COCONUT FIBER REINFORCED POLYMER COMPOSITE FOR NON-LOAD BEARING PANEL WALLS

P. D. Dharmaratne

198049E

Degree of Doctor of Philosophy in Civil Engineering

Department of Civil Engineering

University of Moratuwa

Sri Lanka

September 2022

COCONUT FIBER REINFORCED POLYMER COMPOSITE FOR NON-LOAD BEARING PANEL WALLS

P. D. Dharmaratne

198049E

Dissertation submitted in partial fulfillment of the requirements for the Degree of Doctor of Philosophy in Civil Engineering

Department of Civil Engineering

University of Moratuwa

Sri Lanka

September 2022

Declaration of candidate and supervisor

I declare that this is my work and this thesis/dissertation does not incorporate without acknowledgment any material previously submitted for a Degree or Diploma in any other University or institute of higher learning and to the best of my knowledge and belief it does not contain any material previously published or written by another person except where the acknowledgment is made in the text.

Also, I hereby grant to the University of Moratuwa the non-exclusive right to reproduce and distribute my thesis/dissertation, in whole or in part in print, electronic, or another medium. I retain the right to use this content in whole or part in future works (such as articles or books)."

UOM Verified Signature

20-06-2022

Signature: Date:

The above candidate has carried out research for the Ph.D. Dissertation under my supervision.

Prof. R. U. Halwatura

Department of Civil Engineering

University of Moratuwa

Prof. (Ms.) A. H. L. R. Nilmini

Faculty of Technology

University of Sri Jayewardenepura

Dr.(Mrs) R Jayasinghe

Faculty of Technology

University of Sri Jayewardenepura

Abstract

The study's main aim was to develop a lightweight walling panel for apartment buildings by employing coconut [coir] fiber with waste polyethylene. In this study, the flexural performance of coconut fiber reinforced polymer [CFRP] sandwich panels with different core configurations has studied experimentally and numerically. The numerical investigation was carried out using finite element analysis software "ANSYS 17.2". The coconut fiber reinforced polymer sandwich panel was developed with thin CFRP sheets for the outer faces and cell arrangement for the internal core structure which was made by the same CFRP sheets. The sequences of cells with different core structures were considered to determine the optimum solution for flexural behavior. The first part of this study was the investigation of coconut fiber's physical, mechanical, and chemical properties by using an experimental investigation and a literature review. The next step was to develop the CFRP composites. In this study, the coir fiber was used as reinforced material, and the waste polyethylene was utilized as a matrix material. Composite was developed using hand-layup techniques by varying the coir length and coir weight fractions. This composite material was analyzed using ASTM standards for tensile and bending performance. The sample which optimum results obtained relevant to the coir length and weight fraction were used to develop a composite sandwich panel of 400mm x 400mm in size. The most suitable manufacturing conditions were also studied. The flexural properties of this panel were inspected using experimental and numerical methods. The three-point bending test was carried out to investigate the maximum failure stresses for the panel sample. The next part of this study is to develop the numerical models for the three-point bend test using finite element software. Then, the experimental results obtained from the three-point bend test and numerical outcomes are compared and validated. In the end, the numerical analysis is expanded to examine the sample panel's flexural performance of different cell arrangements. Finally, the failure stresses and the volume at minimum failure stress were identified for each cell configuration. This result concluded that the best cell configuration with minimum weight for wall panels was the result. The proposed wall panel should be durable and low-cost. Therefore, service characteristics and production costs were analyzed. Further, to extend this research, the proposed wall system's life cycle cost and embodied energy were analyzed to identify the long-term benefits of the proposed walling system.

Keywords: Coir fiber, Polymer material, Sandwich wall panel, Mechanical properties, Physical properties.

Acknowledgment

First and foremost, I would like to express my heartfelt gratitude to my research supervisor, Professor R. U. Halwatura, for giving support, guidance, suggestions, and valuable comments to upgrade my research carrier and overall research work. And also wishes to acknowledge Prof. (Ms.) A.H.L.R. Nilmini and Dr. (Ms.) R Jayasinghe has given support to successful research as my co-supervisor.

Next, my sincere gratitude delivers to Prof. S.M.A Nanayakkara (Former Head, Department of Civil Engineering), Dr. L.L. Ekanayake (Senior Lecturer, Department of Civil Engineering), and Prof. (Mrs.) J.C.P.H. Gamage (Research Coordinator, Department of Civil Engineering) for their continuous encouragement, comments, and guidance as my examiners of bi-annual review panels.

And also, I would like to acknowledge Prof. (Mrs.) C Jayasinghe (Head, Department of Civil Engineering), Prof. S Walpalage, (Head, Department of Chemical and Process Engineering), Prof. B. A. J. K Premachandra, (In-charge, Australian, waste-based composite laboratory), Dr. N. D Wanasekara, (Head, Department of Textile and Apparel Engineering), Mr. Sivahar, (Head, Department of Materials science and Engineering), and all academic and non-academic staff of the University of Moratuwa, who continuously given support to successful the research work.

I wish to extend my sincere appreciation for the support given by Technical officers and Lab-Attendants of all relevant Departments at the University of Moratuwa and all staff members, especially Ms. J. P. B. Priyantha Silva, Mrs. W. B. U. Rukma, and Mr. J. A. N. D. Perera in Construction Management Division, Mrs. T.L.K Kumari, Technical officer and Mr. W. L Kumara Lab attendant of the Applied Mechanics Laboratory of the Department of Mechanical Engineering, and all research assistants in Pro- green Laboratory.

Then, I wish to extend my heartfelt gratitude to Dr. (Mrs.) H. Galabada for her invaluable encouragement and guidance in successful this research work. The author wishes to thank all other contributors for completing this project successfully. Finally, I would like to acknowledge the sacrificial dedication of my loving wife, Mrs. Nilakshi Udugama, for her firm support throughout my studies and my son Jaanuka and daughter Supunika for patiently sacrificing some of their entitled time

Table of contents

List of figures

List of tables

1 INTRODUCTION

1.1 General

The population of the world is increasing day by day, and this is adversely affecting the housing requirement of the world. Hence, it is advisable to construct affordable houses in short durations and at a low cost because housing is one of the basic needs of living beings. However, traditional housing construction with conventional materials restricted building construction at low cost and short duration. For example, traditional solid walls such as burnt bricks, solid blocks, and mud concrete blocks cause to increase in the total weight of the structure, forming the requirement of heavy structural elements [1]. Because of the construction material, dead load accounts for a significant amount of the total weight of the structure. It is one of the controlling criteria for the size of structural elements and affects the construction cost and project Duration [2].

Furthermore, the land area does not rise in proportion to the increase in population density and urbanization, making horizontal construction difficult [3]. People are motivated toward vertical structures such as high-rise buildings or apartments to facilitate their living requirements [4]. Moreover, the value of a housing unit of such an apartment governs by the usable or sellable area. Therefore, maximizing the inside space of a building is essential. The use of thinner partition walls instead of the traditional thick wall would be facilitated to increase the useable area inside the apartment by a considerable amount.

In this background, prefabricated lightweight panel walls have gained popularity in the modern building construction industry due to several benefits, including maximizing interior space and being simple to handle, assemble, and disassemble. However, due to limited research on prefabricated lightweight panel walls in Australia, only 3% to 4% of these innovative materials are used in their construction [5].

According to literature, partition wall design is widely used in modern construction to separate the space and interior decoration. Partition walls are used more efficiently in the workplace and to increase user comfort and safety with vital construction features [3],[6].

The walls made of clay bricks, cement blocks, hollow blocks, and other masonry materials are the traditional internal and external partitioning walls. In the modern construction industry, partitions are available in three forms, skeleton partitions, slat partitions, and sandwich panel partitions. The skeleton partition walls are made up of studs and panels. These skeletal partitions are flexible structures that can be constructed to any height. Inside a skeleton partition, any thickness of fireproof and heat-insulating materials can be used. Skeleton partitions include steel stud partition walls, timber stud partition walls, and gypsum stud partition walls, to name a few. The slat partition walls are the other type of partition wall which can be built to a height of the clear height of the room [3]. Sandwich panels are made out of two thin face sheets of substantially greater strength material and a core arrangement that is in between these two face sheets. This core arrangement is made out of lower strength and lower density materials [7].

In addition to maximizing the internal space of the building, the expected other features of these partition walls are the ability to move and disassemble freely, allowing for greater flexibility in indoor space without compromising the essential functional requirements [8]. However, the current issues of existing partition walls lack these important features.

Moreover, these materials' energy consumption, costs, and environmental impacts are higher than the ancient walling materials [9]. It uses internationally available resources with high transportation costs and environmental impact, while most old structures were constructed using local resources.

The rapid growth of the construction industry is creating the most critical environmental problems, such as climate change and greenhouse gas emissions. Therefore, researchers have sought new construction techniques and materials with more sustainable features [1].

The use of polyethylene can be considered one of the leading causes of environmental pollution in recent decades. Polyethylene waste and its way of disposal create harmful impacts on the environment due to its non-biodegradability properties [10]. It has a threat to the long-term viability of the domain. Though the disposal and treatment methods of this waste polyethylene are harmful to the environment, currently, the world production of waste polyethylene is over millions of tons.

One of the leading disposal methods is landfilling. However, it will take thousands of years to degrade. Further, the accumulation of polyethylene in the soil will cause poor vegetation and low water absorption. It roots to increase the temperature in the soil. Because of this, crops could not grow well in polyethylene-contaminated soil [11]-[13].

Burning is the other method of disposing of waste polyethylene. It produces unpleasant gasses and odours. Combustion of polyethylene waste emits dust which is an airborne particulate, and produces volatile organic compounds [VOC] such as paraffin, aldehydes, and dioxins[14], [15].

Moreover, animal plastic ingested persists in the digestive system and can lead to decreased feeding stimuli [16]. According to literature, over 80 seabirds have been found with plastics in their gastrointestinal tracts. These animals with plastic bags in their stomachs ultimately face painful deaths [17]. As such, reducing the usage, recycling, and reuse of plastics would create environmentally and socially positive impacts.

Polyethylene, on the other hand, is a lightweight, odourless, and tasteless substance. It possesses a low water permeability, a strong impact resistance, good organic solvent resistance, and high electrical resistance. In this background, using waste polyethylene for construction material can be a positive way of addressing these issues.

On the other hand, using synthetic fibers such as aramid and glass fibers in the structural elements also causes long-term environmental pollution because they can retain in the open environment for many more years after use. Natural fibers are progressively utilized as a reinforced material due to their essential properties like low density, good thermal insulation properties, good mechanical properties, low price, etc. [18],[19]. Several authors studied natural fibers such as jute, kenaf, flax, sisal, and hemp blended with thermoplastic and then manufactured the composites as substitutes for synthetic fibers [20],[21]. Among such natural fibers, coconut fiber is particularly interested in many industries due to its affirmative characteristics such as high hardness, hard-wearing quality, moth-proof properties, good acoustic resistance, nontoxic properties, and resistant to microbial and fungi degradation [14],[22]. Furthermore, coir fibers are more resistant to moisture than other natural fibers and have a high heat tolerance [23].

Previous research has shown that coir fibers can be a reinforcement material in polymer-based composites with desirable features such as low bulk density and thermal conductivity. Much research has been performed on polymer matrix coconut fiber among several composites produced with coir. Composite is a material that is used in many industries including the construction industry [24]-[30].

Therefore, coir fiber and waste polyethylene are versatile materials in the construction industry in different ways. So it can be used as a raw material to produce composite materials.

Hence, this research focused on developing a composite material by utilizing the readily available coconut fiber as reinforced material and waste thermoplastic as a matrix material. Finally, this composite material is used to develop a partitioning panel wall with the sandwich panel concept in the construction industry.

1.2 Research gap

There has been a lot of research into producing composite materials using various matrix ingredients and reinforcing materials. These composites are utilized for different applications. Natural or synthetic fibers are the most common reinforcing materials. Other polymers such as polypropylene, polystyrene, and thermoset materials are the most common matrix material used to manufacture composite materials. Most composite materials are developed for applications such as the automobile industry, aviation, marine equipment, and asphalting road materials.

Despite waste polyethylene becoming a huge problem globally, there is a gap in knowledge among researchers who use waste polyethylene to manufacture polymer composite. Among several natural fibers, there is a lack of research that involves coconut fiber to manufacture the composite with polypropylene, polystyrene, and thermoset. However, a combination of coir and waste polyethylene is identified as a knowledge gap to be filled.

On the other hand, though the researchers focus on using the composite in several applications, very few researchers have aimed to develop construction material. Since partition walls are an essential part of building construction, using composite to produce thinner partitioning panel walls is significant to fulfilling the novel research problem.

This research is mainly focused on developing a composite material using coir and waste polytene, possibly converting this composite to make a thinner partition wall based on the sandwich panel concept with the necessary properties.

Finally, the study focuses on developing an internal panel wall, which comprises a better flexural performance than the available panel wall in Sri Lanka. This novel panel wall should be lightweight, less installation and demolishing time, less manufacturing cost, and better architectural appearance. Further, it should be long-lasting with less embodied energy and life cycle costing with good sustainable features.

1.3 Aim and objectives

The main aim of this research is to develop a non-load bearing composite sandwich internal panel wall with optimum flexural properties, followed by several objectives:

- To characterize the coconut fibers and waste polyethylene.
- To develop a composite material using coconut fiber and waste polyethylene
- To optimize the internal mechanical structure (core arrangement) using finite elements and actual simulations.
- To study and compare the mechanical and structural properties of the proposed panel wall with available exiting panel walls.
- To evaluate the financial feasibility of this product (panel wall) by comparing the life cycle cost and embodied energy.

1.4 Methodology

1. A detailed literature review is carried out to study the physical, mechanical, and chemical properties of coir fiber and polyethylene and the properties of fiber-reinforced composites and their properties.

2. Prepare a series of composites and carry out the laboratory experiment series to optimize the length of coir fiber, mix proportions, etc.
3. Prepare a series of numerical models by varying the internal mechanical structure and then list the mechanical properties.
4. Simulate a numerical model for sandwich wall panels using "Ansys software" for the selected internal core arrangement and then compare the properties with actual model outcomes.
5. Compare the software outcomes with the standard and mechanical properties of wall panels in Sri Lanka.
6. Calculate this product's life cycle cost and embodied energy and compare it with available non-load-bearing wall panels.

1.5 Main findings

1. The most suitable coir to polyethylene weight ratio was discovered to develop the composite with optimum mechanical properties. The coir to polyethylene weight ratio between 10% to 40% was identified as the most suitable mix proportion for manufacturing the composite.
2. The production factors have an impact on the mechanical properties of composites. Temperature, pressure, and time are the most critical manufacturing factors when developing composites. So, it was discovered that 140^0 C temperature, 4 MPa pressure, and processing time of 6 min. are the optimum production conditions for the composites.
3. The effect of fiber length on the composite's characteristics was determined. At this point, the optimum tensile strength investigated was 12.56 N/mm^2 when the fiber length was 4 cm with 40 % coir weight content. The flexural strength was optimum when the composite consisted of a 3 cm fiber length and a 30 % coir to polyethylene ratio. The composite material's maximum flexural strength was 33.77 N/mm^2. The impact strength was optimum when the fiber content was 40 %, and the fiber length was 2 cm. It was observed that the highest impact strength in the composite was 1.22 kJ/m^2.

4. Compared to the other composite samples with varying fiber percentages, the composites with 40% weight reinforcing fiber exhibited a maximum water absorption capacity of 19.78%. However, after 18 days, water absorption was negligible for all fiber percentages. Furthermore, despite the composite sample's cutting edges being waterproofed against water contact, all samples absorbed water to some extent, according to this observation. As a result, the surface of the samples was expected to absorb some water. So, it was discovered that the composite material's surface should also be treated to minimize water absorption.
5. The horizontal burning rates of the coir fiber polyethylene composites were higher, ranging from 25.33 to 31.91 mm/min. The analyzed samples fall under the HB category according to the UL-94 HB standard. Furthermore, the test findings demonstrated that the burning rate increased as the fiber fraction of the composites rose. It can also be stated that the average horizontal burning rate of the sample is proportional to the coir weight percentage. Coir fiber polymer composites are highly flammable and burn rapidly, which is a significant disadvantage. This proposes the use of flame-retardant chemicals causes to control and delay the burning process.
6. This composite was used to develop a panel wall. The 100 mm x 100 mm square core structure was observed as the most suitable core arrangement to produce the panel wall based on weight and flexural performance.
7. The 3-point bending test was carried out on coir fiber-reinforced polymer composite (FRPC) panel samples and Durra panels. When comparing the values, the FRPC panel showed 2.8 times higher flexural capacity than the Durra panel. In addition, innovated FRPC panel shows less cost and weight than Durra panels. The flexural strength of innovated FRPC panel shows a better concert than Acotec, Micro, and EPCI panels.
8. The panel deformation was within the serviceability limits according to building Code 2006.

9. FRPC panel walls are identified as the best panel wall for buildings by considering the initial cost, embedded energy, operation cost, and life cycle cost.

1.6 Organization of the thesis

The breakdown of the chapters in this thesis is as follows;

- The first chapter discussed the research background, the research gap, the goal and target, and the technique. Then the key findings and outcomes of the research were discussed.
- The second chapter contains a comprehensive literature review that examines the research's background, including fiber material, matrix material, composite material, manufacturing processes, sandwich panel walls, and numerical analysis of panel walls.
- Chapter 3 presents the complete process of developing composite and their flexural performance. Coir fiber and polyethylene characterization were provided. The use of a mixed design for composite preparation and the change of physical parameters to improve mechanical properties were discussed. Water absorption and flammability tests were reported as physical attributes.
- The development of sandwich panels made of composite materials is discussed in Chapter 4. Initially, software validation was carried out using a variety of methods. The finite element approach was then utilized to determine the best core layout.
- Chapter 05 explains how to prepare sandwich panels and test them mechanically. Finally, the flexural properties of existing panel walls are compared to those of the novel panel.
- Chapter 06 compares and contrasts the financial feasibility of the new panel and Durra panel samples. Finally, the panel wall's embodied energy estimates and life cycle costs were examined.
- The research conclusion and recommendations are presented in chapter 7

2 LITERATURE REVIEW

2.1 General

This research focuses on developing a non-load-bearing internal panel wall system using polymer reinforcement composites. The necessary information and data for this study were acquired after thoroughly examining the literature. This chapter covers the literature survey to identify the importance of vertical construction, available walling materials, panel walls for building construction, different composite materials, fibers used in composite materials, and available matrix material.

2.2 Importance of vertical construction

When considering the building industry and the history of shelters, the basic needs of all living beings are shelters. All living beings except human beings are providing their sheltering requirements from nature. But the, human beings are facilitating their sheltering requirements using manmade structures. The majority of the world population has been living in manmade structures [31]. The people are upgrading their manmade structures daily to fulfill their unlimited sheltering requirements [32]. This has been causing a reduction in the usable land area.

Similarly, population growth is a severe issue in facilitating their requirements due to limited land space availability. People have started to think of innovative solutions. Therefore, they started to utilize vertical spaces instead of horizontal land spaces. Hence, this has promoted vertical constructions like multi-storied buildings. Once we go for this type of construction, most of them are reinforced concrete structures. Reinforcement multi-storied buildings are famous in Sri Lanka and worldwide [33]. However, their construction cost is very high. Not only the construction cost but also the construction time [34]. Because significant construction companies and property developers still adhere to traditional construction methods and materials, the total project cost is so high and not bearable for building owners [35]. Because of this, researchers needed to introduce effective alternative materials and methods to rectify this situation as much as possible.

2.3 Available walling materials and panel walls

Building construction plays a significant role when catering to the construction sector. Two major items in multi-storied buildings are load-bearing frame structure and walling elements [36]. The load-bearing frame structure consists of the slab, beam, columns, staircase, foundations, etc. The walling elements consist of brickworks, block works, panel walls, etc. However, the masonry walling elements consume much time during construction [37]. Literature states that the method of wall construction and material usage has a long history and has been continuously developing. In the initial stage, walls were constructed using adobe, cob, cordwood, rammed earth, etc. [38]. However, burn brick, cement sand block, and mud concrete blocks [MCB] are recently used.

These masonry constructions have no full-height constructability. The construction is based on stage construction. As a result, considerable time and high labour requirements are needed for this construction [39]. Since the thickness of the traditional walls is high, room space is consumed by walls unnecessarily [40]. Further, cement-sand plaster or some finishing material is required to achieve a good finish. So, additional costs and time must be incurred for these plastering and finishing works.

Therefore, inventors and researchers want to find a solution to minimize these drawbacks. Hence, they have been developing the wall construction process and techniques. In the end, they have identified that panel walls are more effective than traditional walling systems [41].

Hence, the panel walls now come to the front line because of several advantages such as easy handling, assembling, reassembling, demolishing, etc. In addition, the panel walls' thickness is less than that of traditional walls. Hence, the usable and sellable area also goes up. In addition, panel walls' weight is less than conventional walls. This result causes a reduction in the size of the structural elements and the superstructure weight of the building. In the end, the overall weight of the structure reduces. Because of this, the cost of the project goes down. In this background, panel walls are more effective and significant for high-rise building construction.

Different materials such as laminated timber, gypsum board with papers, cement mix material, fiber with resin material, calcium silicate with paper, lightweight concrete, and some waste material are used for the panel walls [42]. These panel walls are used worldwide as well as in Sri Lanka. M. E. Arslan et al. (2022) further studied that most panel walls consist of synthetic and non-biodegradable material [43]. When considering the available panel walls in Sri Lanka, Acotech panels walls, durra panel walls, micro panels walls, and Expanded Polystyrene (EPS) panel walls are commonly used [44]. Most of the panel walls are manufactured using cement mixing materials. Due to their heavy weight, several people must handle some of the panel walls. In Addition, a skilled, trained labour gang is required to fix the micro panels. Some of the materials in micro panel walls are needed to be imported from other countries, so the final production cost will go up.

The invention of lightweight panel walls results in minimizing and rectifying these difficulties. Most of the panel walls are made out of both synthetic and natural materials [45]. But very few panel walls are made out of natural materials, waste material, and biodegradable material [46]. The study observed a lack of natural or waste material used to develop panel walls.

The sandwich panel comprises two outer face sheets and an inner core arrangement with an adhesive layer [47]. The external face sheets are made out of very stiff and strong material, mostly using laminates or metals. The outer face sheet's expected property is flexural [48]. The inner core may be arranged mostly of non-metallic hollow structures, cellular foams, or some other less stiff, low-density materials. This inner core material provides the shear strength to the sandwich panel resulting in high bending stiffness [49]. After a series of research, Mines et al. (1998) revealed that polymer composite materials can be used as face sheets and inner core [50]. The composites can be simply developed by blending fiber materials with matrix material. So, the data was collected to select the most suitable fiber and matrix material for this development. According to these data, coconut fiber was selected as fiber material from several natural fibers, and the waste polyethylene [LDPE] was chosen as the most suitable matrix material. The selection of natural materials will not affect environmental pollution, and utilized waste materials will be more beneficial to the environment.

2.4 Fiber

Fibers are categorized mainly into three categories such as animal, mineral, and plant fibers. Animal hair, silk fiber, and avian fiber are categorized under animal fibers. Asbestos, ceramic fibers, and metal fibers are categorized under mineral fibers. The seed fiber, leaf fiber, fruit fiber, and stalk fiber are categorized under plant fibers. The classification of fibers is given in Figure 2-1 [51]. Among these fibers, plant fibers are a major type used in the construction industry. According to Rohit and Dixit (2016), the plant fibers were categorized into six basic types. These are blast fibers (jute, ramie, flax, hemp, and kenaf) leaf fibers (abaca, pineapple, and sisal), seed fibers (kapok, coir, and cotton), core fibers (kenaf, jute, and hemp), grass and reed fibers (wheat, rice, and corn), and all other types of fibers (wood and roots) [52]. Out of these six categories, coconut seed fibers are the most used. These fibers are used as raw material for several productions worldwide and in Sri Lanka.

Further, the coir is used in the construction industry also. Hence, coir was selected as one major raw material for the proposed development. The following section will discuss more detail about coir fiber.

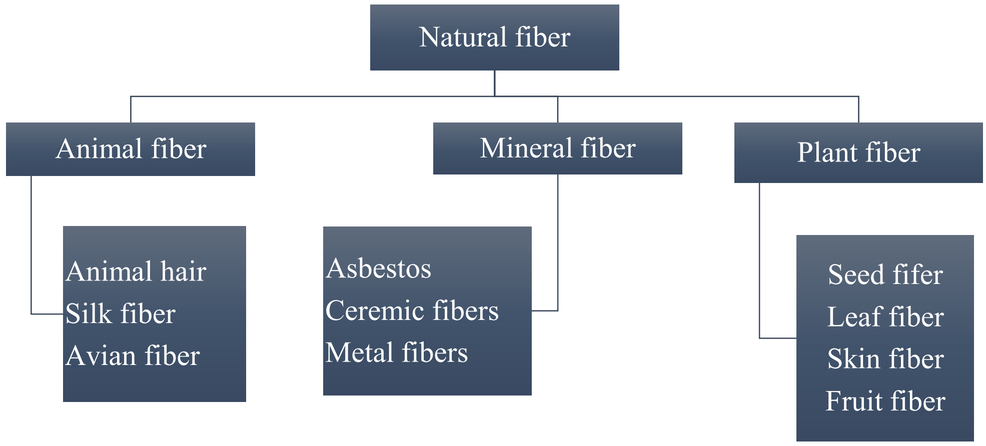

Figure 2-1: Classification of fibers

2.4.1 Coconut fiber

In Sri Lanka, coconut fibers are abundantly available. The outer shell of the coconut fruit (Cocos Nucifera), which belongs to the Arecaceae graminid, is used to extract this fiber [20]. The coconut tree, seed, and fiber are shown in Figure 2-2. Figure 2-3 depicts microscopic images of a fiber's longitudinal and cross-sectional views.

Figure 2-2: Coconut tree, seed, and coir fiber

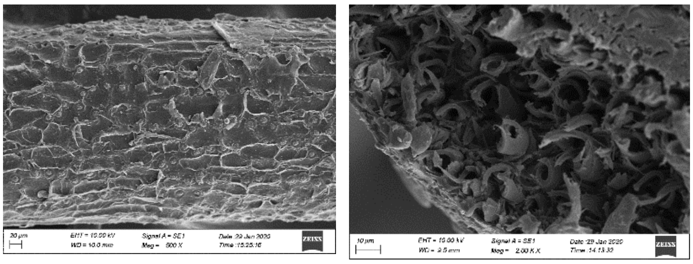

Figure 2-3: Longitudinal and cross-section of a coir fiber

Coconut fibers are divided into two types: white and brown fibers. The images of brown and white coir are shown in Figure 2-4. The smooth, fine, and weak coconut fibers are taken from young coconuts. On the other hand, the fibers recovered from mature coconuts are thick, strong, and abrasion-resistant [53]. According to the requirement, the selection of fiber type will vary. However, brown fibers are frequently used in the manufacturing industry. From the commercial point of view, coconut fibers are classified into three categories: bristle, mattress, and decorticated.

Figure 2-4: brown and white coir

Coconut trees can be found in tropical areas all over the world. The bulk amount of coir fibers is produced in the Philippines, Indonesia, Brazil, India, Thailand, Sri Lanka, Vietnam, and Malaysia [54]. Coconuts are grown on around 12.05 million hectares around the world. In recent years, production has reached 61.1 million seeds per year [20]. According to the official website of the "International Year for Natural Fibers 2009", about 500,000 tons of coconut fibers are produced worldwide from Sri Lanka and India, accounting for most of them. It is estimated to be worth roughly USD 100 million in total. The top exporters are India and Sri Lanka, followed by Thailand, Vietnam, the Philippines, and Indonesia [55]. The coastal region of Kerala state in India accounts for 60% of the entire world's supply of white coir fiber. Sri Lanka produces 36 percent of the world's brown coir fiber [56].

Coconut fiber is a recycled natural material with a longer life span than other fibers due to its high lignin concentration [57],[23]. Coir fibers are also more moisture-resistant than other natural fibers and heat and salt-resistant [58]. Coconut fibers also have several advantages, such as being resistant to fungi and corrosion and having excellent temperature and sound insulation properties [59].

2.4.2 Different usage of coir fibers

Because of its hard-wearing quality, high hardness, good acoustic resistance, moth-proof, nontoxic, and resistance to microbial and fungus degradation, coir fiber has a unique appeal in various industries [58]. Coir fibers have been used to make a wide range of items. It has essential characteristics such as the lowest bulk density and thermal conductivity. As a result, developing a composite material with low thermal conductivity using coir fiber is critical [60] as it would be a good answer to environmental and energy challenges. According to the authors [27], laying coconut fiber on the rooftops can lower the average indoor air temperature by up to 1.20°C. Then temperature of the inside room by up to 3.10°C. As a result, coconut fiber can serve as a thermal insulator [27]. Heatwave transfer through the concrete slab is reduced significantly when coconut fiber is used as a thermal barrier on the roof slabs. Due to this occurrence, indoor temperatures can be more comfortable during the day and night [61].

2.4.3 Physical and mechanical properties of coconut fibers

Many researchers have looked into the characteristics of coconut fibers for various applications. According to the literature, the diameter of coconut fibers is approximately identical, and the value may be between 0.1 and 0.5 mm. Coir fibers have a tensile strength of 100 to 200 N/mm^2 and a density of 0.67 to 1.00 g/cm^3 [62]. The stress-strain relationship of coir fibers is depicted in Figure 2-5. It demonstrates that among natural fibers, coir is the most ductile [63].

Figure 2-6 shows stress-strain relations for natural fibers. It reveals that the coir fibers are 4-6 times more resistant to strain than other fibers [64]. The predicted ranges for physical and mechanical parameters are shown in Table 2-1 [65].

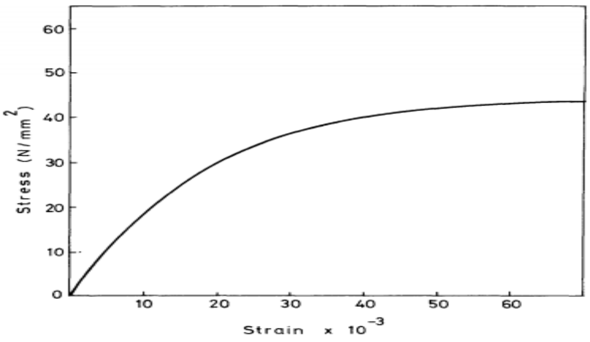

Figure 2-5: Stress-strain variation for coir fiber

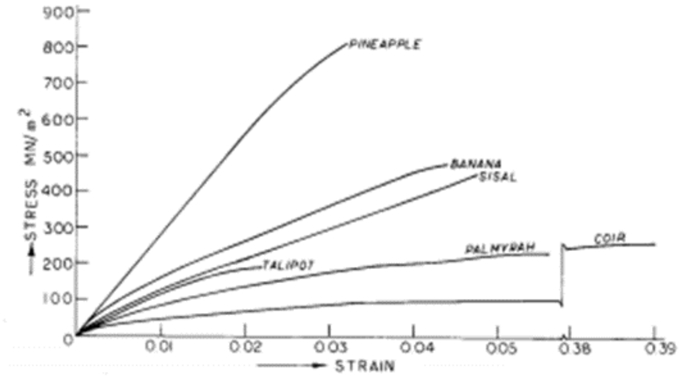

Figure 2-6: Stress-strain curve for natural fibers

Table 2-1: Physical and mechanical properties of coconut fibers

Diameter (mm)	Length(mm)	Tensile strength (MPa)	Elongation (%)	Elastic modulus (GPa)	Density (Kg/m^3)	Reference
040-0.10	60-250	15-327	75			Ramakrishna et al.(2005a)
0.21		107	37.7	2.8	1104-1370	Agopyan et al.(2005)
0.3		69.3		2.0	1140	Paramasivam et al.(1984)
		50.9	17.6		1000	Ramakrishna et al. (2005)
0.27±0.073	50±10	142±36	24±10	2.0±0.3	-	Li et al.(2007)
0.11-0.53		108-252	13.7-41	2.50-4.50	670-1000	Toledo et al.(2005)
0.12±0.005		137±11			870	Munawar et al.(2007)

2.4.4 Chemical properties of the coir fibers

The primary chemical compositions of the coconut fibers are cellulose, lignin, and hemicellulose. These compositions cause the different properties of the coconut fibers. Further, treated fibers change their compositions [42]. Usually, NaOH solutions are used for the coir fiber treatment process [50]. The chemical properties of the coir fiber are summarised in [66].

Table 2-2: Chemical properties of coir fiber

Chemical composition and microfibrillar angle	**Unit (weight %)**
Lignin	40-45
Cellulose	32-43
Hemicellulose	0.15-0.25
Pectin	3-4
Water-soluble	5
Ash	2
Microfibrillar angle (degree)	30-49

Another study was carried out to investigate the tensile properties of composite with sisal fiber with polyethylene having 30% fiber loading. The length was arranged to 5.8 mm. Their results revealed the 14.7 N/mm^2 tensile strength of composite [67]. It indicates that the fiber type also will cause a considerable effect on the tensile strength.

2.5 Matrix material

The composite material is produced by blending reinforced material with the matrix material. According to the literature, different kinds of composites are available such as polymer composite, ceramic composite, and metal matrix composite. This research focuses to develop a polymer matrix composite. Therefore, choosing a suitable matrix material for this development is necessary.

2.5.1 Polymer

The scholarly data reveals three types of the matrix material used in manufacturing polymer composites. They are thermoplastics, thermosets, and elastomers. Generally, plastics are categorized as thermoplastic and thermoset. These plastics are categorized based on their behavior concerning heat. Any polymer that undergoes a temporary physical change is known as thermoplastic. Low-density polyethylene [LDPE], high-density polyethylene [HDPE], polystyrene, polypropylene [PP], polyamide, and polyvinyl chloride [PVC] are considered under thermoplastic polymers [68]. Any polymer that undergoes a permanent chemical reaction is called thermosetting plastic. The thermoset polymers shall not soften under heat due to their strong cross-link chemical bonds. These polymers are harder and more rigid. Hence, it is very difficult to soluble in organic solvents [69]. Epoxy resin, Melamine Formaldehyde, Polyester Resin, Urea Formaldehyde, Vinyl Ester, and Phenolic are frequently used thermosetting polymers [70]. The advantages and disadvantages of thermoplastic and thermosets are given in Table 2-3 [71]. However, this study was carried out using thermoplastic polymers.

Table 2-3: Advantages and disadvantages of thermoplastic and thermosets composites

Material	Advantages	Disadvantages
Thermoplastics	High impact strength	Typically, it will soften with heat
	Attractive surface finish	More difficult to prototype
	Recyclable/ Scrap is reusable	Short workable pot life with some exceptions
	Stick to other thermoplastics	
	Molded or shaped by reheating and No emission	
Thermosets	Easy to process and laminate	Often release emission (Volatile organic compounds)
	May be need pressure or heat to form	Non-recyclable and cannot be reclaimed easily
	Typically, inexpensive	
	strong than thermoplastics	
	Better suited to a higher	

2.5.2 Waste polyethylene

The waste polyethylene creates enormous health, social, and environmental problems, especially in developing countries. Seventy-five percent of total plastic litter generated by the world coming from developing countries, and in which 25% is originated in western countries. The polyethylene, a disposal material from industries, factories and man-made activities, is called waster polyethylene. The majority consists of shopping bags (40%), lunch sheets (29%), plastic bottles (20%), and polyethylene sheets (8%). Out of them, low-density polyethylene is around [LDPE]-57%, high density polyethylene [HDPE] 20%, and polypropylene [PP] is the remaining amount. According to literature data, the LDPE is the most critical problematic waste in Sri Lanka. Hence, an urgent solution is required to rectify this situation.

2.6 Composite material

At least two constituent materials make up a composite material. These constituent materials have considerably various chemical or physical properties, and when combined, they produce a substance with attributes distinct from the individual elements.

The main advantages of the composites are lightweight and high strength-to-weight ratio. According to Verma et al. (2014) the advantages of composite materials can be identified as

- The tensile strength of the composite is four to six times higher than steel.
- Corrosion-free and resistant to the chemical effect
- The low embedded energy when compared with the other structural metallic materials
- Non-conductivity [23],

According to past literature, many composites are made out of coir. Composite with coir fiber and oil palm fiber, composite with recycled rubber and coir, the composite with coir fiber-reinforced polymer composite for the partition wall, coconut-fiber-reinforced thermosetting, coir fiber reinforced polypropylene composite panel, coir fiber reinforced polybutylene succinate resin composites, coir fiber reinforced epoxy composites and short coir fiber-reinforced natural rubber composites are few of them. Detailed evidence is described in the following sections.

There are many advantages of natural fiber composites. It has a high specific strength and low specific weight and stiffness. Natural fiber can be renewable and biodegradable. Since the cost is very low and environmentally friendly, they are better for developing countries [72].

2.6.1 Different composite materials

Different composite materials are manufactured in different fiber materials and matrix materials. The following section describes the composite materials which are developed by some other researchers.

2.6.1.1 Composite with coir fiber and oil palm fiber

"Fiber cement sheets" were made using cement mortar with coir fiber and oil palm fibers. It showed better physical and thermal properties. The 10% weight of coir or oil palm fiber showed the optimum properties of heat insulation in flat cement fiber sheets. The fiber treated with inorganic compounds showed more quality and durability for these fiber sheers. The coir and palm fiber caused to increase in apparent porosity, thermal conductivity, and a decrease in bulk density. In addition, this composite material could be used as a good heat insulator. Further, this composite helps to increase the energy efficiency in residential buildings while helping to reduce the cost of mechanical ventilators and air-conditioners [28].

2.6.1.2 Composite with recycled rubber and coir

The medium-dense fiber [MDF] board composites were fabricated using recycled rubber and coir fiber. In this product, rubber and coir fiber are used as a filler material and polyurethane is used as a resin. Based on the mechanical and physical parameters, the performance of the composite board was observed. According to experimental research, the modulus of rupture and modulus of elasticity grow with the hardness of the board. Further, it was found that the content of fillers and resins plays a vital role in getting better results [29].

2.6.1.3 Coir fiber-reinforced polymer composite for the partitioning wall

The prominent proud of this research work was to explore the opportunity of using coir fiber with a polymer matrix material. The matrix material was polyethylene [used polyethylene covers and milk packets], and the reinforced material was coir. The results were very challenging compared with existing plywood planks. In addition, the composite was tested for threading operation. Further, this product shows a higher load-carrying capacity, good bending and compression strength, and better waterproofing properties than plywood planks. The tensile strength was very close to the plywood planks, and these sheets are more flexible than the plywood [73]

2.6.1.4 Coir fiber reinforced polypropylene composite panels

The coconut fiber reinforced polypropylene [PP] composite panels were studied for their physical and mechanical properties in this research. Coir fiber weights 40%, 50%, 60%, and 70% were combined with PP powder, and 3 % maleic anhydride grafted polypropylene [MAPP] powder. It was discovered that increasing the coir fiber harms the composite's characteristics. Furthermore, when coir fiber content is increased up to 60%, composites' flexural strength, tensile strength, and hardness improve. In addition, the flame resistance developed with incrementing the coir content. Ultimately, the optimal composition of 60% coir fiber, 37% PP powder, and 3% weight MAPP was observed for the automotive interior application [58].

2.6.1.5 Coir fiber-reinforced polybutylene succinate [PBS] resin composites

The study investigates how alkali treatment affects the surface morphology and mechanical characteristics of coir fibers, as well as the interfacial shear strength [IFSS] of PBS resin composites. With altering fiber mass, the mechanical characteristics of coir fiber PBS resin composites were investigated. Both treated and untreated fiber composites were studied for these qualities. A five percent NaOH solution was used to treat the coir fibers. According to the findings, the highest IFSS was roughly 55.6% greater than untreated coir fibers.

Similarly, the mechanical properties of the treated fibers were far superior to those of the untreated fibers. The best mechanical properties were found when the fiber mass content reached 25%. It reveals that tensile strength grew by 54.5%, tensile modulus increased by 141.9 %, flexural strength improved by 45.7%, and flexural modules increased by 97.4%. The alkali-treated coir fiber induced increased fiber surface roughness, which resulted in these increases. It significantly improved mechanical interlocking between the fiber and the PBS matrix in composites. The optimum strength and mechanical properties were found in coir fiber with PBS resin matrix, according to the findings of the experiments [74].

2.6.1.6 Coir fiber reinforced epoxy composites

The natural fiber-based polymer composites described in this study included coir as a reinforcement material and epoxy resin as a matrix material. The reinforcement materials were untreated coir, and the glue was epoxy. The mechanical characteristics of the produced composites were studied. The study aimed to see how fiber length affected the mechanical performance of these epoxy-based polymer composites. The scanning electron microscope [SEM] was also used to investigate the surface morphology of cracked surfaces. The length of the fibers increased up to 20 mm, while the hardness values declined. The microhardness value improved to 16.9 Hv after that moment. The findings revealed that fiber lengths had a significant effect on material properties. The observed tensile strength, tensile modulus, flexural strength, and impact strength were 13.05 MPa, 2.064 GPa, 35.42 MPa, and 17.5 $kJ/m^{2,}$ respectively [75].

2.6.1.7 Short coir fiber-reinforced natural rubber composites

The natural rubber was reinforced using chopped untreated coir fibers for manufacturing coir fiber reinforced rubber composite. This study involved altering fiber lengths and treating them with a 5% NaOH solution. These composites were vulcanized at a temperature of 150°C. These composites' vulcanization parameters, processability characteristics, and stress-strain properties were investigated. Untreated coir fiber composite was compared to alkali-treated coir fiber composite in terms of reinforcing qualities. Green strength measurements were taken to determine the degree of the composite's fiber orientation. The investigation was conducted to measure anisotropic swelling, fiber strength and alignment, and rubber adhesion. Finally, the mechanical properties of different fiber lengths, processability, orientations, and surface treatments were studied.

The results showed that the mechanical properties were better when the material was in the longitudinal direction and the coir length was 10 mm. The composite of treated coir with a 5 % sodium hydroxide solution for 48 hours had the highest tensile characteristics. SEM studies demonstrated a greater bond between natural rubber and alkali-treated coir fibers. Anisotropic swelling investigation revealed poor adhesion between natural rubber and untreated coir fiber [76].

2.7 Panel wall

This study aims to develop a non-load-bearing interior panel wall that can be used as a partitioning wall in multi-story buildings. After reviewing a literature series, the appropriate information and suitable data were gathered for this study. The followings were included in the literature.

2.7.1 Existing panel walls

The different kinds of non-load bearing elements have been used in building structures, and they are employed in different locations such as walls, floors, ceilings, doors, windows, etc. [9]. Among these elements, non-load-bearing walls contribute a greater portion. Different types of non-load-bearing walls are currently used in the construction industry. They are made out of other materials with varying manufacturing technologies [77]. The panel walls constructed on different materials extracted from literature are depicted in Table 2-4.

According to the study conducted by Aghaee and Foroughi (2013), the lightweight panels which are made out of textile waste are more environmentally friendly and can be used as non-structural walls in a building. This panel wall is a low-cost alternative solution in the construction industry. Moreover, these experiments revealed that the lightweight materials, with the confinement of textile mesh glass fiber, the post-crack behavior also improved. The average compressive strength of perlite lightweight concrete was 9.19 $N/mm^{2,}$ and its specific gravity was 1,269.8 kg/m^3. This type of concrete is considered semi-structural lightweight concrete [78].

Table 2-4: Summary of different wall panels

Source	Country	Product	Raw materials used
(Kamran Aghaee and Mohammad Forough)	Iran	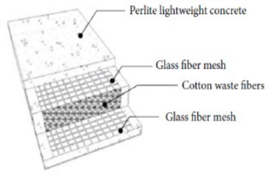	Textile waste, Textile mech glass fiber, Light wt perlite concrete
(M. K. Hassan et al 2020)	Australia	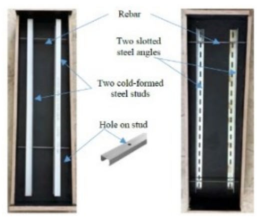	Cement, lime, fly ash, fine sand, and expanded glass aggregate with stud
M. Kippel et al 2014)	Switzerland	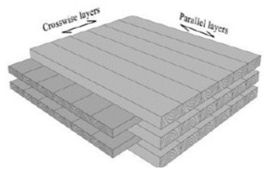	Cross-Laminated Timber
W. K. Chow C. W. Leung	China	 	Timber and Glue
Ref No: CE/GA/17/ST/2014/675)-Civil Department - UOM)-Sri Lanka	Sri Lanka	 	Cement, Sand, Aggregate
(Ref No: CE/GA17/ST/2005/118)-Civil Department – UOM-Sri Lanka	Sri Lanka		Waste paddy straw, Kraft sheets
Ref No: CE/GA17/ST/2010/33)-tested by Dept of Civil Engineering, UOM, Sri Lanka	Sri Lanka	 	Three-dimensional welded-wire space frame. Polystyrene insulation core, Plastered on both sides with Cement sand mortar

Nahro Radi et al 2013	India	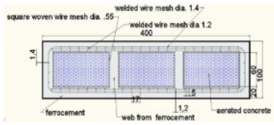	Cement, Fine Aggregate, Admixture, Al powder, Wire mesh
Fernando et al. 2017	Sri Lanka		Expanded Polystyrene (EPS). Cement, sand, fly ash
Harikrishnan et al. 2020	Brisbane, Australia		16 mm thick Gypsum plasterboard, lipped channels, stud
Juan et al. 2016)	Argentina		
D. Gawatre et al 2020	India	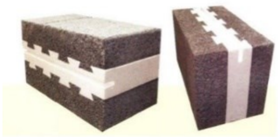	1.EPS Thermocole Material, Cement, Crushed sand, Water
W. K. Chow & C. W. Leung	Hong kong		Gypsum and Papers
			Calcium Silicate and papers
		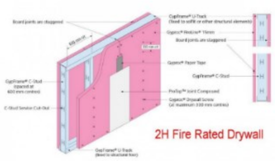	Fire retarder material with Gypsum

Fernando et al. (2017) introduced lightweight concrete panel walls made by mixing mechanically recycled expanded polystyrene (EPS), cement, sand, and fly ash together, as shown in Table 2-5.

This experiment was performed to evaluate the properties of panel walls which are made out in two different ways. Type I was made out of the same material but fixing the two asbestos sheets are either side, and in type II, the panel was made out of the above material mixing. The density of this foam concrete is maintained between 600 -700 kg/m^3 to keep the panel's weight under control. The panels were cast in sizes of 0.6 m x 2.4 m to 75 mm, 100 mm, or 150 mm thickness [44].

Table 2-5: Properties of EPS panel

Property	Type I 	Type II 
Compressive strength (N/ mm^2)	4.06	2.13
Elastic modulus (kN/mm^2)	1.15	0.75
Flexural capacity (N/mm^2)	1.64	0.31

EPS-based lightweight panels can also be used in various other applications, such as apartment buildings, hotels, and commercial structures. In these concrete board foams, the moisture effect is insignificant. When moisture is present, though, they tend to strengthen. The panel uses tongue and groove joints for connections, which could reduce building time while still giving the walls an excellent finish. As a result, the usage of plaster on the wall surfaces is no longer necessary.

The prefabricated lightweight composite [PLC] wall panels made from steel studs and lightweight concrete is another study carried out by Hassan et al. (2020) [5]. Various steel studs/angles and material types were used to manufacture these panels. According to the author, the present PLC wall panels are weak under the flexural load. Therefore, additional reinforcement bars are employed to increase the flexural strength of the panel. The usage of reinforcement bars also contributes to increasing density and corrosion issues. Lightweight composite wall panels have recently been created using foam concrete and cold-formed steel. The flexural strength of those wall panels is relatively high. Expanded glass aggregate and cold-formed steel studs/slotted steel angles were used to create the prefabricated lightweight composite wall panels. The mechanical properties of lightweight concrete were investigated according to AS 1012.10 for tensile strength and AS 1012.9 for compressive strength. The average compressive strength and tensile strength of the PLC wall panel were 27.52 MPa and 1.64 MPa, respectively. The compressive strength of lightweight concrete expanded glass aggregates was 27.52 MPa, and the density was 1367.11 kg/m^3. Split tensile strength was lower than that of ordinary lightweight concrete. The prefabricated lightweight composite wall panels with high flexural strength were proposed for the walls. Three slotted steel angels PLC wall panels provide the maximum flexural strength and stiffness, and one slotted steel angle PLC wall panel offers relatively high deformation.

A cross-laminated timber wall is another type of partition wall studied by Kippel et al. (2010). Cross-laminated timber [CLT] is a wood product made of modest softwood boards with thicknesses ranging from 10 to 40 mm and widths ranging from 80 to 240 mm. In glued-laminated timber boards, the layers are oriented crosswise. As a result, a two-dimensional structural system can carry loads in longitudinal and transversal directions. As a result, CLT can be utilized as a floor, roof, or wall material. CLT has several advantages in the building, including excellent thermal and structural properties. In North America, light-frame wood construction dominates the low-rise building industry. CLT has the potential to be used in mid and medium-rise buildings in the government and private sectors. These buildings with seven to nine stores have also been constructed in Sweden, the United Kingdom, and Italy. Because of the minimal connecting details, CLT constructions have a fast and industrialized manufacturing method and a very short assembly and construction time [79].

Thermo-cool sandwich concrete bricks in sizes 200 mm x 100 mm x100 mm is another partitioning walling block made of cement, crushed sand, and expanded polystyrene

[EPS]. The cement and crushed sand were used to manufacture the block's exterior layer, while expanded polystyrene thermo-cool was used to build the interior layer. The average water absorption value was 14.33%, and the density was 1792.49 kg/m^3. This block has a flexural strength of 3.45 N/mm^2 and compressive strength of 1.9 N/mm^2 [80].

Gypsum wallboards [GWB] are also used for partitioning in 50%-95% of commercial buildings and offices, especially when wet partitions are not permitted. The low cost, ease of installation, tremendous flexibility, lightweight, and non-combustibility are only a few of the benefits. The GWB can be built in single or multiple layers, horizontally or vertically. The void between the two layers might be filled with mineral wool or glass fibers to guarantee optimal sound insulation. Most gypsum boards are made in standard dimensions of 1200 mm wide, 2400 mm high, and 12 mm thick. They have a one-hour fire resistance time and are non-combustible. To strengthen the fire resistance of this board, fire retardant paints or coatings can be put on the surfaces. In general, the distance between successive studs is approximately 2400 mm and if the height of the partition is increased, additional stiffeners should be added [77]**.**

According to BS 476: Part 4 and Part 7, the calcium silicate boards are classified as non-combustible materials and are used especially in high-quality projects similar to gypsum wallboard partitions. They are tough with excellent impact resistance, good water resistance properties, and long-term durability conditions. This wall type is made of two calcium silicate boards supported by steel or wood studs on top and bottom. The cavity was filled with mined wools. The boards are usually built to the dimensions of 1220 mm long, 2440 mm wide, and 6 mm to 60 mm thick [77].

Plywood wall panels were common partitioning material before people began using gypsum wallboard partitions. The main disadvantage of plywood partitions is that they are more time-consuming to install than gypsum wallboard systems. Fixing operations include cutting the plywood, using studs to the correct sizes, and then the top coating for final finishes. Because of these reasons, the labour costs are considerably high. However, plywood has advantages such as less environmental impact and less health risk to humans [77].

Fire-rated partitions are made of fire-resistant material and fully meet international regulations such as BS 476: Part 22. However, these wall panels are more expensive than the gypsum wallboard and plywood partitions. Therefore, designers would only choose fire-rated partitions in response to insurance company requests [77].

Durra panels manufacture by pressing waste paddy straw and adhering the paper outside the panel to have a smooth finish. The 50 mm and 58 mm thick wall panels are made in this process. These panels are mainly used for the internal non-load-bearing walls. And also, these durra panels were used not only for wall panels but also for interior wall claddings and ceilings. These panels are available in 8' x 4' sizes. This wall system has a fire-resistance value of up to 100^0 C and a fire control rating of 1-2 hours. These rated values adhere to the British Standard 476, Part 22, 1987 code. This wall system is non-asbestos and eco-friendly. The other main advantage of this system is the low cost, less construction time, less labour, acoustic performance, strength, durability, and re-usability of materials. Durra Panel is a naturally fire-resistant building material. It has a 1-hour fire rating from panel to panel. The fire resistance level [FRL] of 60/60/60 is assigned, and some essential properties of this panel are summarized in Table 2-6. [Experimental investigation for durra panels as partition and ceiling boards (Ref No: CE/GA17/ST/2005/118)-Civil Department -UOM]

Table 2-6: Properties of durra panel

Density(kg/m^3)	370 – 400
Axial Load Capacity (N/mm^2)	-
Flexural Strength (N/mm^2)	2.50
Thermal Resistance (m^2k/w)	0.62 – 0.72
Sound Insulation (dB)	32 – 34
Fire Resistance (hours)	2
Axial Load Capacity (N/mm^2)	-
Thermal conductivity (W/mk)	0.081

ACOTEC precast panel walls are made of concrete containing cement, sand, and aggregate in thicknesses of 75 mm, 100 mm, and 140 mm. The available heights of wall panels are 2700 mm, 3000 mm, and 3300 mm. It has superior quality and faster construction and needs to allocate less labour during construction. According to the manufacturer data, these walls can be erected at 5 m^2 per man day. The main application is to adopt them for commercial buildings, different institutes, and private and public office buildings by replacing traditional materials such as brick and cellular blocks. This system is more popular for the partitioning of residential buildings. Some advantages are summarized in Table 2-7. The comparison of another conventional wall according to the manufacturer is shown in Table 2-8, and the physical properties of Acotech panels are shown in Table 2-9. [Test report of ACOTEC panels (Ref No: CE/GA/17/ST/2014/675)-Civil Department -UOM].

Table 2-7: Advantages of physical properties of Acotec precast wall panels

Higher Productivity	80% saving on labour	In conventional blocks 1m^2 per labour day but here it is 5 m^2 per labour day
Less machinery usage	40% less weight	Eliminate lifting of plaster material to the site
Faster installation and finishing	5 times faster than blockwork	
No need for plaster on both sides	Zero cost of plastering	Only a 3 mm skim coat is enough
Full height constructability	Full height once	Continuous construction up to 3.3 m
Panel with larger dimension (600 mm x 3,000 mm)	Larger coverage capacity	One panel is equivalent to 25 Cellular blocks

Table 2-8: Comparison of physical properties of Acotec panel

Property	**Conventional brick wall**	**Cellular block wall**	**AAC/CLC block wall**	**ICC-ACOTEC wall**
Fire rating (hr)	1-2	1-2	2	1.5-2.5
Sound insulation (Db)	35	38	42	43
Compressive strength (N/mm^2)	2.50	3	5	5-6
Thermal conductivity (W/Mk)	0.13	0.88	0.18	0.56
Thermal resistance (m^{2}k/W)	0.80	-	0.75	0.18
Moisture absorption	30	10	15	8

Table 2-9: Physical properties of Acotec precast wall panels

Property	**Acotec precast wall panels**
Density(kg/m^3)	1,200 – 1,400
Axial Load Capacity (N/mm^2)	5.47
Flexural Strength (N/mm^2)	0.80-1.08
Thermal Resistance (m^{2}k/w)	0.40
Sound Insulation (dB)	41 - 43
Fire Resistance (hours)	2.0

The thermal efficiency of R-18 is achieved by covering a 101.6 mm expanded polystyrene core with 50.8 mm of concrete layer on each side. Higher R-values can be achieved by combining polyurethane insulation with 38.1 mm of concrete on both sides. The panels have a fire rating of two hours, and the properties of this system are shown in Table 2 10 [Tests on 3D insulated micro panels for compressive and flexural strengths (Ref No: CE/GA17/ST/2010/33)-tested by Department of Civil Engineering, UOM, Sri Lanka]3D micro panels are another type of lightweight partitioning walling system, and they can be utilized as flooring materials, load-bearing exterior or interior walls, partitions, curtain walls, roofs, and floor slabs. A welded-wire space frame encloses a polystyrene insulating core to manufacture these welded wire sandwich panels (3D micro panels). A layer of shotcrete is sprayed over the wire mesh. The shear connectors are soldered between these two-wire meshes on each side of the panel, providing strength and rigidity to the element. However, the resulting structure fulfills the composite behaviour with good stiffness and shear strength.

Table 2-10: Properties of 3D micro panels

Density(kg/m^3)	1000
Axial Load Capacity (N/mm^2)	1.57
Flexural Strength (N/mm^2)	1.70
Thermal Resistance (m^{2}k/w)	-
Sound Insulation (dB)	44
Fire Resistance (hours)	2

2.8 Chapter summary

The different natural fibers are available in Sri Lanka as well as in the world. Out of those fibers, the coir fiber has special properties, according to literature. People have been using these fibers in different applications. So, the people are pleased to develop composite material using coir fiber. Composites are developed by blending fiber material with matrix material.

Different polymers are used as matrix materials in the composite development process. This study selected the waste low-density polyethylene as a matrix material. The panel wall was developed using FRP composite which is manufactured by coir fiber blending with waste polyethylene. According to the literature data, the composites were developed by varying the matrix material such as rubber, polypropylene, polybutylene succinate, and epoxy composites.

In the building industry, there are diverse varieties of panel walls available. Most of them are made out of synthetic and bio-degradable materials. Some of the materials are natural. However, the researchers are trying to develop lightweight, low cost and thick panel walls to optimize their mechanical and physical properties and as a solution to the current economic crisis in the world.

3 DEVELOPMENT OF COMPOSITE

3.1 General

Composite is a material made using two or more main materials called matrix and fiber. The fiber-reinforced polymer composite mainly combines fiber (synthetic or natural) and any type of polymer. In this study, the fiber-reinforced polymer composite was made out using waste LDPE as matrix material and coir fiber as reinforcing material. The development process was completed in several steps, as shown in Figure 3-1. This chapter described the process of developing the composite material and concluded optimum mix proportions of composite material. The other significant factors and their effect and limitations also were discussed.

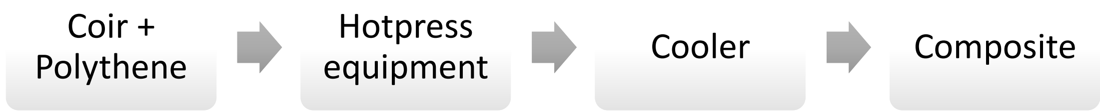

Figure 3-1: Development process of composite

3.2 Raw material characterization

Before starting the composite development process, it is important to know about raw materials' properties and how they affect the composite. Therefore, the physical, mechanical, and chemical properties of coconut fiber and the chemical properties of LDPE were studied.

Under the physical properties, the diameter, density, SEM analysis, and TGA analysis were carried out for coir. The tensile strength of coir fiber was studied under the mechanical properties. Under the chemical properties, the chemical composition of the fiber was studied, and its effect on the mechanical properties of the composite.

The surface area of the fiber material is directly proportional to the fiber's diameter; this surface area is directly affected by the bond characteristics. Hence, it is essential to study the diameter of the fiber before starting the manufacture of the composites [81]. Further, the density of coir is directly affected by the composite material's weight. During the mix design process of composite, the coir to polyethylene ratio by weight is influenced by the density of the coir. The use of high-density coir produces a composite with less amount of coir and on the other hand, the use of low-density coir produces a composite with a high amount of coir. This amount of variation in coir percentage affects the bonding characteristics of polyethylene and coir inside the composite. This bonding strength is directly affected by composite's bending and tensile properties [82]. The SEM analysis helps to study the surface morphology and cross-sections of fiber. These morphological features are directly affect the interfacial bond between fiber and matrix material [83]. TGA helps to study the thermal stability of the material concerning temperature. During the manufacturing of composite, materials are heated up to 140^0 C. If the coir decomposes before that temperature, usage of the coir is useless. This manufacturing of composite is undergone the heating process. Therefore, understanding and studying the decomposition temperature of coir is more important to maintaining the manufacturing temperature [84]. The mechanical properties of composites depend on the tensile properties of fiber material. Hence, studying the tensile properties is significant [85]. The chemical properties of waste polyethylene were observed through the FTIR analysis to identify the selected polyethylene.

3.2.1 Characterization of coir fiber

According to previous literature, coir fiber has considerable properties and can be employed as a reinforcing material in composites made of polymers. As a result, numerous studies using coconut fiber-based polymer matrix composites have been conducted [26],[86]-[88].

Coir fiber is considered one of the versatile and sustainable construction materials in the construction industry due to its easily decomposable and renewable properties. Further, it has very energetic properties such as low thermal conductivity, bulk density, etc. The coir is abundantly available at a low price, and many products can be fabricated [65]. If coir fibers could be used to create construction materials, they would be a good substitute for currently used environmentally hazardous materials [89]. Therefore, coir fiber is selected as the reinforcement material for this research.

Since the coir is one of the mainly used materials when manufacturing the composite, its properties would be affected by the properties of the composite. Hence, it is very important to find out the characteristics of the coir fiber. Further, based on their genetic varieties, age of the coconuts from which the fibers are extracted, time of extraction, method of extraction, zone in which the coconut trees are cultivated, type of soil in the growth area, testing method, and conditions of experiments, fiber characteristics can vary significantly according to the literature [90].

This makes the different properties of the particular composite. Many studies were carried out to study the properties of the coir fiber in many ways. Therefore, coir fiber's physical, chemical, and mechanical properties were investigated through the characterization process.

In Brazil, Mathura and Cree (2011) investigated the ultimate tensile strength, young’s modulus, and elongation of the lignocellulose coir fibers. as 118 - 143 MPa, 1.3 - 2.7 GPa, and 25 - 60% respectively [91]. Another research was performed and obtained by Ho et al. (2012) the ultimate tensile strength, young’s modulus, and elongation of the lignocellulose as 175 MPa, 4 - 6.02 GPa, and 30 % respectively [92]. The diameter range of coir fiber was measured to be 0.272 mm to 0.513 mm and the crystallinity index for lignocellulosic coir fiber calculated using Segal empirical method was recorded to be 47.82% by Lomelí-Ramírez in 2018 [93].

Besides, the characterization of coir fiber in Sri Lankan context is essential before beginning the manufacture of composites because the characterization process of coir fiber has not been performed up to now. Hence, a scientific characterization of coconut fiber in the Sri Lankan context was performed. More literature is available outlining the characterization process of coir fibers, including methods of extraction, different treatment methods, and their properties.

In this research, the physical properties of coir fiber such as diameter, average density, property changes with temperature [TGA], and surface morphology of coir fiber were analysed. The chemical characterization was performed using Fourier Transform Infrared Analysis [FTIR] and X-Ray Diffraction analysis [XRD]. The mechanical property was evaluated using the tensile test.

3.2.1.1 Sample collection and testing procedure

Sri Lanka offers three different coconut fibers: brown (bristle) coir, mix coir, and mattress coir fiber, as shown in Figure 3-2. The brown coir fiber was selected for this research. The mix coir and mattress coir are mostly wasted during coir production. The fiber required for the study was collected from the western province, and used the same fiber throughout the experiment to avoid the effect of external factors on the results.

(a) Brown (bristle) coir *(b) Mix coir* *(c) Mattress coir*

Figure 3-2: Available coconut fibers

3.2.1.2 Physical properties

When determining the physical properties of coir fiber, the average diameter and density, surface and cross-sectional feature of coir fiber, and behaviour of coir with temperature by using thermogravimetric analysis [TGA] were studied.

Diameter measurement

The diameter of the coconut fibers was measured using an optical microscope [CX 410, Olympus, Tokyo, Japan]. The diameters were measured at three equally spaced points because the sectional characteristics and diameter of the coir varied along its length. Next, the average diameter was determined, which might be regarded as the mean diameter of each fiber. The average diameter from fifty numbers of randomly selected coir fibers was undergone in this measurement for more generalized results. The surface area of the fiber material is directly proportional to the diameter of the fiber. This surface area directly affects the bond characteristics. So it is essential to study the diameter of the fiber before starting the manufacture of the composites [94].

Density measurement

The density of coir fiber was measured using the psychometric method [95]. The selected fiber samples were dried for 96 hours in a silica-containing desiccator, and the dried fibers were then divided into segments of 5 mm to 15 mm in length. The fibers were immersed in a toluene solution for two hours before the density measurements to get rid of any microbubbles attached to the fibers. These fibers were divided into 5 sets and one set out of those 5 sets was tested for density and repeated the same procedure for each set at a time. Then the average value was calculated to have more accurate results. The density of the coir fiber " ρ_f " was calculated using Equation 3-1[96].

$$\rho_f = \frac{(m_2 - m_1)}{(m_3 - m_1)(m_4 - m_2)} \rho_t \qquad \textit{Equation 3-1}$$

Where,

m_1 - Mass of the empty pycnometer (g),

m_2 - Mass of the pycnometer filled with segmented coir fibers (g),

m_3 - Mass of the pycnometer filled with toluene (g),

m_4 - Mass of the pycnometer filled with segmented coir fibres and toluene (g),

ρ_t - Density of toluene (g/cm3) which is 0.866 g/cm^3

Scanning electron microscopy analysis [SEM]

SEM was used to examine the surface morphology and cross-sectional characteristics of fibers. The coir samples were first coated with a thin conductive gold layer using a plasma sputtering device to prevent the potential development of electrical charges during the examination. Different magnifications were used to study the fibers' longitudinal and cross-sectional images [89], [91]. The plasma sputtering apparatus and scanning electronic microscope are shown in Figure 3-3 (a) and (b), respectively.

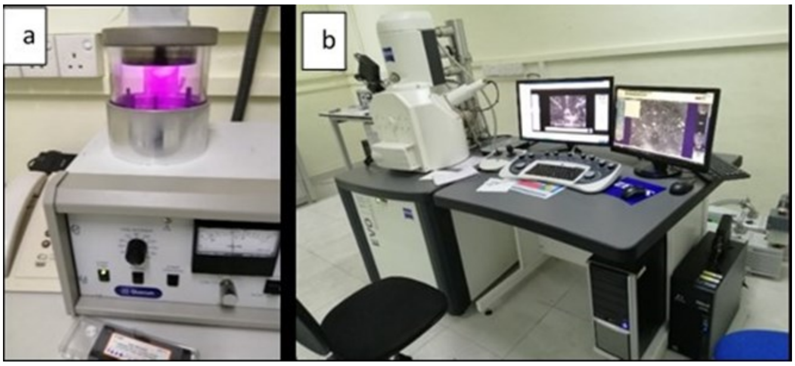

Figure 3-3: Plasma sputtering apparatus and SEM equipment

Thermogravimetric analysis [TGA]

The thermal stability of coir fibers was investigated using a thermo-gravimetric analyzer (TGA- SDT-650). The 5 mg of fiber sample was weighed and placed in an aluminium pan and then heated from 20°C to 850°C at a heating rate of 10°C/min at a flow rate of 100 ml/min under an argon atmosphere. The weight changes of coir fiber in the percentages as a function of increasing temperature with a constant heating rate were recorded [97].

3.2.1.3 Mechanical properties

The tensile strength, young’s modulus, and elongation of coir were investigated to obtain the mechanical property of coir fiber, and tests were performed according to the ASTM D 3822-07 standard.

Tensile strength

The tensile test was carried out using a universal testing machine of “INSTRON tensile tester, Model 4465”. The test was implemented on the ambient temperature with 65% relative humidity and a temperature 20^0C. To ascertain its impact on the tensile characteristics, the gauge length was changed. The test included fiber samples with different gauge lengths of 10 mm, 20 mm, 30 mm, 40 mm, and 50 mm, and the crosshead speed were kept at 6, 12, 18, 24, and 30 mm/min, respectively [93],[98],[99]. Pneumatic grips held the fibers in place during the test at a pressure of 0.4 MPa. The average values of ultimate tensile strength [UTS], young's modulus, and elongation were determined by testing more than 30 samples of each gauge length due to the variability of natural fibers [92],[98]. Natural fiber tensile properties are primarily influenced by test conditions, fiber species, and fiber dimensions [100].

3.2.1.4 Chemical properties

Fourier transform infrared analysis and X-ray diffraction analysis were performed to evaluate the chemical properties of coir fiber. When performing these testing, the procedure described in past literature was used as a reference.

Fourier transform infrared analysis [FTIR]

To ascertain the chemical characteristics of the brown coir, a "Perkin Elmer Spectrum" instrument was used to determine the Fourier transform infrared spectra of the coir fiber using the Attenuated Total Reflectance [ATR] approach [101] using an FTIR spectrometer with 32 scans per minute and a resolution of 4 cm^{-1} spanning the wavenumber range of 4000 to 500 cm^{-1} [98]. The infrared radiation [IR] spectrum was acquired and analyzed. A sample holding arm was used to force a coir fiber sample onto the sample plate. FTIR determines the functional groups in fiber based on the size and shape of the peaks in spectroscopy [102].

X-ray diffraction analysis [XRD]

The X-ray diffraction analysis was performed using the "Ragaku, Ultima IV X-ray Diffractometer" system with Ni-filtered CuKα radiation. The powdered sample was used for X-ray diffraction analysis. The diffracted intensity of CuKα radiation was recorded within the 2θ range, varying from 3º to 70º at 45 kV and 40 mA. The speed of the goniometer was 20 min^{-1}. The Crystallinity Index (CI) was calculated using Segal empirical method, which is given using Equation 3-2.

$$CI = \frac{I_{200} - I_{am}}{I_{200}} \times 100\% \qquad \textit{Equation 3-2}$$

Where I_{200} and I_{am} are the maximum intensity of diffraction of the lattice peak at a 2θ angle between 220 and 230, representing both crystalline and amorphous materials. The amorphous material's diffraction intensity is taken at a 2θ angle between 18^0 and

19^0 where the intensity is at a minimum, respectively. Crystallite Size [CS] was calculated using Scherrer's formula Equation 3-3 [103].

$$CrS = \frac{0.89\lambda}{\beta COS\theta} \qquad \textit{Equation 3-3}$$

Where

Scherrer's constant- 0.89

β - the peak's full width at half-maximum of the peak

λ - the wavelength of the X-ray (0.154 nm)

θ - the Bragg's angle

3.2.2 Characterization of LDPE polyethylene

When considering polyethylene as a raw material for composite development, there may be a possibility to collect the mixture of the LDPE, HDPE, and PP samples from the market. If this happens, it will seriously affect the test results. So, the author needs to confirm whether the selected polyethylene is confidently LDPE or any other material. Hence, carrying out the characterization for the LDPE is very significant. For this, the "FTIR" analysis for LDPE was performed at the University of Moratuwa [UOM]. Finally, this confirms that the selected waste polyethylene comprised the LDPE in this research.

3.2.2.1 Sample collection and testing procedure

Waste polyethylene was collected from a selected factory and washed in potable water with washing powder to remove impurities and unwanted material. After that, the cleaned polyethylene was kept under natural air for a day. One polyethylene sample was placed on the diamond crystal sample plate and pressed with a sample holder arm to analyze the Attenuated Total Reflectance mode [ATR] technics. Using an FTIR spectrometer with 32 scans per minute and a resolution of 4 cm^{-1} spanning the wavenumber range of 4000 to 500 cm^{-1}, the infrared radiation [IR] spectrum was acquired and analyzed [98]. The functional groups contained in polyethylene can be identified with the help of the peak's size and shape [102].

3.2.3 Results and discussion of material characterization

In a material development study, the properties of individual materials are studied to predict the property variation of the outcomes. Hence, the physical, chemical, and mechanical properties of the coir fiber were studied. When we consider the diameter of the fiber, the diameter is directly related to the surface area of the fiber material. This surface area is directly affected by the bond characteristics. So, it is vital to study the diameter of the fiber before starting manufacturing the composites.

Similarly, the density of coir is directly affected by the composite material's weight. So high-density coir needs to add a very less amount for the composite. The low-density coir needs to add more. It will affect the bending and tensile properties of composite material. SEM analysis helps to study the surface morphology and cross-sections of fiber. These morphological features are directly affecting for the interfacial bond between fiber and matrix material. In addition, SEM analysis is used to interpret and identify the fractured surface and the reasons for the fractures of materials. TGA helps to study the thermal stability of material concerning temperature. During the development of composite, materials are heated up to 140^{0}C. If the coir decomposes before that temperature, usage of the coir is useless. So, studying the decomposition temperature. The flexural properties of face sheets are significant in wall panel developments. If the reinforcement material has better tensile strength, it will cause to increase in the flexural properties of composite material [104].

This description reveals whether the reinforcement material is appropriate for a specific composite application. Hemicellulose and cellulose that have been chemically bound together make up a sizable portion of coir. Coir consists of a large amount of hemicellulose and cellulose, which are bonded together. As a result, during the development of composites, the perfect bonding between fiber and matrix material could be noticed [101].

3.2.3.1 Diameter of coconut fiber

Figure 3-4 displays the diameter of the coir fiber as measured using an optical microscope. The results obtained for the five coir samples across three successive distances are shown in Table 3-1. The determined average diameter was 0.30 mm.

Table 3-1: Measured diameter of the coir

Sample No.	Diameter / mm			
	Point-1	**Point-2**	**Point-3**	**Average**
1	0.26	0.31	0.33	0.30
2	0.36	0.33	0.3	0.33
3	0.31	0.28	0.28	0.29
4	0.34	0.31	0.30	0.32
5	0.28	0.28	0.29	0.28
	Average Diameter			**0.30**

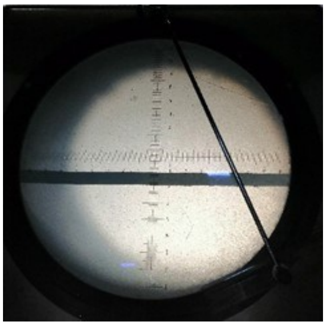

Figure 3-4: Image of coir fiber through the microscope

3.2.3.2 Density of coconut fiber

The average density of the coir fiber was obtained at 1.018 g/cm^3. However, when compared with the densities of another natural fiber, higher values of densities can be seen than the coir fiber [105]. Those fibers also could be used to satisfy the reinforcement requirement of the development of composites. However, the final product should be lightweight. Since the fiber density is less compared to others, it will cause us to develop the lightweight panel by fulfilling our final objective [93].

Density values would vary depending on the plant's growth rate and the environment [102]. Additionally, the method used to harvest the fiber, the fiber's available moisture content, and the state of the soil in which the plant is grown have all contributed to variations in densities [106]. E-glass and carbon fiber are commonly used synthetic fibers, with densities of 2.56 g/cm^3 and 1.4–1.8 g/cm^3, respectively [107]. Some of the densities of synthetic and natural fibers are displayed in Table 3-2 [105].

Table 3-2: Density of fibers

Fiber	**Density (g/cm^{3})**
Natural Fiber	
Coir	1.02
Jute	1.30
Flax	1.50
Hemp	1.47
Kenaf	1.30
Sisal	1.50
Banana	1.35
Synthetic Fiber	
E-glass	2.56
Carbon fiber	1.4–1.8

3.2.3.3 Scanning electron microscopy analysis

The fiber surface inconsistencies may cause during the extracting process because of the fiber age, ecological effects, and variation of soil. Therefore, the manufacturer should be keen on when the preparation of samples [108]. The SEM offers magnified, high-resolution images of the fiber focusing the electron beam on the cross-section and longitudinal surface of the fiber [109].

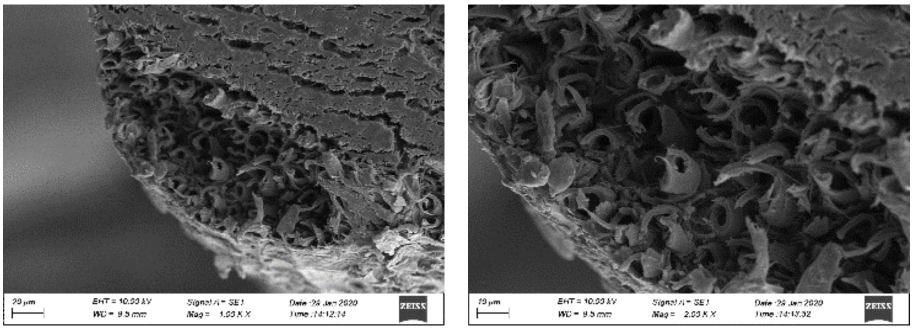

Magnification 1000 times *Magnification 2000 times*

Figure 3-5: Cross-sectional micrographs of coir fiber

Figure 3-5 shows the sectional micrographs of scanning electron microscopic brown coir fiber in different magnifications. The microfibrils are of different sizes and consist of thick walls [93]. The surface roughness of coir fiber may help to bond fiber with matrix material, and it influences mechanical interlocking between fiber and matrix material [108]. Further, understanding the behavior of acoustic and thermal properties, and studying the surface morphology of the coir fiber is very significant [98].

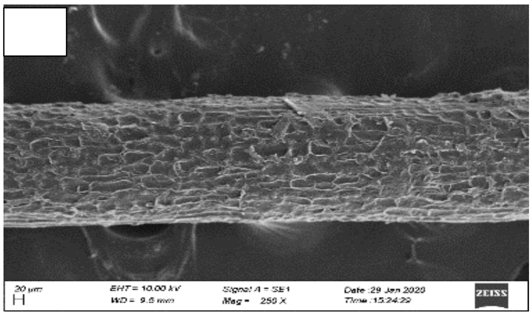

Magnification 250

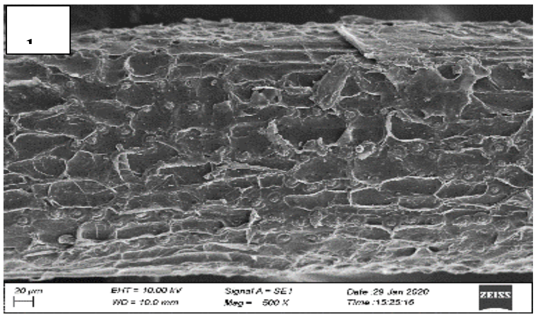

Magnification 500

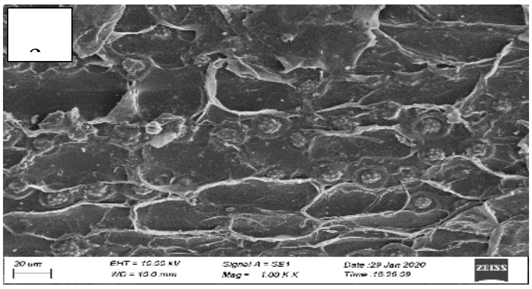

Magnification 1000

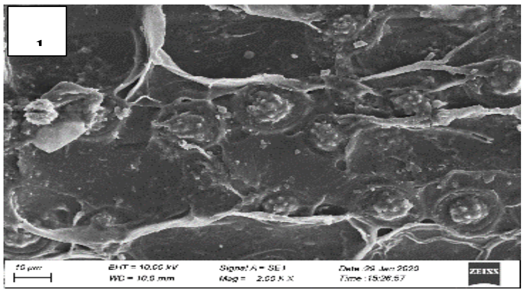

Magnification 2000

Figure 3-6: Longitudinal SEM micrographs of brown coir

The longitudinal micrographs of brown coir fiber are shown with different magnifications in Figure 3-6. When studying the fiber surface firmly, the porous medial of the coir can be observed on the fiber's surface in Figure 3-6 a, b, c. The white bands indicate the hemicellulose content on the fiber surface in Figure 3-6 (d).

Smooth fiber surfaces would prevent the adhering properly of matrix and fiber. The fiber must then have its surface modified to get appropriate mechanical properties for creating composites [102]. Fiber surface characterization, such as surface roughness, pore size, and material chemical composition, is essential for evaluating the mechanical properties of composites [104].

3.2.3.4 Thermogravimetric analysis

Thermogravimetric analysis is conducted to investigate the thermal stability of natural fibers and the composites made from them. As the temperature rises while being heated continuously, the physical and chemical properties can be evaluated [109]. The second-order phase transitions, vaporization, sublimation, absorption, adsorption, and desorption are only a few examples of the physical properties that can be evaluated using TGA. Additionally, chemical characteristics can be identified, including de-solvation, chemisorption, solid-gas interactions, and breakdown [102]. Additionally, as the temperature rises, hemicellulose, cellulose, lignin, wax, and other components contribute to the thermal degradation of natural fiber [102].

The Thermogravimetric analysis is carried out to study the thermal stability of natural fibers and their composites. The physical and chemical properties can be determined as a function of increasing temperature while maintaining a steady heating rate TGA is used to assess information regarding specific physical properties, such as absorption, adsorption, desorption, second-order phase transitions, vaporization, and sublimation. It is also possible to determine chemical properties such as de-solvation, chemisorption, solid-gas reactions, and decomposition. Further, the thermal degradation of natural fiber occurs from hemicellulose, cellulose, lignin, wax, and other components with an increment in temperature. The TGA and DTG curves of the powdered brown coir fiber sample are shown in Figure 3-7.

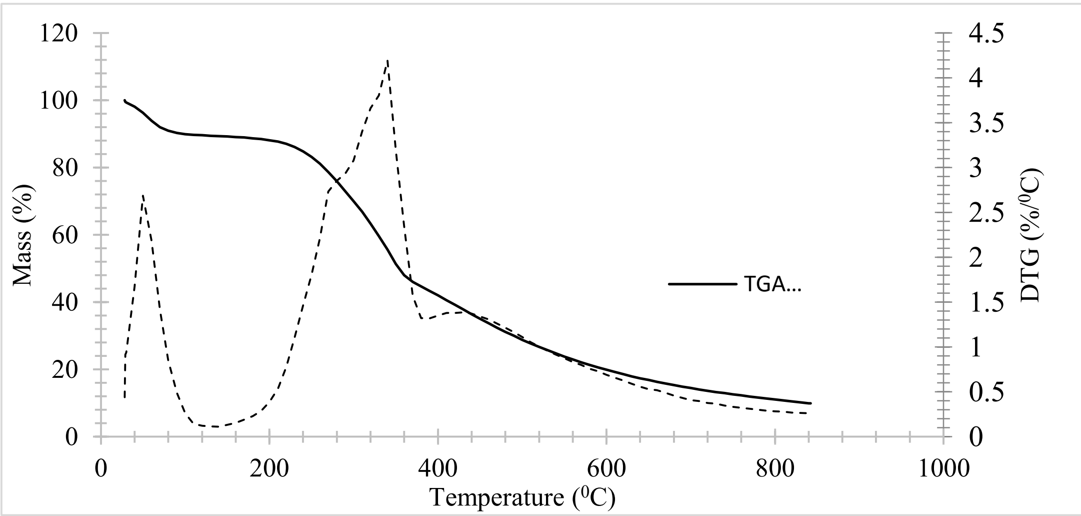

Figure 3-7: Thermogram of brown coir fiber

It has been noted that a slight weight loss happens up to 125^{0}C due to the sample's volatile organic component and moisture evaporating. Until 220^{0}C, there isn't much weight loss, which shows that the fiber retains strong thermal stability as the temperature rises [108]. Only coir fiber showed the second degradation peak, which occurred between 280^{0}C and 340^{0}C and is related to hemicellulose and pectin degradation. Thermal degradation of cellulose is represented by the third 340^{0}C–380^{0}C peak. Lignin was visible as a thin peak spanning the temperature range of 220^{0}C to 680^{0}C [110].

3.2.3.5 Fourier transform infrared analysis in coir fiber

One method for characterizing the chemical composition of natural fibers is this one. Identification of the molecules and functional groups present in natural fibers is important. Fourier Transform Infrared spectra were seen between 500 and 4000 cm^{-1}, demonstrating that the availability of the hydroxyl (-OH) group in the cellulose group in fiber material led to the most significant absorption peak being measured at 3338 cm^{-1} [111],[112]. The peaks at 2845 cm^{-1} bring attention to the wax substance that is spread throughout the coir fiber (C≡C stretching). The hemicellulose content of coir fiber was indicated by the peak appearing at 1600 cm^{-1} due to the stretching of the C=O group [105],[96]. The C=H group's lignin content category correlates with the region between 1252 and 1439 cm^{-1} [113]. The availability of the following components in the chosen brown coir fiber may then be determined after researching the chemical composition of cellulose, hemicellulose, and lignin.

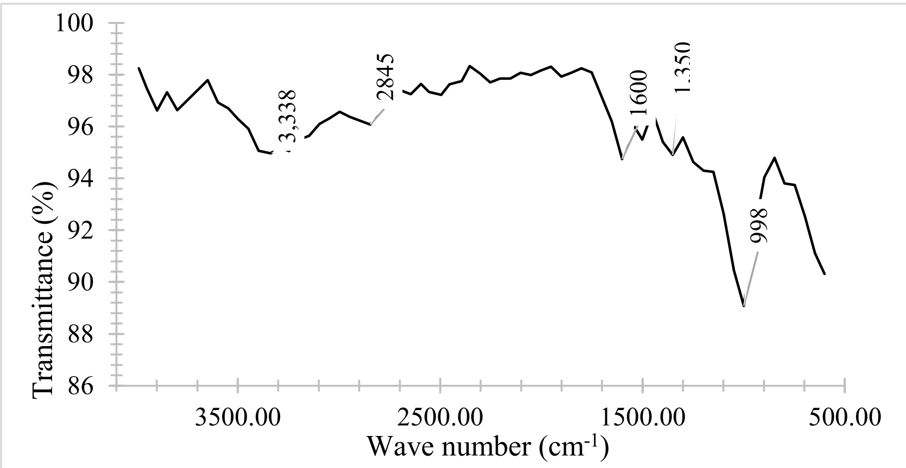

Figure 3-8: FTIR spectra for the coir fiber

3.2.3.6 X-ray diffraction analysis

X-ray diffraction examination was used to assess the natural fibers' crystallinity index. The primary crystalline peak, which corresponds to the crystallographic plane of cellulose-I, was shown to arise at 22.48° C. The fiber contains more amorphous components such as hemicelluloses, amorphous cellulose, lignin, and pectin, as seen by the lower-intensity peak at 17.48° [114]. According to Figure 3-9, I_{200} and I_{am} heights of the peaks at 904.2 cps and 658.63 cps, respectively. The calculated crystallinity index using Equation 6-2 was 37.28 %, for the coir, which is less than other natural fibers reported are Wrightia tinctoria seed fiber (49.2%), ramie fiber (58%), Sansevieria cylindrica leaf fibers (60%), Raffia textiles (64%), sisal (71%), jute (71%), flax (80%), hemp(88%), Date palm (38.5%) [99], [115]. However, the crystallite size of the coir was determined as 0.4331°nm using Scherrer's formula in Equation 3-3. The crystallite size for some natural fibers is R.textilis (32 nm), ramie fibers (16 nm), cotton fibers (5.5 nm), cornstalk fibers (3.8 nm), and flax fibers (2.8 nm) [99].

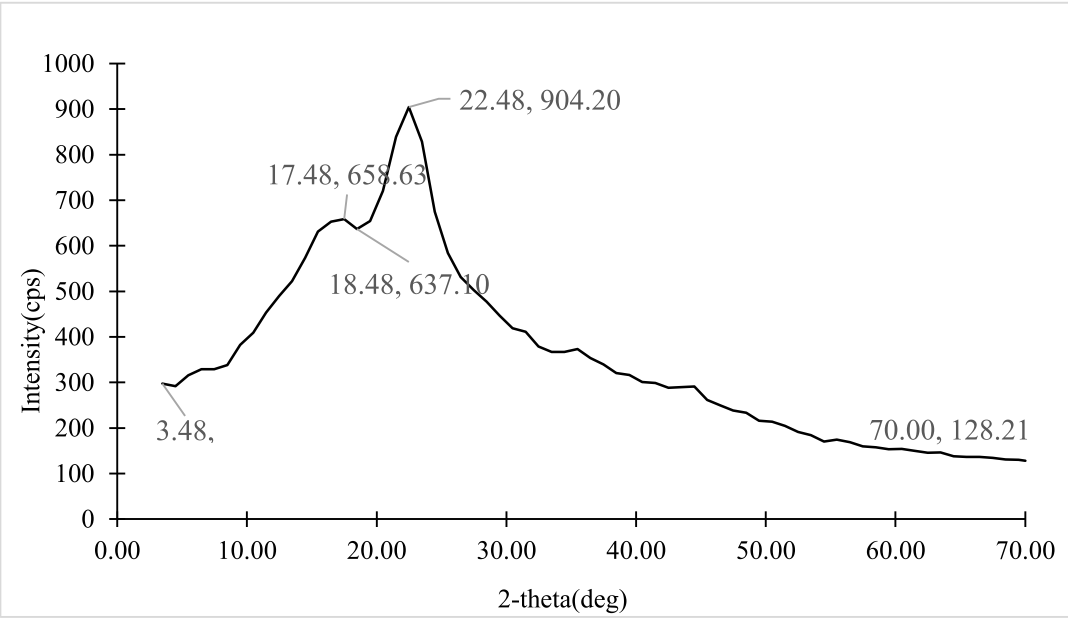

Figure 3-9: XRD spectrum of brown coir fiber

3.2.3.7 Tensile strength of coir

According to the results obtained from more than 30 coir fiber samples, it can be seen that the tensile strength varies when increasing the gauge length of the coir due to variations of diameter along with the fiber. Therefore, the change in tensile strength will indirectly impact this diameter [107]. But in the current investigation, the coir fiber's ultimate tensile strength, young's modulus, and elongation were between 94-159MPa, 1.2 - 1.8 GPa, and 21%- 67% percent, respectively. Table 3-3 [116]–[118] shows the published values of natural fibers' aforementioned mechanical properties. However, comparing the ultimate tensile strength of coir with other natural fibers shows lesser values.

Table 3-3: Tensile properties of coir fiber and other natural fibers

Fiber	**Tensile Strength (MPa)**	**Young's Modulus (GPa)**
Jute	400-773	10-30
Flax	500-1500	27.6
Cotton	200-400	5.5-12.6
Ramie	400-938	61.4-128
Hemp	690	70
Pineapple	362-748	20-80
Kenaf	930	53
Sisal	511-635	9.4-22
Abaca	756	31.1
Henequen	500	13.2
Banana	700-800	27-32

3.2.3.8 Fourier transform Infrared analysis for waste polyethylene

All polyethylene types show characteristic doublets due to CH_2 asymmetric stretching at 2915 cm^{-1} and 2848 cm^{-1} [116]. The wavenumbers 1471 cm^{-1} and 1463 cm^{-1} represent CH_2 bending deformation doublet [117]. The other doublet, around 729 cm^{-1} and 719 $cm^{-1,}$ represents the rocking deformation of CH_2 [118]. These signals are strictly related to the chemical structure of polyethylene. The low-density polyethylene [LDPE] shows the Carbon [C] and Hydrogen [H] atoms, which comprising of repeating methylene groups [CH_2].

However, the three weaker bands at 1377 cm^{-1}, 1366 $cm^{-1,}$ and 1351 cm^{-1} assist to govern the relevant type of polyethylene out of the HDPE, LDPE, and LLDPE [117]. If the peak at 1366 cm^{-1} is most relevant to LDPE [117]. The different types of functional groups were identified after investigating the wavenumber and spectrum band. The FTIR spectrum shows nearly the same size peaks in 1377 cm^{-1} and 1366cm^{-1} wavenumbers. This confirms the waste polyethylene collected for this research consists of an LDPE. Figure 3-10 shows the FTIR spectrum for waste polyethylene.

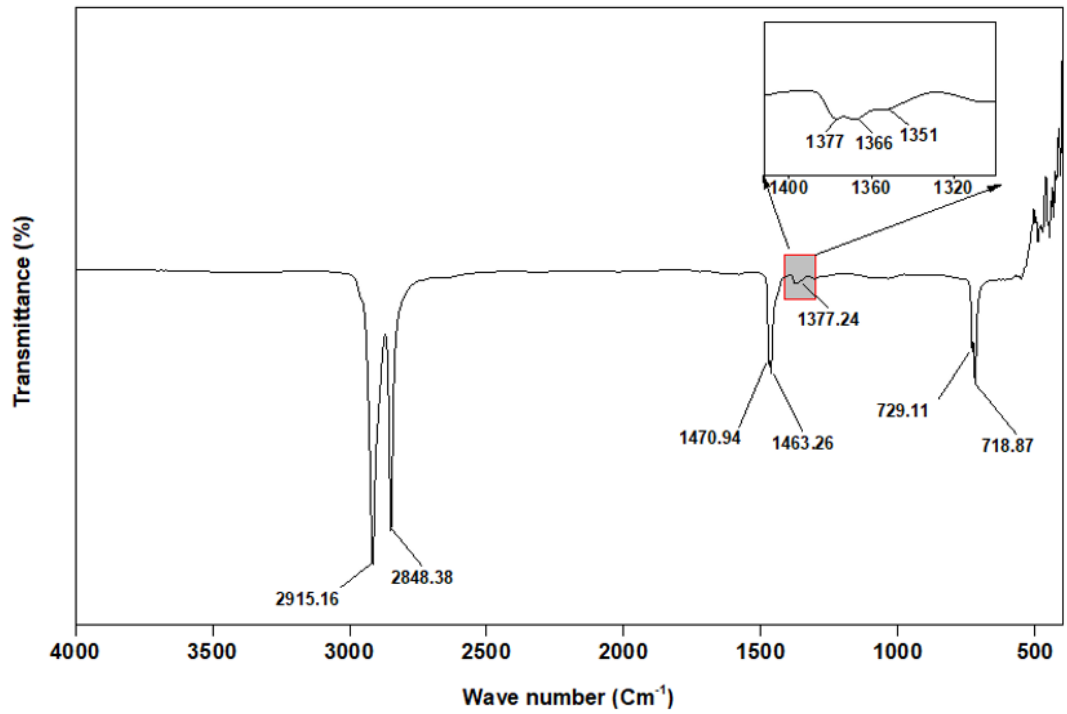

Figure 3-10: FTIR spectrum of waste polyethylene

3.2.4 Summary of material characterization

Randomly selected coir samples from the purchased coir heap for the research were undergone for the characterization process. The mechanical, chemical, and physical characteristics of coir fibers were identified. Coir fiber had an average diameter and density of 0.31 mm and 1.018 g/cm^3, respectively. The surface characterization of properties such as roughness, pore size, interfacial bonding between the fiber and matrix, and available impurities was achieved using SEM analysis. The FTIR detected the chemical analysis of the coir fibers, and it was possible to identify the molecules and functional groups present in Sri Lankan coir fibers, confirming the presence of cellulose, hemicellulose, lignin, and wax content, among other components. The crystallinity index and crystallite size of coir fiber were computed using the X-ray diffraction analysis, and the results were calculated as 37.28 percent and 0.4331 nm, respectively. These values were lower than reported for other natural fibers [119]. During the tensile test, the coir fiber's ultimate tensile strength, young's modulus, and elongation varied from 94 - 159 MPa, 1.2 - 1.8 GPa, and 21% - 67%, respectively. The thermogravimetric study showed Sri Lankan coir fibers to be thermally stable below 220^0C.

The purchased waste polyethylene was characterized by FTIR and was identified as having LDPE. Low-density polyethylene typically shows the carbon and hydrogen atoms comprising repeating methylene groups [CH_2]. The obtained FTIR spectrum shows nearly the same size wave numbers [1377 cm^{-1} and 1366 cm^{-1}] related to the chemical structure of polyethylene.

3.3 Mix design for composite material

The theoretical overview of mix design, the material collection, the cleaning process of coir and polyethylene, and the preparation of composite to determine the most suitable coir to polyethylene ratio are presented in this section.

3.3.1 Theoretical overview

Before starting the composite development process, the knowledge of material properties, bond characteristics of fiber and matrix material, and physical properties like temperature, pressure, and time taken to composite preparation are very significant. And also, awareness of the mechanical properties of composite and their behavior causes the development of a suitable material very effectively.

However, the mechanical properties of a fiber-reinforced polymer composite depend on the properties of fiber, applied load transmitted to fiber, and fiber-matrix bond characteristics. Literature further states that three parameters directly affect the critical fiber length of composites. They are the diameter of the fiber, the ultimate tensile strength of the fiber, and fiber-matrix bond strength.

$$\sigma_f = \sqrt{\frac{2E\gamma_0}{\pi a}} \qquad \textit{Equation 3-4}$$

The formula shown in Equation 3-4 highlighted the inverse relationship between the strength of fiber with fiber diameter. It reveals that the fiber diameter is lesser and lesser, and the strength of the fiber will be higher.

3.3.2 Conditioning of the raw materials for composite preparation

Coconut fiber and waste polyethylene were used as the primary raw materials. Coir fiber was purchased from a local agent in Colombo, and the waste polyethylene used for this study was donated by Rapid Creations (Pvt) in Colombo, Sri Lanka. Both raw materials were collected and stored at once to minimize the variation of raw material properties from batch to batch. The raw material used to manufacture the composite are shown in Figure 3-11.

Purchased coir fiber *LDPE sample* *Shredded LDPE*

Figure 3-11: Raw material used to manufacture the composite

3.3.2.1 Preparation of coir fiber

The cleaning process of coir fiber was performed to remove the undesirable foreign matter and pith on the surface of the fiber. The cleaned fiber was washed in running potable water for around 30 minutes for further cleaning. Then, exposed to a natural drying process at room temperature and placed in an oven under a 50^0C temperature for around 10-12 minutes to remove the residual moisture in the fiber surface. The cleaned coir fiber was used throughout the research to produce composite material.

3.3.2.2 Preparation of polyethylene

The collected waste LDPE was washed in potable water with washing powder to remove impurities and unwanted material and then dried at room temperature. The cleaned polyethylene was shredded into tiny particles around the 1- 4 cm range because it is essential to use small particles to achieve a uniform mixture during the hand layup process.

3.3.3 Investigation of the most suitable polyethylene to fiber ratio

Among several identified variables, mixed proportions are mandatory to optimize the mechanical properties of the composite. Hence series of experiments were carried out to select the optimum mix proportions of coir to polyethylene by weight. In this stage, the other variables, such as applied temperature 140^{0}C, and pressure 4 MPa, was kept constant.

3.3.3.1 Preparation of composite

The composite was prepared in two steps, and the schematic diagrams of the sample preparation procedure are illustrated in .

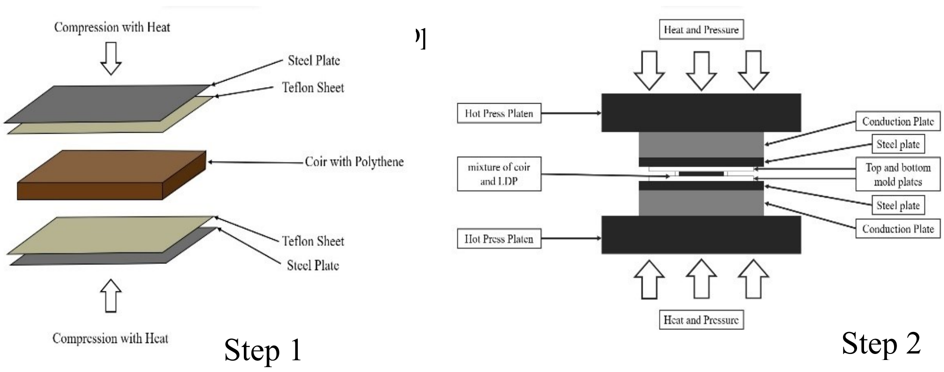

Figure 3-12: Schematic diagram for preparation of composites

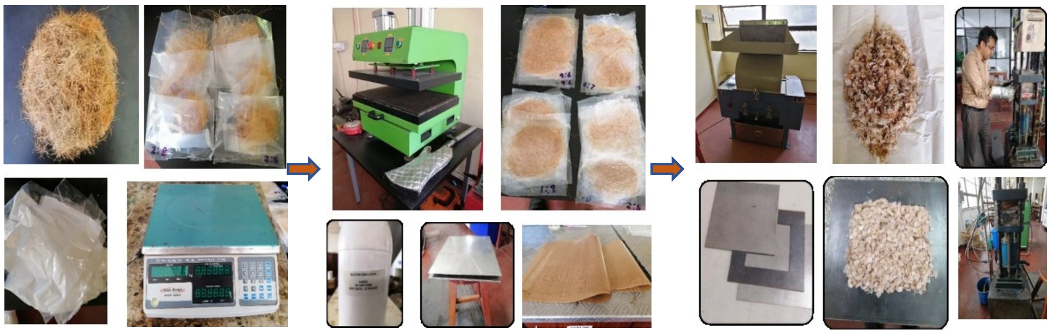

Figure 3-13: Composite development process

In the first step, the cleaned fiber and shredded polyethylene were mixed to have a uniform mixture. The hand layup method was adopted to lay the mixture uniformly between two Teflon sheets and place it in the laminated machine to make the laminate sheets. The Teflon sheets help to prevent the adhesion of composite material with the surface of the laminated machine.

Feeding the material to the laminated machine was performed manually and operated according to the given safety precautions. After that, the laminated sheets were shredded into small pieces, and these shredded pieces were used to prepare the composite material. In the process of preparation of composite material, the shredded mixture was laid in a steel mold and placed on the hot press machine to prepare the composite samples by employing the compression molding technique. The machine and equipment used for the composite manufacturing process are shown in Figure 3-14. Figure 3-15 shows the weighted raw material samples and initial steps of prepared samples. Figure 3-16 shows the composite sample prepared inside the steel Mould. These two steps were repeatedly followed for a series of experiments to prepare the composites to finalize the optimum coir to polyethylene mix proportion and study the conditions of composite preparation.

When selecting the mix proportions, it could be identified that a few variables affected the properties of a composite. These main variables are the fiber-to-polyethylene ratio and fiber length. The specified testing conditions are the temperature and pressure applied by hot-press equipment. The following section describes the experimental procedure.

Laminated machine *Hot-press Equipment* *Shredded machine*

Figure 3-14 Equipments for manufacturing composites

Weighted coir *Weighted polyethylene* *Laminated samples* *Shredded samples*

Figure 3-15: Weighted raw material samples and sample preparation steps

Steel Mold *Shredded sample filled to mold* *prepared composite*

Figure 3-16: Preparation of composite

3.3.3.2 Preparation of samples for mechanical testing

The test samples were prepared according to ASTM standards, as shown in Table 3-4: ASTM Standards for mechanical test.

The 2.5 mm samples were used to study the tensile properties, and the 3.2 mm thick samples were used to find flexural properties. These sheets were cut to the required length using a hand saw, as shown in Figure 3-17. Tensile testing was carried out according to ASTM 3039, and the flexural test was carried out on ASTM 790.

Sample preparation *Tensile test sample* *Flexural test sample*

Figure 3-17: Sample preparation for testing

Table 3-4: ASTM Standards for mechanical test

Property	Standard	Sample size (mm)
Tensile properties of polymer matrix composite material	ASTM D 3039	250 x 25 x 2.5
Flexural properties of reinforced plastic material	ASTM D 790-03	150 x 12.7 x 3.2

3.3.3.3 Experimental procedure for testing mechanical properties

The tensile, bending, and impact tests were carried out to examine the mechanical properties of composites. The ASTM standards were followed during the testing. In addition, the SEM analysis was also carried out on the fractured surface to evaluate the interfacial bond between the fiber and the polymer matrix. According to the literature, the interfacial adhesion between fiber and the polymer matrix influences the properties of fiber-reinforced composites [120].

Six samples from each mix proportion were prepared for the tensile test, and nine samples were ready for the bending test. Tensile and flexural tests were carried out using the "INSTRON 5500R" universal testing machine. The morphology of the fractured surface of tensile test samples was studied using SEM "CARL ZEISS EVO 18 RESEARCH" equipment.

The dimensions of the samples, different sample sizes and the test standards are shown in Table 3-5. The samples before and after bending and tensile testing are shown in Figure 3-18.

Table 3-5: Mechanical test parameters

Experiment	**Sample size (mm)**	**Total numbers of samples N = i x j**	**Standard**
Tensile test	250 x 25 x 2.5	i=6, j=5, (N= 30)	ASTM D 3039
Flexural Test	150 x 12.5 x 3.2	i=9, j=5, (N= 45)	ASTM D 790

i- Numbers of samples used for one set

j- Varying in coir weight percentage (from 10 % to 50 % at 10% increment)

	Tensile test	Bending test
Test Equipment		
Samples before test		
Samples after test		

Figure 3-18: Test samples before and after testing

3.3.3.4 Results and Discussion

The main aim of these mechanical tests was to investigate the optimum range of mix proportion of polyethylene to coir. For this, both tests were conducted by selecting the possible practical range. Both tests were conducted from 9:1, 8:2, 7:3, 6:4, and 5:5 polyethylene to coir mix proportions.

Tensile test

The test results obtained in the tensile strength test were used to calculate the maximum tensile strength at breaking point, elongation at break, and tensile modulus with different fiber weight fractions, and those were tabulated in Table 3-6. The variation of tensile strength of composite material versus different coir weight fractions is graphically represented in Figure 3-19.

This indicates that tensile strength increases with the increment of coir weight %, decreasing with the further increment of coir weight fractions. The maximum tensile strength could be observed when the coir weight fraction is between 10% - 40% of the total weight, and it was 6.75 N/mm^2. So, this coir weight % range was selected as the practically possible range for future work.

According to the results, it can be seen that the tensile strength decreases with increasing fiber content. This is related to the poor interfacial adhesion bond between coconut fibers and the polymer matrix [121].

Table 3-6: Variation of tensile strengths

Sample No	**Coir weight fraction from total Wt. (%)**	**Tensile strength at breaking point (N/mm^2)**	**Elongation at breaking point (mm)**	**Tensile modulus (kN/mm^2)**
1	10	5.00	27.20	18.38
2	20	6.64	48.40	13.72
3	30	6.46	10.70	60.33
4	40	5.12	6.10	84.01
5	50	3.50	6.10	57.38

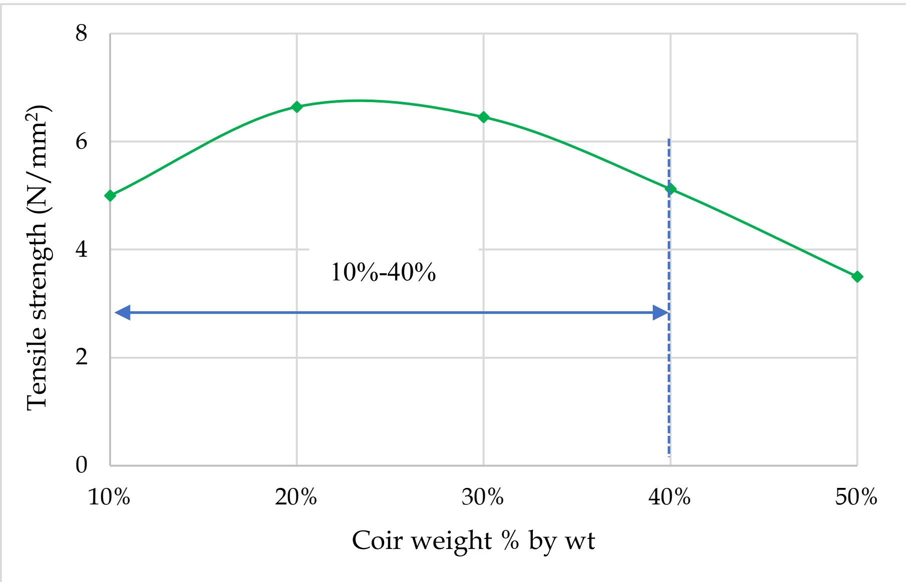

Figure 3-19: Variation of tensile strength with coir weight fractions

Flexural strength test

The flexural strength increases with the increase of coir fraction up to 10% - 25%, and then it decreases due to further increment of coir weight fractions. The maximum flexural strength of 29.85 N/mm^2 occurs when the coir weight fraction is 25%. This is supported by Rao and Rao (2007), and according to their observations, the flexural properties of coir fiber-reinforced composites are dependent on the volume fraction of fibers within the composite [106]. This relationship is essential to determine an optimal fiber content corresponding to the maximum flexural strength. The results obtained in the flexural strength test are illustrated in Table 3-7.

Table 3-7: Variation of flexural properties

No.	Coir weight fraction from total wt. (%)	Load (N)	Flexural strength (N/mm^2)
1	10%	40.625	25.864
2	20%	45.250	29.525
3	30%	43.625	29.026
4	40%	33.500	24.000
5	50%	27.167	19.030

The variations of flexural strength versus coir weight fraction are graphically presented in Figure 3-20. Therefore, it can be concluded that both tensile and flexural strength increases with the coir weight fraction, and then optimum results are observed when the coir weight fraction is between 10% - 40% by total weight.

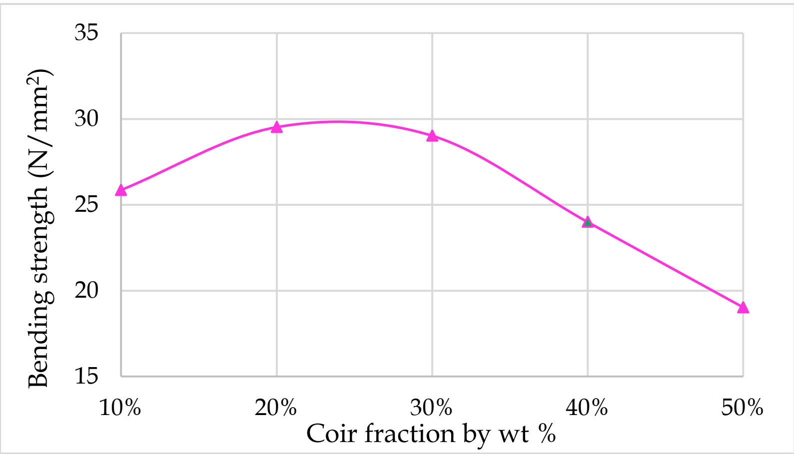

Figure 3-20: Variation of bending strength with coir fraction

SEM analysis on the fractured surface

The morphology of the fractured surface of tensile test samples was studied using SEM "CARL ZEISS EVO 18 RESEARCH" equipment. The sample was mounted on stubs with silver paste in the testing procedure. Then, a thin film of the platinum layer was vacuum-evaporated to enhance the conductivity of the samples.

Figure 3-21 exhibits the surface morphology of coir fiber through Scanning Electronic Microscopy. It shows the irregularity of the coir surface, including impurities and the presence of a cerumen layer covering the fiber.

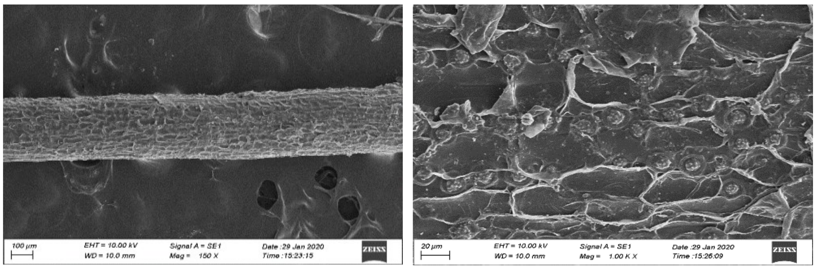

150 magnifications *1000 magnification*

Figure 3-21: Longitudinal SEM micrographs of brown coir fiber

The SEM images in Figure 3-22 depict the fractured surface of composite material undergone to the maximum tensile strength out of a series of test samples which consists of a coir weight fraction of 30%. Figure 3-22 (a) depicts that the fibers detached from the matrix/polyethylene material, and Figure 3-22 (b) show the fiber pull-out state due to applied stress. The SEM results indicate that the adhesion between fiber and matrix material was lost, and the failure process was dominated due to poor interfacial bonding between fiber and matrix material.

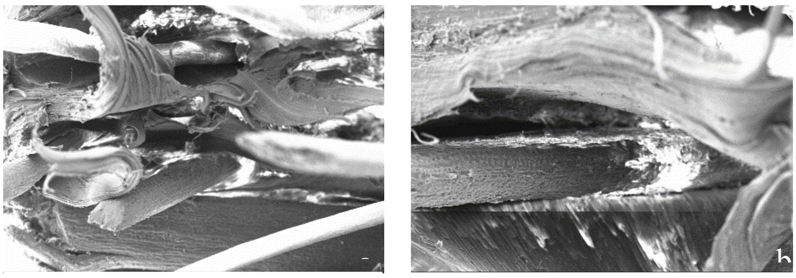

Figure 3-22: SEM micrographs of the fracture surface of composites

The surface morphology of the pull-out fibers in Figure 3-20 (b) shows a similar appearance to the morphology of the coir fiber given in Figure 3-20 (a). It also implies that the bonding between polyethylene and coir fiber is poor.

The literature said that the interfacial adhesion between the fiber and the polymer matrix is directly influenced by surface features of the fiber, such as surface roughness, pore size, chemical content, and homogenization of the dispersion with the polymer matrix. These factors play a significant role in the composite's mechanical performance and interlocking behavior [122],[104].

A similar study by Singh et al. (2013) highlighted that gaps between fiber surface and matrix material were visible. This gap arises due to insufficient physical bonding between the coir fiber and polymer matrix. Similarly, the presence of lignin and other waxy components on the coir fiber prevents the coir fiber from adhering to the polymer matrix, resulting in poor fiber-matrix bonding [123].

According to the observed results of tensile and flexural tests, it was selected that the optimum coir fiber to polyethylene ratio is 15-35% of coir by total weight. Therefore, the next step was to evaluate the applied temperature effect on the properties of composite and select the most suitable temperature to optimize the mechanical properties for the composite manufacturing process. The following section presents the testing procedure and the results obtained.

3.3.4 Summary and discussion

Selection of practical possible coir to polyethylene ratio in which the mechanical properties of the composite may be optimized was performed as the initial step of the research. For that, the tensile and flexural strength of the composite was selected as testing parameters. The composites were prepared by changing the coir to polyethylene ratio (1:9, 2:8, 3:7, 4:6, 5:5), and a series of testing were performed according to ASTM standards to determine the tensile and flexural strength of all the manufactured composite samples. During the composite manufacturing process, it was observed that the best possible coir to polyethylene weight ratio is between 10% and 40 %. Further, according to the results of the testing series, it was observed that the best mechanical parameters also were observed within this range. Therefore, this weight range was used for future investigation.

3.4 Investigation of production criteria

In the composite production process, it was identified that several parameters were to be considered, which will have affected the properties of the composite. The specified criteria were the applied temperature and the pressure on the hot press machine during the composite manufacturing process. Therefore, the most suitable temperature and the pressure which gives the optimum properties of the composite were analyzed.

3.4.1 Investigation of optimum temperature

The behaviour of mechanical properties with varying the applied temperature was studied. This test series forces us to investigate the optimum temperature required for the production process with more energy efficiency during the composite preparation. Initially, a series of samples were prepared with varying temperatures for the coir to polyethylene weight ratio and underwent the tensile test. This study was continued using tensile test variation. In this situation, the pressure and time were kept constant. When observing the outcomes, the tensile strength with temperature would be optimum at 140^0C. This temperature was recommended for future material development works. When the temperature increases, the tensile strength variation will be constant from 140^0C temperature. So, it is evident that we cannot achieve higher tensile strength by increasing the manufacturing temperature. So, it is recommended to manage 140^0C temperature as the optimum temperature. Tensile strength variation with temperature is shown in Figure 3-23.

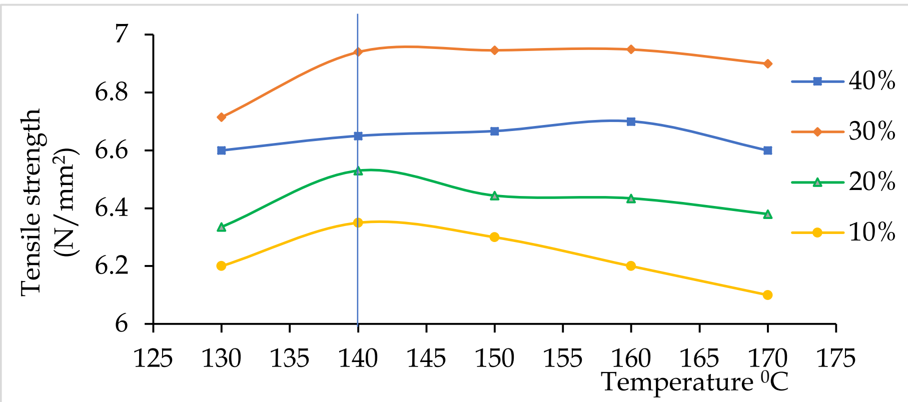

Figure 3-23: Tensile strength variation with varying temperature

3.4.2 Investigation of the optimum pressure

The behaviour of mechanical properties with varying applied pressure was studied. The series of tests focused on investigating the optimum pressure required for the production process with more energy efficiency during the composite preparation. Initially, a series of samples were prepared with varying pressure for coir to polyethylene weight ratio, and it underwent the tensile test. Here, the optimization was carried out based on the tensile test. In this situation, the temperature and time were kept constant. When observing the outcomes, the tensile strength with pressure would be optimum at the molding pressure is 4 MPa. This pressure was recommended for future material development works. When increasing the pressure, the variation of tensile strength will be at a peak value, and then it starts to decrease. The investigated maximum pressure is 4 MPa. So, it is evident that we cannot achieve higher tensile strengths by increasing the manufacturing pressure unnecessarily. So, it is recommended to manage 4 MPa molding pressure as optimum. Tensile strength variation with pressure is shown in Figure 3-24.

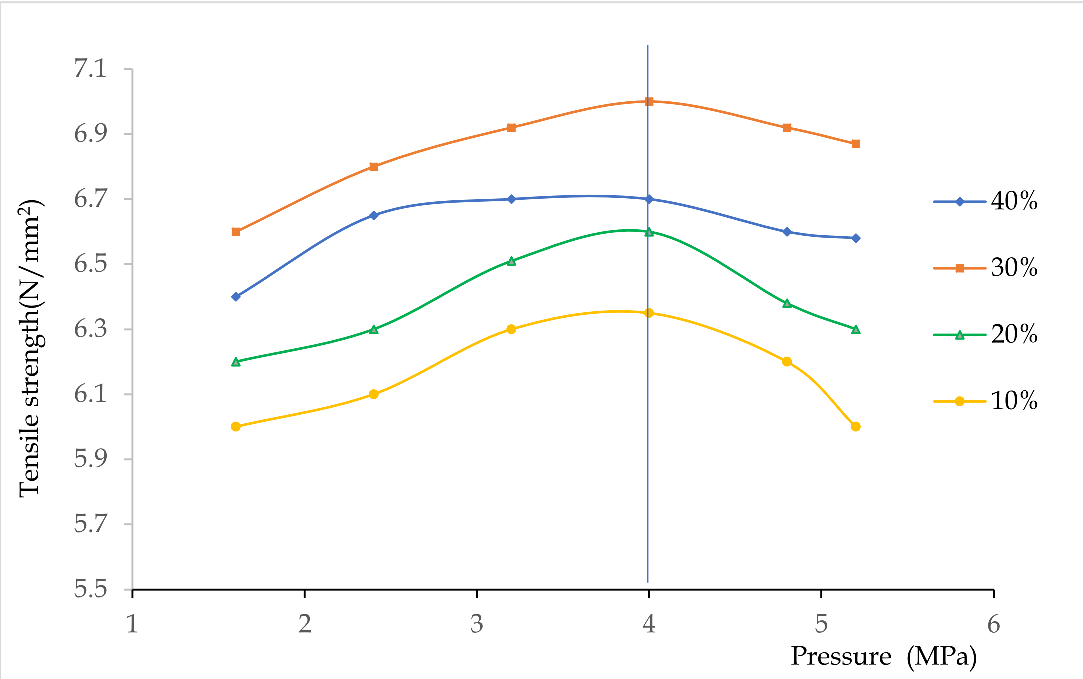

Figure 3-24: Tensile strength variation with varying pressure

3.4.3 Summary and discussion

Different manufacturing conditions were identified during the composite preparation process described in the above sections. It could be directly affected by the mechanical properties of composites. Out of them, temperature and pressure were identified as the major variables. Therefore, it was significant to locate the molding temperature and pressure, which gives the maximum mechanical properties. Hence, a series of the composite were prepared (1:9, 2:8, 3:7, 4:6) according to ASTM standards and tested by changing the applied temperature and pressure. And then performed the tensile test series. Under this test series, it was identified that the 140^0C temperature and 4MPa pressure are the optimum molding temperature and pressure to manufacture the composites.

3.5 Selection of optimum fiber length

The effect of tensile strength of the composite with varying fiber length was investigated by Kuburi et al., and they observed that the maximum tensile strength of 7.1 N/mm^2 resulted when the fiber length was 30 mm [124]. The mechanical properties of a fiber-reinforced polymer composite depend on the properties of the fiber as well as the degree to which an applied load is transferred to the fibers via the matrix phase, according to the literature [125], [126], [127]. The strength of the interfacial bond between the fiber and matrix phases determines the load transmittance value. The matrix deformation pattern is schematically depicted in Figure 3-25 as a result of the fiber-matrix bond weakening near the fiber's termination. This indicates that there is no load transmittance from the matrix at each fiber edge.

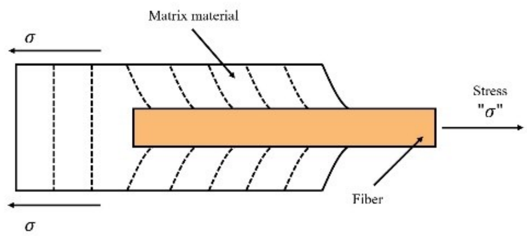

Figure 3-25: Deform of matrix material surrounding a fiber

However, some critical fiber length (l_c) given in Equation 3-5 is necessary for the effective strengthening and stiffening of the composite material. This critical length is dependent on the diameter of the fiber (d), its ultimate tensile strength (σ^*_f), and fiber-matrix bond strength τ_c (Interfacial bond strength) [125].

$$l_c = \frac{\sigma_f^* d}{2\tau_c} \qquad \textit{Equation 3-5}$$

The above equation could be used for the uniformly distributed unidirectional fiber alignment composite when the load applies in the direction parallel to the fiber. Furthermore, Arib et al. observed that the equation for the rule of mixture Equation 3-5 fails to produce a good match when comparing the experimental and theoretical tensile strengths for pineapple leaf fiber-reinforced polypropylene composites. This is because laying the fiber is unidirectional, and the uniformity of the mixture is a talented process in practice. Therefore, the experimental procedure was recommended to find the critical length and the effect of fiber length on mechanical properties [128].

Therefore, the composite samples were prepared to find the effect of fiber length on composite properties. The purchased coir was cut into different lengths [1 cm to 5 cm at each 1 cm interval] and cleaned as described in section 3.3.2, shown in Figure 3-26.

Purchased coir sample *Cut coir samples* *After cleaning and drying*

Figure 3-26: Prepared coir samples into required length

3.5.1 Preparation of samples

Then, the samples were prepared using this coir with different lengths and prepared waste polyethylene as described in section 3.3.2. The coir weight percentage varied from 10% to 50% at 10% intervals for each coir length. The detailed mix proportions of these composite samples are given in Table 3-8.The sample preparation process is shown in Figure 3-27.

The shredded polyethylene and fiber length were mixed according to the selected proportions and laid uniformly, as shown in the hand layup method used for this process, and carefully laying the material is very important to maintain the uniformity of the composite material. In this composite preparation stage, hot-press equipment, a cooler, was used but not a shredder. Figure 3-28 shows this equipment with prepared composite sheets. Although it was challenging to lay the fiber as unidirectional, the uniformity of the mixture was maintained by engaging skilled technicians during this composite manufacturing process.

In previous sections, the outcomes of optimum temperature and pressure were applied as constant values. The applied constant temperature and constant pressure were 140^{0}C, and 4MPa, respectively. The temperature and pressure were applied for 6 minutes period.

Figure 3-27: The sample preparation process

Hot-press equipment *Cooler* *Composite sheets*

Figure 3-28: Equipment and composite sample

Table 3-8: Mix proportions of composite samples

Sample No.	Coir wt. (%)	LDPE wt.(%)	
$A_{(i,j)}$	10	90	**Where**
$B_{(i,j)}$	20	80	i = Coir length in cm and i= 1-5,
$C_{(i,j)}$	30	70	j=j^{th} sample
$D_{(i,j)}$	40	60	j= depends on the required number of
$E_{(i,j)}$	50	50	samples for each test

3.5.2 Preparation of test specimen

After developing the composite sheets, test specimens were prepared according to ASTM standards. The test specimens were cut into the required size, as shown in Figure 3-29, using the handsaw machine.

Figure 3-29: Test specimen preparation in the carpentry shop

3.5.3 Experimental procedure for testing mechanical properties

Experiments were conducted to evaluate the variation of mechanical properties with different fiber lengths and fiber weight percentages of composite materials. The tensile test, bending test, and impact test were performed to evaluate the mechanical properties of the composite, and SEM analysis was carried out to study the bond performance between coir and matrix material. The ASTM standards were followed during the test. The size and numbers of the samples prepared for each test are given in Table 3-9. Table 3-10 shows the summary of samples before undergoing mechanical testing. Flexural tests and tensile tests were carried out using the "INSTRON 5500R" universal testing machine, and the impact test was carried out using the “Universal impact tester” from Hung Ta Instrument Co Ltd Testing equipment. The morphological and cross-sectional features of the fractured surface of the tensile test samples were studied using SEM "CARL ZEISS EVO 18 RESEARCH" equipment. All the equipment used for the above analysis is shown in

Figure 3-30

Table 3-9: Size of samples, the total number of samples, and test standards

Test Name	**Sample size (mm)**	**Total numbers of samples N = i x j x k**	**Standard**
Tensile test	250 x 25 x 2.5	i=7, j=5, k= 5, (N= 175)	ASTM D 3039
Flexural	150 x 12.5 x 3.2	i=6, j=5, k= 5, (N= 150)	ASTM D 790
Impact test	110 x 12.5 x 3.0	i=5, j=5, k= 5, (N= 125)	ASTM D 256
i-	Numbers of samples used for one set		
j-	Varying in lengths (from 1cm to 5 cm at 1 cm intervals)		
k-	Varying in coir weight percentage (from 10 % to 50 % at 10% increment)		

Tensile & flexural test equipment *SEM equipment* *Impact test equipment* *Notching machine*

Figure 3-30: Equipment used for testing

Table 3-10: Prepared specimen before undergoing mechanical test

Length	9:1	8:2	7:3	6:4
1 cm				
2 cm				
3 cm				
4 cm				
5 cm				

3.5.4 Results and discussion

The tensile strength, young's modulus, bending strength, and impact resistance were conducted evaluated with the experimental results. SEM analysis was carried out to assess the properties variation with bond performance.

3.5.4.1 Tensile strength

The test was carried out, and samples were prepared according to the ASTM standard. Mix proportions were arranged according to the results of the previous tensile test. The tensile strength of composites increases with an increase in the fiber length to some extent, and the strength starts to decrease with further increasing fiber length. Results depict that when the coir weight percentage of 10% and 20%, tensile strength achieves its optimum value when the fiber length is 3 cm. Further increase of fiber length, it was noticed that the tensile strength decreases in this weight percentage.

Nevertheless, increasing the coir percentage from 30% to 50%, incrementally variation of tensile strength shows for higher lengths than 3cm as in Figure 3-31and

Figure 3-32. The optimum tensile strength gives a fiber length of 4 cm for 30% to 50%. Eventually, it is observed that the critical length could be observed for the length of fiber of 4cm at 40% weight. Hence, it is concluded that the fiber content and length are affected by the tensile strength of the composite.

This variation may be due to the change in adhesion between coir and matrix material. According to William et al. (2020) the load transmittance through the interfacial bond between the fiber and the matrix phases is significant when considering the mechanical properties of composites. As the fiber content increases, fibers gathering may occur. The fibers cannot bond properly with the matrix due to the non-entrance of matrix material [LDPE] in-between the two adjacent fibers. Because of this, the applied load transmitted to the fibers through the matrix phase could be less. Therefore, the possibility of failure or slip increases with the increase in fiber-to-fiber interaction [125]. According to the experimental outcomes, the maximum tensile strength of the composite material was 12.56 N/mm^2 which comprised 40% fiber content and 4 cm length in fiber.

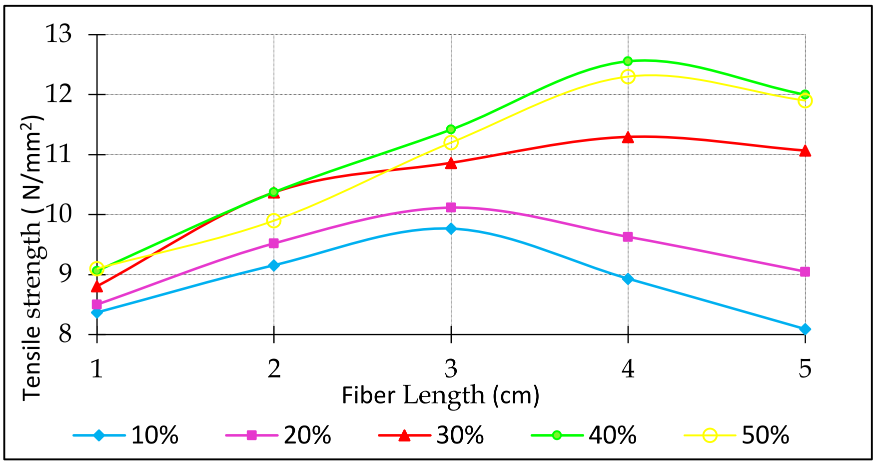

Figure 3-31: Tensile strength variation with fiber length for fiber content

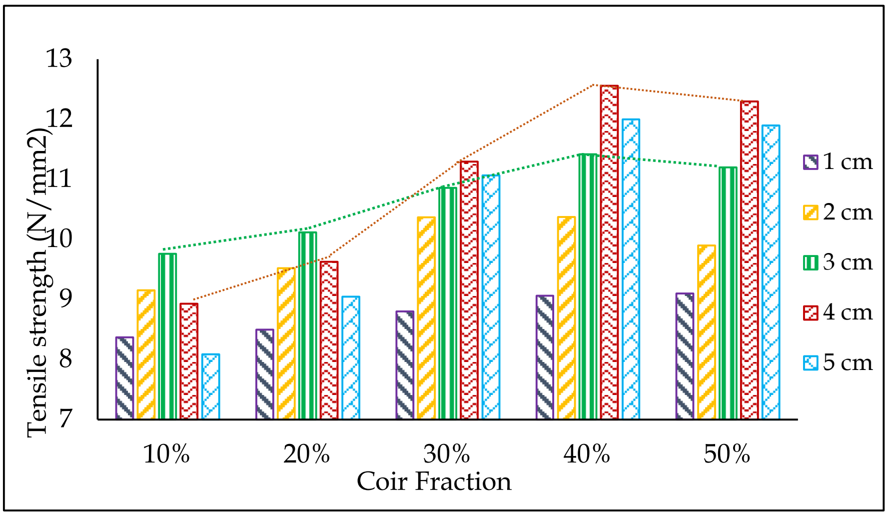

Figure 3-32: Tensile strength variation with coir fraction for different fiber length

Figure 3-33 shows the SEM images on the sample's fractured surface, which shows the optimum tensile strength. Figure 3-33(a) depicts the fibers detached from the matrix/polyethylene media, and Figure 3-33(b) shows the fiber pull-out state due to applied forces. The SEM images further explain the form of poor dispersion of the matrix material within the fiber.

The SEM results designate that the adhesion between fiber and matrix material vanished, and the failure process was dominated due to poor interfacial bonding between fiber and matrix material. The surface morphology of the pull-out fiber appears similar to the surface of coir fiber given in Figure 3-32 (b). This implies that there is no damage to the surface of the coir.

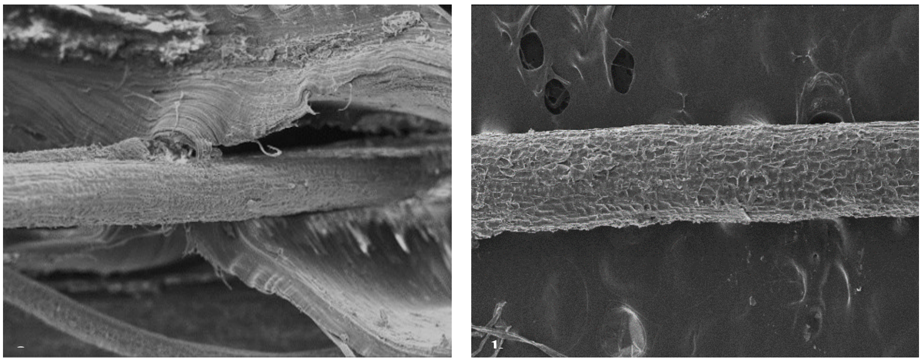

Figure 3-33: SEM micrographs of the fracture surface after tensile tests

The experimental results reveal that the young's modulus increases slightly with the fiber length increase up to 4 cm. With a further increase in fiber length, the decrement of young's modulus was observed. However, it is investigated that the low percentage (10%) of fiber content shows a lesser young's modulus. The maximum young's modulus of 0.46 GPa was obtained for 4cm fiber length and 50 % fiber content. The effect of fiber length on the young's modulus of composites is shown in Figure 3-34.

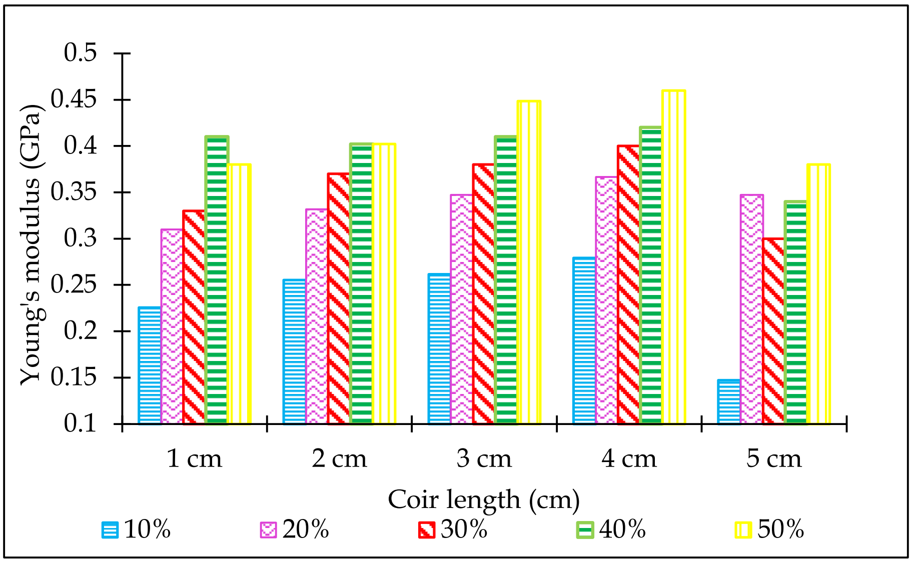

Figure 3-34: Variation of young's modulus with varying fiber length and content

3.5.4.2 Flexural strength

The variation of flexural strength of coir fiber reinforced polymer composites at different fiber lengths and fiber content is shown in Figure 3-35. According to the experimental results, the flexural strength increases with the increment of fiber content up to 30%, then decreases. The maximum flexural strength of 33.77 MPa was observed for the composites with a 3 cm fiber length and 30% fiber content. It trails a similar trend observed in tensile behavior also. Studying the fiber-matrix interfacial bond strength could easily demonstrate the reason for this incremental behavior. However, the further increment of fiber content courses a poor interaction bond between fiber to the matrix due to the gathering of fibers.

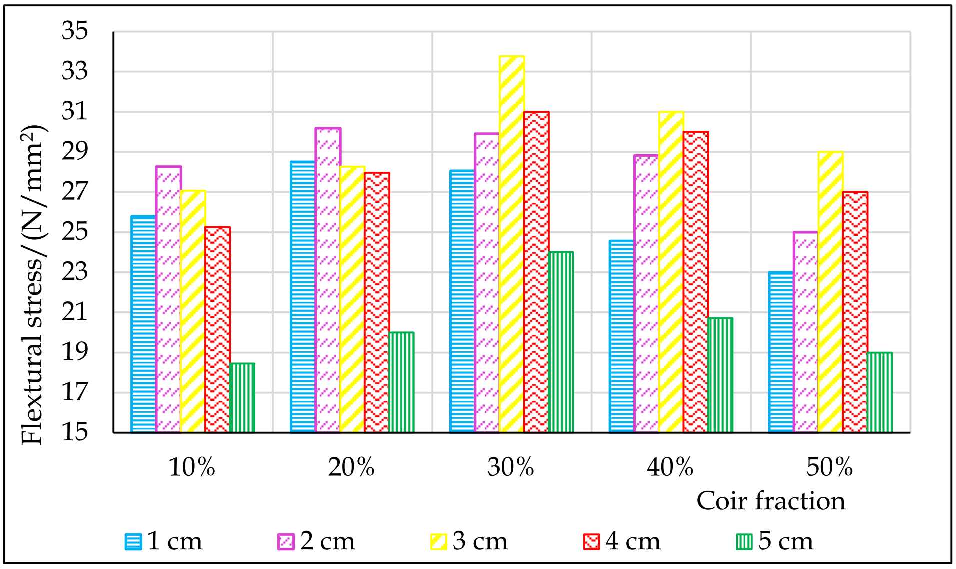

Figure 3-35: Flexural strength variation with fiber percentage

3.5.4.3 Impact strength

The impact strength of fiber-reinforced polymer composites mostly depends on the fiber-matrix interfacial bonding, type of fiber, and type of polymer [119]. The fiber is capable of absorbing energy. The energy absorption increases due to the increment of fiber content [129]. The matrix material affects the bond between the fiber and matrix. Increment in fiber content causes poor fiber-matrix interfacial bonding. Hence, the slip between fiber-fiber occurs when applying the impact load. Because of this, absorbed energy could decrease. Figure 3-36 shows the variation in impact strength of composites with the increase in fiber content and the effect of fiber length. According to the experiment results, it is detected that the impact strength increases with the increase in fiber content by up to 40%. With a further increment of composite fiber percentage, the impact strength decrement was observed. The maximum impact strength of 1.22 kJ/m^2 was gained for composites with a 2 cm fiber length and 40% fiber content.

According to the literature review carried out, several authors have investigated the mechanical properties of composites on dissimilar fibers with different matrix materials. Ultimately, it was revealed that the mechanical properties of composites depend on the physical and mechanical properties of fiber and matrix materials. Table 3-11 represents the experimental results obtained by the different investigations conducted by other authors.

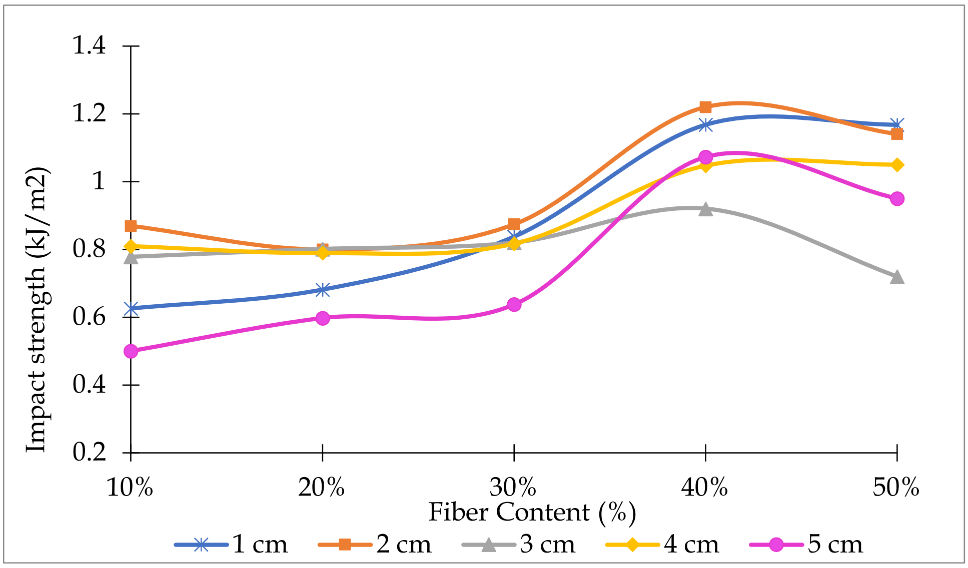

Figure 3-36: Impact strength variation with fiber content

Table 3-11: Mechanical properties of different fiber-reinforced composites

Composite Material				Mechanical Properties				Source
Fiber type	**Matrix material**	**Fiber length (mm)**	**Fiber Content in wt. %**	**Max. Tensile strength (MPa)**	**Max.Elastic Modulus (GPa)**	**Max.Flexural Strength (GPa)**	**Impact Energy (KJ/m^2)**	
Coir	epoxy	12	15 %	24.71		29.43	13.54	[130]
		15	20 %		2.27			[130]
Banana	Epoxy	5	12 %	16.39	0.652		2.23	[131],
Oil palm	Epoxy		30 %		1.342			[133]
Sisal fiber			20 %			22.3		
Coir fiber	Epoxy LY 556	30	30 %	13.05	2.064	35.42	17.5	[134]
Pineapple	Polypropylene		10.8 % by volume	37.28				[128]
Coir	Waste LDPE	40	40%	12.56				Experimental results
		40	50%		0.46			
		30	30%			33.77		
		20	40%				1.22	

3.5.5 Summary of production criteria

In this section, composite samples were prepared to identify the effect of fiber length on the properties of the composite. Composite were prepared by varying fiber length and keeping all the other parameters constant. After preparing the composite material, the test specimens were undergone to the mechanical test. According to the tensile experiment outcomes, the optimum tensile strength investigated was the 4 cm fiber length with 40% coir weight content. The maximum tensile strength of the composite material was 12.56 N/mm^2. The 3 cm fiber length with a 30 % coir to LDPE ratio showed the optimum flexural properties. The maximum flexural strength of the composite material was 33.77 N/mm^2. Further, it was observed that the impact strength increases with the increase in fiber content by up to 40% with a 2 cm fiber length. The maximum impact strength shown for the composite was 1.22 kJ/m^2.

Since the critical parameter of the panel wall is bending stiffness, it was decided to select the 3 cm fiber length to prepare the composite for wall panel preparation.

3.6 Serviceability characteristics of composites

Natural fiber-reinforced polymer composites [FRPC] have undergone extensive research to improve their properties, particularly their water absorption tendency [135],[136]. Various chemical treatment procedures have been applied to minimize the hydrophilic nature of the fibers and improve fiber surface adherence to the surrounding matrix.

Kabir et al. found five parameters that influence the qualities of composites: fiber structure, thermal stability, length of fiber, loading and orientation of fiber, presence of voids, and fiber water absorption [137].

According to Carvalho et al., the reinforcing materials absorbed more water than the matrix. The water absorption values of “macambira” fiber reinforced polyester composite, and pure polyester composite were measured in their investigation. The water absorption values for both composites were found to be 14% and 1%, respectively [138].

One of the physical features of FRPC is its ability to absorb water. The fiber absorbs water from the atmosphere because it contains hydroxyl groups. The transport of water molecules, diffusion, and capillary effect are three fundamental mechanisms of water absorption in FRPCs. Diffusion is a random process in which water moves from high-concentration areas to low-concentration areas. In polymeric composites, diffusion follows both Fickian and non-Fickian diffusion theories. On the other hand, the capillary transportation mechanism occurs in the gaps in the fiber-matrix interface spaces. Water absorption is a problem because it can induce matrix cracking, dimensional instability, and a reduction in the mechanical properties of fiber-reinforced polymer composites [139].

FRPC is susceptible to moisture due to the hydrophilic nature of natural fibers. After the water is absorbed, fibers swell, weakening the adhesion between fibers and matrix interfaces and affecting the composites' mechanical characteristics and dimensional stability. As a result, the hydrophilic nature of the fibers can be changed chemically, eliminating the hydroxyl groups [140].

Most investigations have focused on treatments that minimize fiber moisture absorption while also improving matrix-fiber adhesion to reduce FRPC water absorption. Water absorption in FRPC is linked to two fundamental mechanisms, according to Kakroodi et al. (2013). The first key mechanism was the natural fiber's hygroscopic property (absorbing water from the environment), which boosts the composites' hydrophilic behavior. The second mechanism was to create voids that store water at the interface due to structural inhomogeneity between fibers and matrix [141]. According to Pandian et al. (2016), the kind of fibers used for reinforcement, the interfacial bond between the fiber and matrix, and the existence of voids in the composites are all significant determinants of the water absorption behavior of FRPCs [142]. The epoxy composites made from treated fibers exhibit the lowest water absorption compared to the composite made from untreated fiber due to Gupta and Srivastava [143]. When compared to untreated composites, the water absorption of bagasse-reinforced epoxy composites manufactured from fibers treated with 1% NaOH for 30 minutes and then submerged in 1% acrylic acid for an hour was somewhat reduced [144].

By employing fibers treated with vinyl trimethoxy silane to make black sugar palm reinforced polypropylene composites, Zahari et al. (2015) discovered that treated fibers had somewhat lower water absorption than untreated fiber composites [145]. The polypropylene composite reinforced with wood fiber and wheat husk treated with benzylation displayed significantly less water absorption than the composite formed from untreated fibers [146]. It is well known that when fiber concentration rises, composite materials absorb more water [145],[147]. Similar results were reported by Paul et al. (1997), who discovered that sisal fiber-reinforced polyethylene composites' capacity to absorb water rose as fiber loading was carried out. The fibers' sizes affect how FRPC absorbs water and behaves when it swells [148]. Thakur and Singha used pine needle particles, and short and long fibers to create fiber-reinforced PF composites. Long fibers inflated more and absorbed more water than short fibers and particles, owing to their larger dimensions and higher water attraction in the composites. The strength and modulus of the composites were significantly affected by fiber length variation [149]. The treatment of fiber was largely responsible for the FRPCs' reduction the water absorption [150] according to Kalaprasad et al. According to Ichazo et al., insufficient matrix-fiber adhesion resulted in the formation of capillaries with a suction effect in the composite structure, which boosted water uptake [151]. Li et al. (2009) examined the water absorption behavior of bio composites made of flax fiber reinforced polyethylene that had undergone five various chemical treatments, including alkaline, silane, potassium permanganate, acrylic acid, and sodium chlorite [152]. Compared to untreated fibers, all five treatment methods had lower water uptake.

On the other hand, Acrylic acid-treated fiber had the lowest water absorption compared to the other treatment procedures. The water absorption of the composites was greatly reduced after treatment with “acrylic acid, silane, and potassium permanganate”, but not after treatment with sodium chlorite or alkali. Acrylic acid > potassium permanganate > silane > sodium chlorite > alkaline has the highest efficiency in terms of water absorption improvement.

Before fabrication of reinforced polyethylene composites, Paul et al. (1997) treated sisal fibers with alkali, stearic acid, benzoyl peroxide, dicumyl peroxide, permanganate, isocyanate, and acetylation treatments. The treated fiber's hydrophilic character was reduced. The water molecules absorbed by the cellulose fibers could not accommodate the composite due to a strong bonding at the boundary of treated fiber and polyethylene [148].

Many researchers have looked at the physical and mechanical properties of coir and sisal fiber composites. These characteristics are determined by the fiber's nature and morphology, matrix properties, and fiber-matrix interaction. Environmental concerns drive the adoption of cellulosic fibers, yet their composites have worse flammability than glass, carbon, and other fiber-reinforced composites [153], [154].

The use of advanced polymer matrix composites [PMC] is constantly expanding, especially in the industrial, structural, and automotive sectors. Flammability is vital in many industrial applications, particularly in the transformation sector, where compact spaces make fires a significant risk [155].

The fire resistance behavior of flax fiber and glass fiber-reinforced epoxy resin composites was compared by Chai et al. (2003). According to their investigation, flax fiber reinforced composites burn faster, produce more heat, and their structure deforms significantly during combustion [156].

The fire-retardant performance of polyester resin and sansevieria fiber reinforced polyester resin composite was investigated by Ramanaiah et al. (2012). According to their findings, sansevieria fiber-reinforced composite catches fire faster and produces more carbon dioxide and total smoke during combustion than unreinforced polyester resin. Although the commercial applications of natural fiber-based polymers are rapidly expanding, many elements of their behavior, such as fire-retardant properties, are still poorly understood. With this background in mind, the current research project's purpose is to manufacture a sisal/coir fiber reinforced epoxy resin bio-composite and assess its burning rates [157].

3.6.1 Investigation of water absorption properties

Water absorption is a problem for the FRPC because it induces matrix cracking, dimensional stability, and a reduction in mechanical properties. Suppose the availability of voids causes high water absorption due to the capillary action of composite material. After the water is absorbed, fibers swell, weakening the adhesion between fibers and matrix interfaces and affecting the composites' mechanical characteristics. The reinforcing materials absorbed more water than the matrix.

The panel wall was developed using 3 cm long coir fiber and 30% coir to the polytene composite material. The water absorption behavior was investigated for the above composite samples. The experiments were conducted in two different ways. The first test series were carried out for all four edges and two surfaces of the samples exposed to pure water. In the second test series, only two surfaces were exposed to water, and other sides were sealed adequately with waterproofing material. The study aimed to identify the water absorption capacity and arrange suitable rectification methods to minimize it.

3.6.1.1 Experimental method

Water absorption capabilities of the produced composites' were examined following the "ASTM D 570: Standard test method for water absorption of plastics" [158]. The test specimens were made in the shape of a bar with dimensions of 76.2 mm long, 25.4 mm width, and 3.2 mm thickness from the composite sheets by using a hand saw. The sawing process is slow enough that the material does not become overheated. The samples were clean, to have crack-free edges and finished with finer sandpaper to smooth out the cut edges. Three specimens were chosen for each mix percentage for 3cm fiber length. All specimens were dried for 24 hours at 50^0 C before being placed in a desiccator to cool. The following measurements were obtained and weighted to the nearest 0.001 g. The conditioned specimens were completely immersed in purified water and kept at room temperature. The specimens were withdrawn from the distilled water after 24 hours, with all external water rubbed off using a dry cloth, and weighed to the nearest 0.001g by a digital balance within 1 minute of removing them. As a result, evaporation at the surface is negligible. For each weight percentage, three replicates were examined, and the average findings were reported. After weighing, samples were returned to the distilled water container to complete the sorption process and reweighed until steadiness was reached. The water absorption test was performed for numerous days until the sample came a stable weight [159].

The composite's percentage weight gain (W %) was measured at steady time intervals and calculated using Equation 3-6 [160].

$$W\% = \frac{W_t - W_0}{W_0} \times 100\ \% \qquad \textit{Equation 3-6}$$

Where W_t is the weight of the specimen at a given immersion time, and W_0 is the initial weight of the specimen after oven drying. The composite specimens immersed in water have shown in Figure 3-37.


Figure 3-37: Composite specimens immersed in water

3.6.1.2 Results and Discussion

The percentages of weight gain followed by water absorption were calculated. Water absorption percentage (%) with testing time duration in days is graphically interpreted with different fiber content for the first test series in Figure 3-38 (i.e., composite without applying waterproofing material). Figure 3-39 shows the variation of water absorption in graphical presentation with different fiber content for four selected days for the same samples.

The results have shown significantly low values for weight gain percentages followed by water absorption for all different fiber loadings of thermoplastic composite samples. It may be associated with the hydrophobic nature of the coir fiber [161]. The matrix material polyethylene is also a hydrophobic polymer. The results show that the composites with higher reinforced materials offered higher water absorption values than composite materials with lesser reinforced materials.

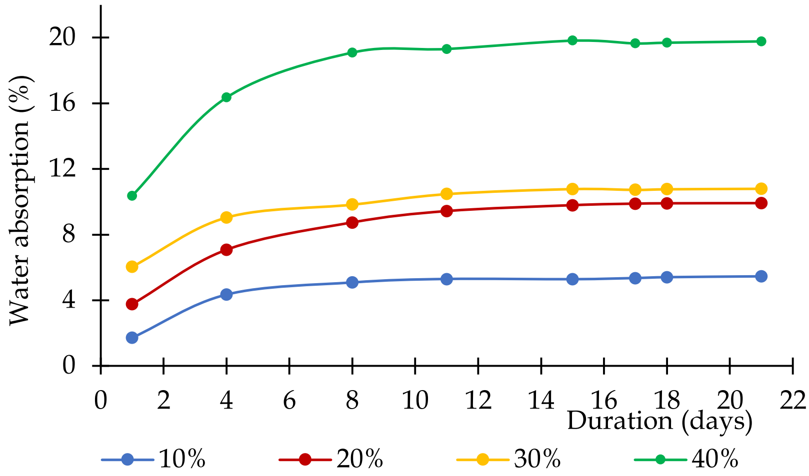

Figure 3-38: Variation of water absorption with time in different fiber content

According to Figure 3-39, the composites with 40 % wt. of fiber presented the highest water absorption of 19.78 % compared to the other samples of composites with different fiber contents. Usually, the water absorption rises with the increasing fiber loading in the fibrous composites [162], which is depicted in Figure 3-39. Thus, the FRPC developed in this study, the composites that were reinforced with 40 wt.% fibers provided the highest percentages of weight gain, while the composite reinforced with 10 wt. % fibers provided the lowest percentages of weight gain.

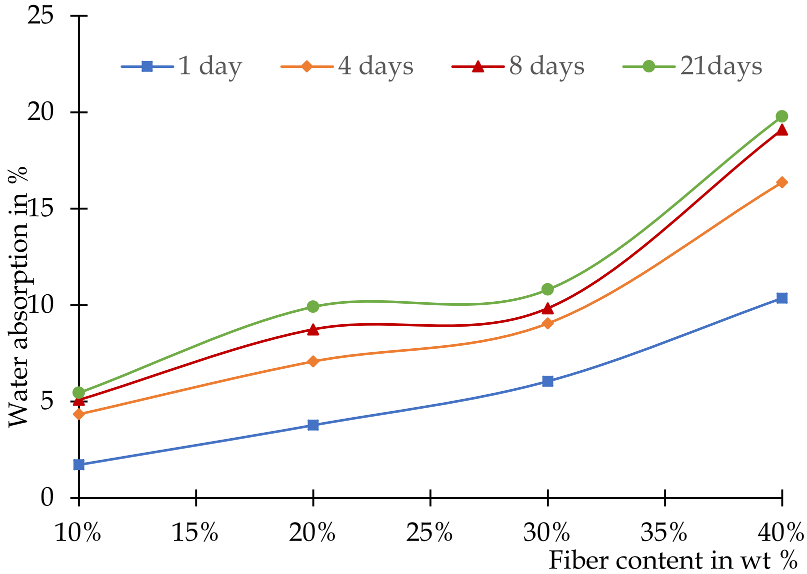

Figure 3-39: Variation of water absorption with different fiber content

The water absorption rate depends on the weight fraction of the fibers in the composites. It was observed that the water absorption was completed approximately 432 hours (18 days) and achieved equilibrium for all the FRPC developed in this research. The water absorption is negligible in all composite samples after 18 days.

Additionally, even the 40 % wt. fiber-reinforced composites provided a lower water absorption value than the commercially available wood particleboards (< 70%) [163]. Moreover, the developed composites in this research show lower water absorption compared to the particleboards developed using sunflower stalks and poplar wood reported in the literature (< 52%) [164].

Next, the water absorption of composite by applying waterproofing chemicals was evaluated. The observations revealed that the water absorption of the composite can be partially prevented by applying waterproofing chemicals at a significant level.

Figure 3-40 shows the overall behavior of water absorption of different weight coir %. Figure 3-41 shows how to reduce composite material's water absorption after applying the waterproofing chemicals. Though the normal composite absorbs water continuously for up to 18 days, the composite which applied waterproofing chemicals showed negligible water absorption for up to 7 days.

Further, according to this observation, although the composite sample's cutting edges were waterproofed against water contact, all samples also absorbed water at certain levels. This predicted that the surface of the samples' absorbed some amount of water. Therefore, finally, it revealed that the surface of the composite material should also be treated to prevent water absorption.

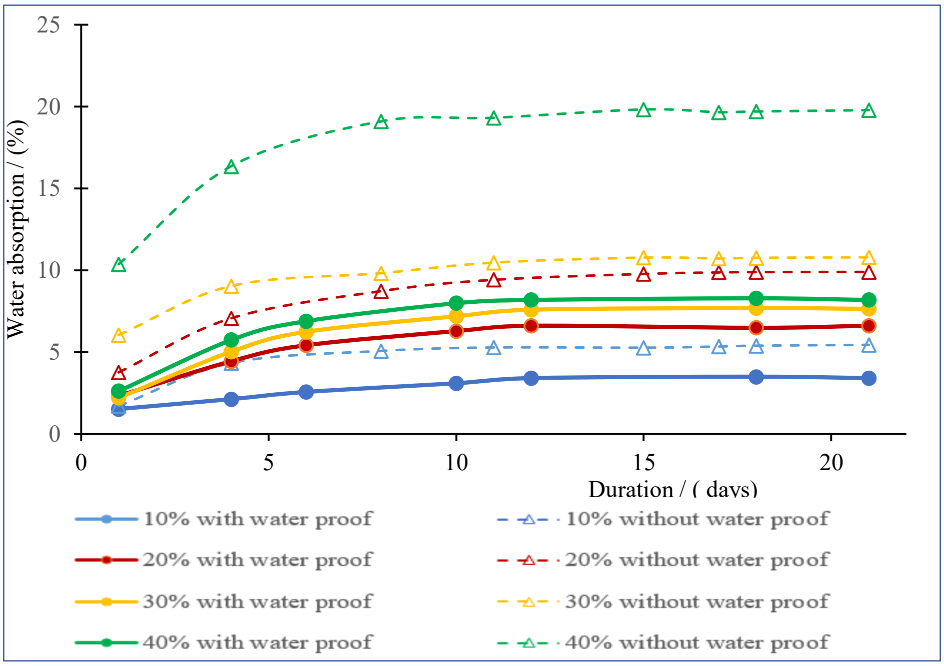

Figure 3-40: Variation of water absorption on waterproof composite

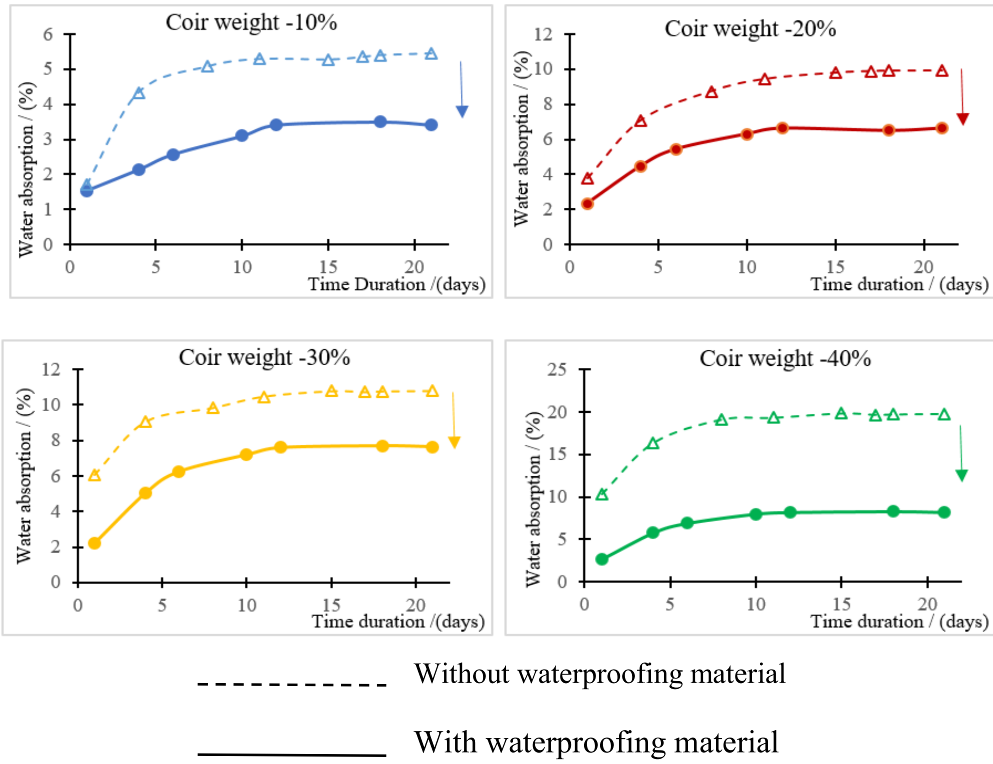

Figure 3-41: Water absorption behavior of composite

3.6.2 Investigation of flammability characteristics

The flammability characteristics of the selected composite, which comprises 30% weight of 3 cm long coir were studied. This physical property is vital in many industrial applications, including the construction and aircraft, and automobile industries. This study aimed to investigate the flammability properties of developed composite material and recommend fire-retardant methods to control the burning rate.

3.6.2.1 Experimental Methods

The flammability performance of the composites was determined using the UL-94 horizontal flame propagation test method for polymers [161]. The test was conducted in a flammability chamber at laboratory room temperature. The horizontal burning tested three specimens from each composite sample (9:1, 8:2, 7:3, 6:4, and 5:5 polyethylene to coir ratio). The specimen size was 120 mm × 10 mm × 3.2 mm. Two lines were marked in each sample at 25 mm and 100 mm from one end of the specimen. The sample was placed horizontally from one side of the sample holder in the flammability chamber. The burner's flame was applied to the sample on the other side for 30 s at a 45° angle. In this case, a controlled Bunsen burner flame was used. If the specimen continues to burn after the test flame has been extinguished, the distance traveled by the flame between two lines was timed, and the burning rate was expressed in millimeters per minute. The flammability test specimens are shown in Figure 3-42.

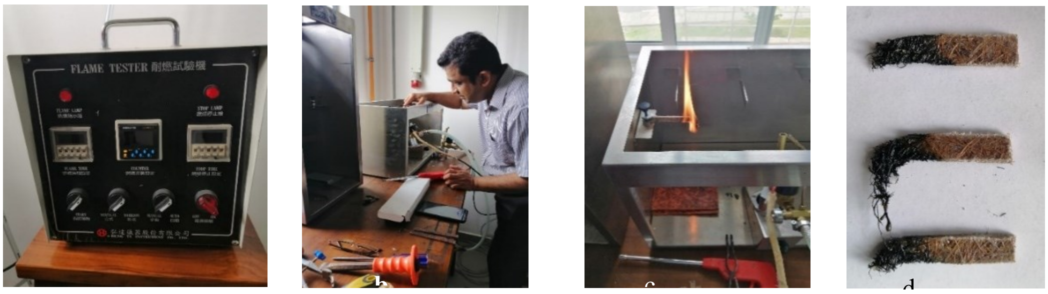

Flame Tester *Fixing the samples* *Test is in progress* *Tested Samples*

Figure 3-42: Flammability test process

The ranking was determined by calculating the speed of flame propagation. The samples were classified as Horizontal Burning (HB) rating only if:

- The samples may not have a burning rate of more than 40 mm/min over a 75mm span, or
- The samples stop burning before the flame reaches the 100 mm mark

3.6.2.2 Results and Discussion

The fifteen rectangular specimens, three from each fiber weight fraction, were tested for flammability properties through the horizontal UL-94 test. The test results are summarized in Table 3-12.

Table 3-12: Burning rate and results

Polyethylene to coir weight ratio	Average burning rate (mm/min)	Result
9 : 1	25.33	HB
8 : 2	26.69	HB
7 : 3	28.19	HB
6 : 4	30.00	HB
5 : 5	31.91	HB

The coir fiber waste polyethylene composites burned with higher horizontal burning rates in 25.33-31.91 mm/min. The results revealed that the burning rate of the composites has increased with increased fiber content. According to the standard given in UL-94 HB, tested samples are in the HB category. Generally, polyethylene is considered a highly flammable material, while the polyester fabric is not a highly flammable material [165]. Although polyester fabric tends to be slow to ignite, it can melt quickly at high temperatures. However, once it is ignited, severe burning and dripping occur at a higher rate [166], which is also observed from the results. Figure 3-43 shows the average horizontal burning rate variation with coir weight percentage.

A major disadvantage of coir/fiber polymer composite is that these are highly flammable materials that can burn at a higher rate. This suggests incorporating flame-retardant additives to delay and control the burning.

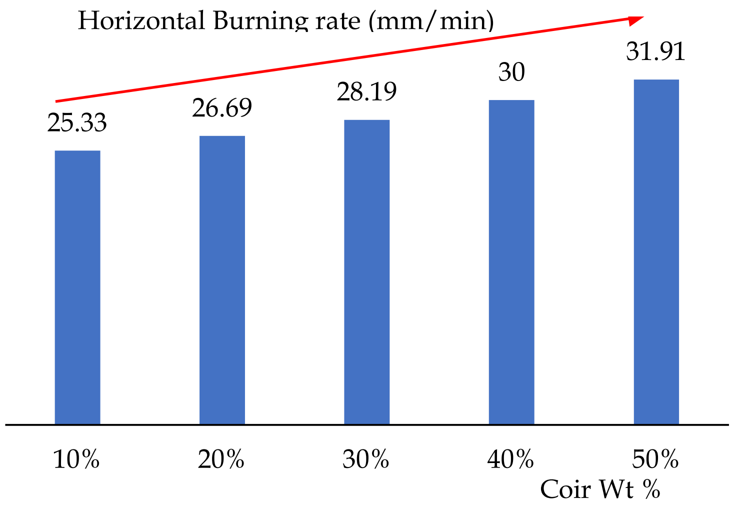

Figure 3-43: Average burning rate of FRPC with different wt. content

3.6.3 Summary of serviceability checks

Though the manufacturing parameters of the composite were concluded in the above section, this section was to understand the serviceability characteristics of the composite. Here, the water absorption property and flammability were selected as two important properties which can be affected serviceability performance. Generally, the water absorption in fibrous composites typically increases as fiber loading increases [162],[145]. Compared to the other composite samples with varying fiber percentages, the composites with 40% weight reinforcing fiber had the maximum water absorption capacity, which is 19.78%. The FRPC with 40 weight% fibers offered the highest percentages of weight growth, while composites reinforced with 10 wt.% fibers provided the lowest percentages of weight gain, obeying past research data.

Flammability test results show that the horizontal burning rates of the coir fiber waste polyethylene composites were greater, ranging from 25.33 to 31.91 mm/min. The burning rate of the composites increased as the fiber percentage increased, according to the findings. The examined samples fall within the HB category, according to the UL-94HB standard. Polyethylene is generally regarded as a highly flammable substance [167]. According to the results obtained, it can be concluded that the average horizontal burning rate of the sample is a function of coir weight percentage. The fact that coir and fiber polymer composites are very flammable and can burn faster is a significant disadvantage. This suggests using flame-retardant additives to control and delay the burning process.

3.7 Chapter Summary

It is significant to investigate the material characterization before commencing the material development work. The primary raw material of this study was coconut fiber and waste polyethylene. The diameter, density, surface morphology, and degradability temperature were studied under the physical properties of the coir. The tensile strength of coir was studied as a mechanical property. The studying chemical properties of coir and polyethylene were evaluated using a standard test.

The coir fiber had an average diameter of 0.31 mm and a density of 1.018 g/cm^3, respectively. The surface characterization of roughness, interfacial bonding between the fiber and matrix, pore size, and accessible contaminants was achieved using SEM examination. The FTIR distinguished the chemical characterization of the coir fibers. It was cleared to identify the molecules and functional groups present in Sri Lankan coir fibers, confirming the presence of cellulose, hemicellulose, lignin, and wax, among other things.

The crystallinity index and crystallite size of coir fiber were calculated using X-ray diffraction analysis and were found to be 37.28 percent and 0.4331 nm, respectively, which were lower than other natural fibers reported. In the tensile test, the coir fiber's ultimate tensile strength, young's modulus, and elongation ranged from 94 to 159 MPa, 1.2 to 1.8 GPa, and 21 to 67 %, respectively. According to thermogravimetric analysis, Sri Lankan coir fibers are thermally stable below 2200 C. The carbon and hydrogen atoms are visible in the low-density polyethylene, which is made up of repeated methylene groups (CH_2). The resulting FTIR spectrum reveals approximately identical wave numbers (1377 cm^{-1} and 1366 cm^{-1}) related to polyethylene's chemical structure.

Then, practically possible coir to polyethylene ratio, in which the mechanical properties of composite optimized was found out during the research, Tensile and flexural tests was performed for this purpose. It was discovered that the best mechanical properties were optimized when the coir to polyethylene weight ratio was between 10% and 40%. Accordingly, this weight range was chosen for further research.

The mechanical properties of composites are directly affected by various manufacturing conditions. The temperature and pressure are the two most essential manufacturing conditions among them. Therefore, it was vital to understand what temperature and pressure would provide the peak mechanical characteristics of the composite. After the tests, it was determined that the 140^0 C temperature and 4 MPa pressure are the optimum temperature and pressure to manufacture the composites.

Next, the composite samples were prepared to identify the effect of fiber length on the properties of the composite. The composite was prepared by varying fiber length and keeping all other parameters constant. After preparing the composite material, the test specimens were undergone to the mechanical test. According to the tensile experiment outcomes, the optimum tensile strength investigated was the 4 cm fiber length with 40 % coir weight content. The maximum tensile strength of the composite material was 12.56 N/mm^2. The 3 cm fiber length with a 30 % coir to LDPE ratio showed the optimum flexural properties. The maximum flexural strength of the composite material was 33.77 N/mm^2. The impact strength optimizes at the 40 % fiber content with a 2 cm fiber length. The composite had a maximum impact strength of 1.22 kJ/m^2.

Since the critical parameter of the panel wall is bending stiffness, it was decided to select the 3 cm fiber length with 30 % fiber content to prepare the composite for wall panel preparation. Finally, specific recommendations were made based on experimental results in this chapter. The best composite manufacturing criteria were the 140^0 C temperature, the pressure of 4 $N/mm^{2,}$ and a processing period of 6 minutes.

The composites with 40 % wt. Reinforcing fiber had the highest water absorption capacity of 19.78 % compared to the other composite samples with different fiber percentages. However, for all the fiber percentages, the water absorption became zero after 18 days.

The coir fiber waste polyethylene composites had higher horizontal burning rates, ranging from 25.33 to 31.91 mm/min. According to the UL-94HB standard, the investigated samples fall under the HB category. Further, the test results show that the burning rate of the composites rose as the fiber fraction increased. And it can say that the sample's average horizontal burning rate is proportional to the coir weight percentage. Coir and fiber polymer composites are extremely combustible and burn quickly, which is a severe disadvantage. To control and prolong the burning process, this proposes employing flame-retardant chemicals.

The mix design and manufacturing criteria for composite material prepared using coconut fiber and waste polyethylene were concluded. The next step of this research is to develop a lightweight panel wall using this developed composite material with optimum flexural properties. Hence, the next chapter describes the wall panel's experimental methodology, results, and development process.

4 DEVELOPMENT OF SANDWICH PANEL WALL

4.1 General

The sandwich panel was fabricated using the developed composite material described in chapter 3. Among different concepts of designing partition walls, the concept of the sandwiched panel was used to develop a lightweight partitioning panel wall in this research. Sandwich panels which are used for partitioning walls, consist of three elements comprising two thin face sheets with significantly higher strength material and a lightweight core arrangement. The core consists of a lower-strength material sandwiched between both face sheets. This core can be arranged in different ways. The internal core material can also be in the same or any other material. In this research, the same material was used to prepare both face sheets and internal core arrangement. These sandwich panels are well-known in light panel designs [168].

There are dissimilar types of internal core arrangements such as square, triangular, honeycomb, circular and rectangular [169]. The challenge is to select the most suitable core arrangement out of which optimum properties such as lightweight, minimum use of materials, maximum flexural capacity, and cost-effectiveness. Therefore, sandwich panels with five different alternative core configurations with different cell sizes were analyzed in this research.

In the past research, different software such as Ansys and ABAQUS was used to analyze the sandwich panels [170]. Hence the finite element models of the sandwich panels were developed to select a suitable core configuration with necessary properties.

Many researchers globally have used finite element analysis to study the mechanical properties and their failure behavior for the sandwich panels [171]-[173]. Chang et al. (2005) studied the corrugated sandwich panels by applying the flexural loadings using finite element methods. During the analysis, the simply supported and clamped edges were arranged in each panel as the boundary conditions. The corrugated angle, core to face thickness ratio, pitch to corrugated depth ratio, and corrugated depth to core thickness ratio were considered as the variable parameters. The bending moment and the central deflection of the panels were studied [174]. However, among several software Ansys software was selected to use in this research. First, the validity of the software for this study was evaluated and identified.

4.2 Software validation

The numerical outputs are to be validated with the experiment results before using the selected software to analyze the different core configurations. Thus, the flexural properties of the composite material were desired and validated using experimentally, numerically, and analytical outcomes.

4.2.1 Experimental method

The material properties of the panel wall were determined experimentally. The test specimens were prepared with selected mix proportions according to the investigated manufacturing conditions. Then, the tensile and flexural tests were carried out as per ASTM standards. Figure 4-1 shows the experimental test setup for the 3-point bend test.

Figure 4-2 shows the force Vs. Strain graph for the 3-point bending test. According to the given outcomes, the evaluated flexural strength was 38 N/mm^2 at the failure stage.

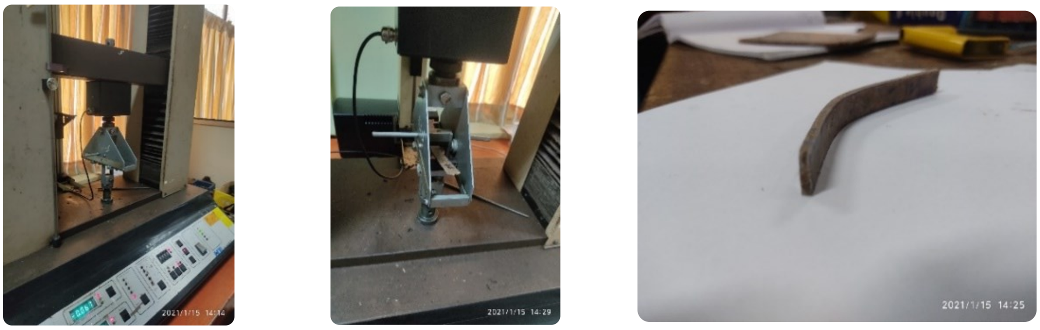

Test equipment *Sample fix for test* *Sample after bending test*

Figure 4-1: Experimental test setup for the 3-point bend test

Figure 4-2: Force Vs. Strain graph for the 3-point bending test

4.2.2 Analytical calculation

Maximum bending stress was calculated using an analytical method with simple bending formula, as shown in Figure 4-3. The following calculation describes the process of bending stress calculation. According to the calculations, the maximum bending stress evaluated from the analytical method was 42.18 N/mm^2.

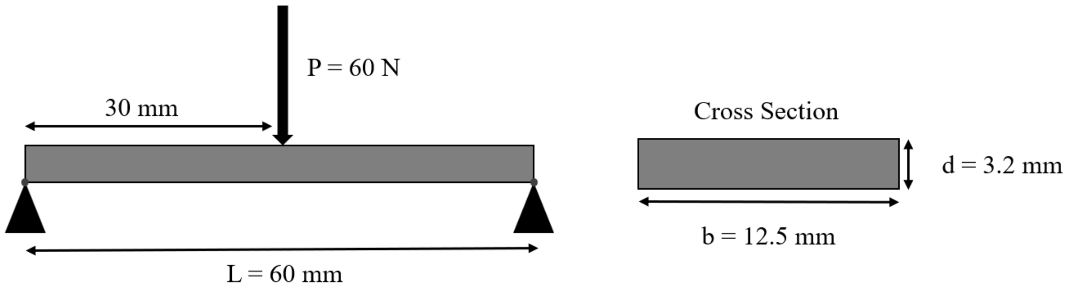

Figure 4-3: Schematic diagram for 3-point bend test

Calculations

$$M = \frac{PL}{4} = 60 \times \frac{60}{4} = 900\ Nmm$$

$$\frac{M}{I} = \frac{\sigma}{y} = \frac{E}{R}$$

$$\sigma = \frac{MY}{I} = \frac{M \times {}^{d}/_{2}}{\frac{1}{12}bd^3} = \frac{6M}{bd^2} = \frac{6 \times 900}{12.5 \times 3.2^2}$$

$$\boldsymbol{\sigma = 42.18\ N/mm^2}$$

4.2.3 Numerical simulation

Numerical simulation was performed to study the flexural behavior of the composite material using ANSYS Workbench 17.2. Young's modulus value of composite is required as input data during the simulation process. Since this composite material is a new product, Young's modulus value is not available. Therefore, Young's modulus value is calculated first.

4.2.3.1 Evaluate Young's modulus of the composite

The highest bending performance was observed at the 3 cm coir length with a 30% volume fraction. During Young's modulus calculation, similar mix proportion composite samples were used. Figure 4-4 shows the force Vs. Elongation graph for the selected composite sample. When modeling this software, young's modulus of composite material is required as input data. Therefore, young's modulus of composite material was calculated as shown in below specimen calculation. After that, separate calculations were carried out for five test samples, shown in Table 4-1, and the average value of 0.38 GPa was taken as young's modulus of composite material for future uses.

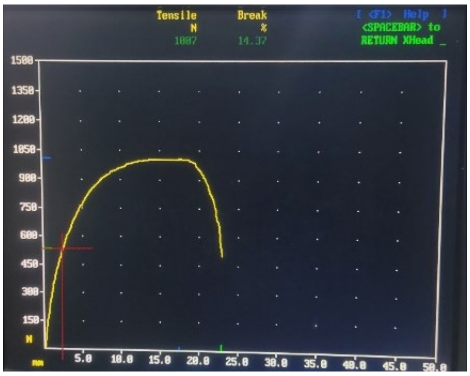

Figure 4-4: Force Vs. Elongation graph for tensile test

Specimen calculation

Effective Length of the Sample	= 159 mm [Gauge Length]
Width of the sample	= 25 mm
Thickness of sample	= 3.98 mm
Force applied	= 530 N
Elongation	= 2.5 mm

$$\text{Stress} = \frac{Force}{Cross\ sectional\ Area}$$

$$= \frac{530\ N}{25\ mm \times 3.98\ mm}$$

$$= \underline{\mathbf{5.327\ N/mm^2}}$$

$$\text{Strain} = \frac{Elongation}{Initial\ Length}$$

$$= \frac{2.5\ mm}{159\ mm}$$

$$= \underline{\textbf{\textit{0.016}}}$$

$$\text{Young's Modulus} = \frac{Stress}{Strain}$$

$$= \frac{5.327 N/mm^2}{0.016}$$

$$= \underline{\textbf{0.34 GPa}}$$

Table 4-1: Young's modulus calculation for five test specimens

Sample No.	Force (N)	Thickness of Sample (mm)	Elongation (mm)	Stress (MPa)	Strain	Young's Modulus (GPa)
1	530	3.98	2.5	5.327	0.016	0.34
2	515	4.07	2.2	5.061	0.014	0.37
3	640	4.09	2.5	6.259	0.016	0.40
4	580	3.81	2.6	6.089	0.016	0.37
5	500	3.31	2.3	6.042	0.014	0.42
Average value						**0.38**

However, theoretical validation is required to emphasize the accuracy of the experimental values. Jr and Rethwisch, Callister's suggested below mention Equation 4-1 [125] to calculate young's modulus of discontinuous and randomly oriented fiber-reinforced composites as shown in Figure 4-5. Since the FRPC also behaves similar pattern, this equation can be used to calculate young's modulus of FRPC. Therefore, the young's modulus of the composite was calculated as shown below using Equation 4-1, and the estimated value is 0.37 GPa.

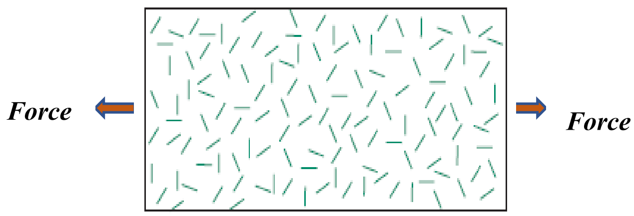

Figure 4-5: Discontinuous and randomly oriented fiber-reinforced composites

$$E_{cd} = KE_fV_f + E_mV_m \qquad \textit{Equation 4-1}$$

K = 3/8

Young's modulus of coir fiber; E_f = (1200+1800)/2 = 1500 MPa

Volume fraction of coir fiber; V_f = 0.4

Young's modulus of matrix material; E_m = (200 + 300)/2 = 250 Mpa

Volume fraction of matrix material; V_f = 0.6

Young's modulus of composite material =0.37 GPa

When comparing these values, it was revealed that they are almost identical. Then it was concluded that the theoretical value validates the experimental value. Hence, the given results can be used for future work.

Then, the bending strength of the sample was obtained using finite element analysis. During this analysis, the point load of 60N load was assigned at the midpoint of the model. Figure 4-6 shows the numerical outputs from Ansys software. According to the numerical output of the software, it was observed that the maximum bending strength of the sample was 41.456 N/mm^2.

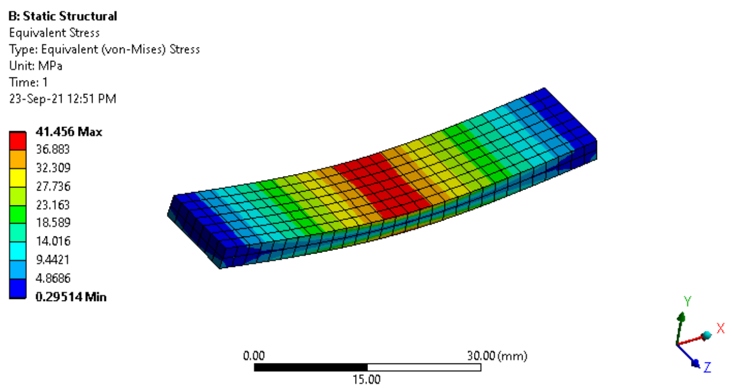

Figure 4-6: Numerical results from Ansys software

4.2.4 Discussion for validation

Software validation was carried out by associating the results obtained in the above three methods. It reveals no significant differences in maximum bending strength since the received values are almost identical. The summary of the outcomes is given in Table 4-2. Hence, the software values which is used for numerical analysis could be validated. Therefore, it is concluded that the Ansys software is valid for future analysis. Hence this software was used to find the optimum core configuration for the sandwich panel.

Table 4-2: Maximum failure stresses in three different methods

Test Method	**Max bending stress / (N/mm^2)**
Experimental results	38.00
Analytical results	42.18
Numerical results	41.45

4.3 Selection of optimum core configuration

Five different core arrangements were selected, and the flexural behavior of the sandwich panels was numerically analyzed using Ansys software. The selected different sizes of different core arrangements (square, rectangular, circular, triangular, and hexagonal) of sandwich panels are shown in Table 4-3. Those were numerically analyzed to investigate the optimum flexural properties and then selected the most suitable configuration based on flexural characteristics with the minimum weight. Since the governing criteria of the non-load-bearing panel wall is bending stiffness, research forcus to optimize the flexural properties.

The finite element helps to study the actual behavior in the digital platform. It can be minimized the unnecessary cost incurred during the experimental testing work. Figure 4-7 shows the flow diagram of the numerical analysis process. Space claim solid modeling CAD software was used to prepare the geometric model. This is a special tool to develop the 3-dimensional solid model in Ansys. The 400 mm × 400 mm × 25 mm geometric model was created to represent the sample sandwich panel. Two face sheets of 3.0 mm thickness were glued to the internal core comprising a 3.0 mm cell arrangement. The overall height of the core was 19.0 mm. The entire geometry was built as a single solid object. The boundary conditions of four sides were assigned as simply supported. A 3.0 mm mesh was assigned during the analysis to achieve a high-quality mesh. The quality mesh is essential to obtain more accurate results in numerical analysis.

Figure 4-7: Flow diagram for finite element modeling

Table 4-3: Selected different core arrangements and sizes

	Square Arrangement	**Rectangular Arrangement**	**Circular Arrangement**	**Honeycomb Arrangement**	**Triangular Arrangement**
Plan view	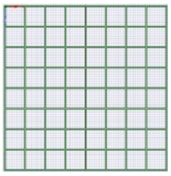	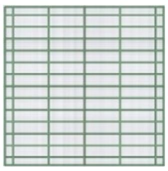	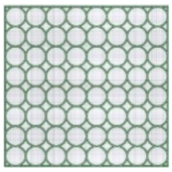	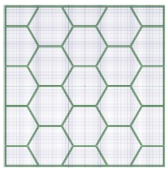	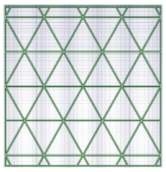
3D view	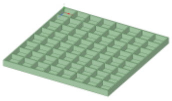	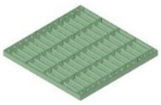		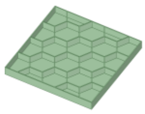	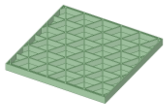
Selected Sizes (mm)	25x25	20x60	25	50	25
	30x30	30x90	50	60	50
	40x40	40x120	75	75	75
	50x50	50x150	100	100	100
	80x80	60x180	125	125	125
	100x100	70x210		150	
	125x125	80x240			
		90x270			

4.3.1 Engineering data

Assigning engineering data to the software is the first step of the process. So, the coir fiber polymer composite material properties were assigned to the software. The value of density, young’s modulus, and Poisson's ratio of the composite material was assigned as 915 kg/m^{3,} 0.380 GPa, and 0.3, respectively [175], [176]. The density value was evaluated experimentally using a simple density test, and the young's modulus of the material was found using a tensile test conducted under section 4.2.3.1. The Poisson's ratio was extracted from past literature [177].

4.3.2 Finite element model

The 3-dimensional finite element models were developed to evaluate sandwich panels' total deformation and maximum bending stress. Figure 4-8 shows the finite element model of the sandwich panel.

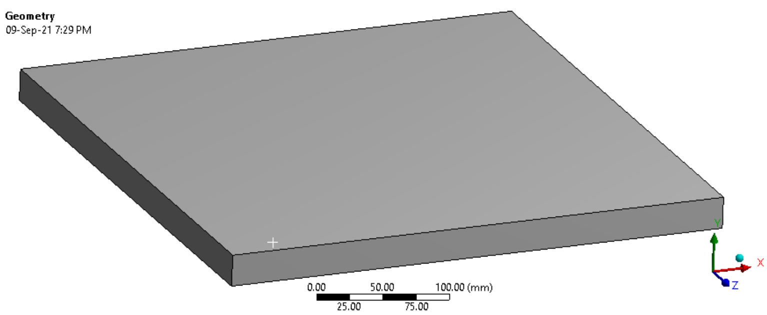

Figure 4-8: Finite element model for sandwich panel

4.3.3 Support conditions

Before starting the flexural test, the support conditions were assigned to the numerical model. During this analysis, one edge of the panel was displacement restrained in all x, y, and z directions. The edges on the other three sides were displacement restrained only in the y-direction, as shown in Figure 4-9.

.

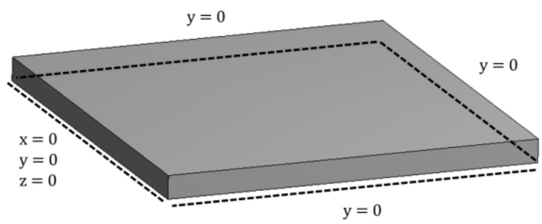

Figure 4-9: Boundary conditions of the model

4.3.4 Loadings

A uniformly distributed load of 1 kN/m^2 was applied to the panel to study the flexural behavior and deformation of the panel. Figure 4-10 shows the assigned load on the numerical model.

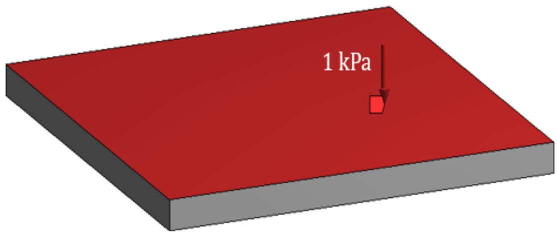

Figure 4-10: Applied load on the model

4.3.5 Solving and outputs

The model was solved using "Ansys Mechanical." This is a separate tool for analyzing the structural elements in Ansys. The solving time depends on the mesh quality and geometry. The 3.0 mm mesh was assigned to achieve the most accurate results. The model was run, and output results were observed. Von missed stress, and the total deformation was received as the output of this analysis.

4.3.6 Results and discussion

Evaluated the flexural stresses relevant for the five different core arrangements. Then, studied the flexural stresses by changing the cell sizes in each core arrangement. The core arrangement, which consists of the least volume, including maximum flexural stress per unit load, was selected as the optimum core arrangement. The deformed amount was compared to check the serviceability criteria.

4.3.6.1 Flexural stresses in different cores

Sandwich panels with five different core arrangements with varying sizes of cell were analyzed using the Ansys workbench, and the results were obtained. This Ansys workbench is the primary tool in Ansys software to guide static structural analysis. After processing the software, the maximum von mises stress was obtained by applying a 1kPa uniformly distributed load. The analysis recorded the flexural stress and the corresponding load on the panel of the bottom side of the top face sheet's midpoint were recorded. Thirty-one different core sizes from five different shapes of core arrangements were analyzed. This is shown in Table 4-4. after that, the results von mises stress of all thirty-one panels are shown in Annex 1. Table 4-5 summarizes the von mises stress of all five core arrangements with different core sizes. The von mises stress variations of five different core arrangements Vs. Core sizes in the flexural analysis are graphically interpreted in Figure 4-11.

Table 4-4: Core arrangement with core configurations

The shape of the core arrangement	**Nos of core configurations**
Honeycomb	6
Square	7
Triangular	5
Rectangular	8
Circular	5
Total	**31**

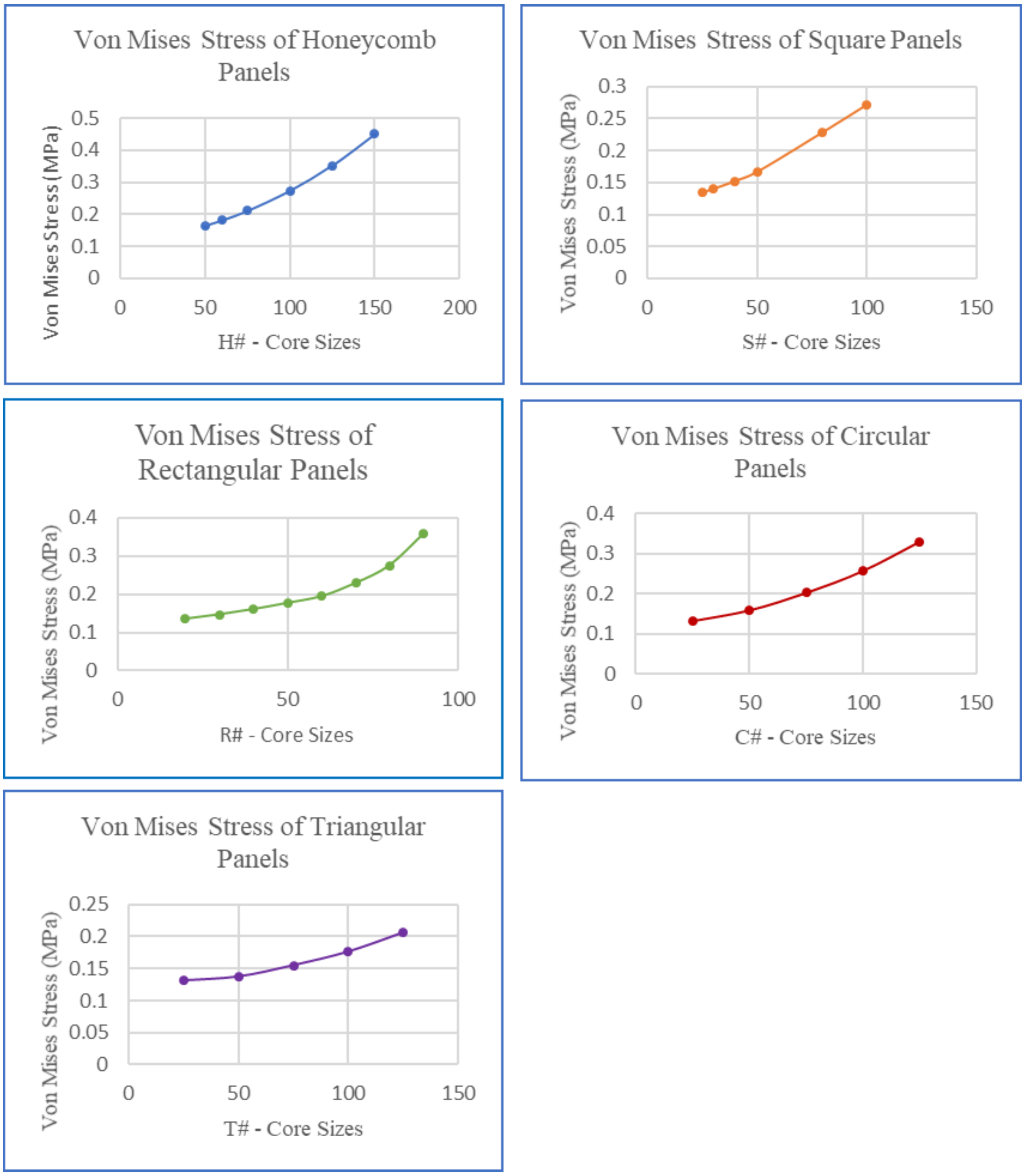

Figure 4-11: Graphical representation of maximum stress variation with core size

Table 4-5: Summary of von mises stress in all panels

Honeycomb		**Square**		**Triangular**		**Rectangular**		**Circular**	
Distance between parallel side (mm)	**Von Mises Stress (MPa)**	**Side length (mm)**	**Von Mises Stress (MPa)**	**Side length (mm)**	**Von Mises Stress (MPa)**	**Width x length (mm)**	**Von Mises Stress (MPa)**	**Diameter (mm)**	**Von Mises Stress (MPa)**
50	0.164	25	0.135	25	0.131	20x60	0.135	25	0.133
60	0.181	30	0.140	50	0.137	30x90	0.147	50	0.159
75	0.211	40	0.152	75	0.155	40x120	0.161	75	0.203
100	0.273	50	0.166	100	0.176	50x150	0.177	100	0.258
125	0.353	80	0.229	125	0.206	60x180	0.194	125	0.330
150	0.449	100	0.271			70x210	0.219		
		125	0.354			80x240	0.275		
						90x270	0.358		

4.3.6.2 Deformations of different core arrangements

Figure 4-12 to Figure 4-16 shows the variation of deformation with all cell sizes of five different core arrangements. Figure 4-17 shows the graphical presentation of deformations, while Table 4-6 shows the summarized deformation values in other cell arrangements. According to the results obtained, the reduction of cell sizes of the cores causes the reduction in the deformation and Von mises stresses of the model.

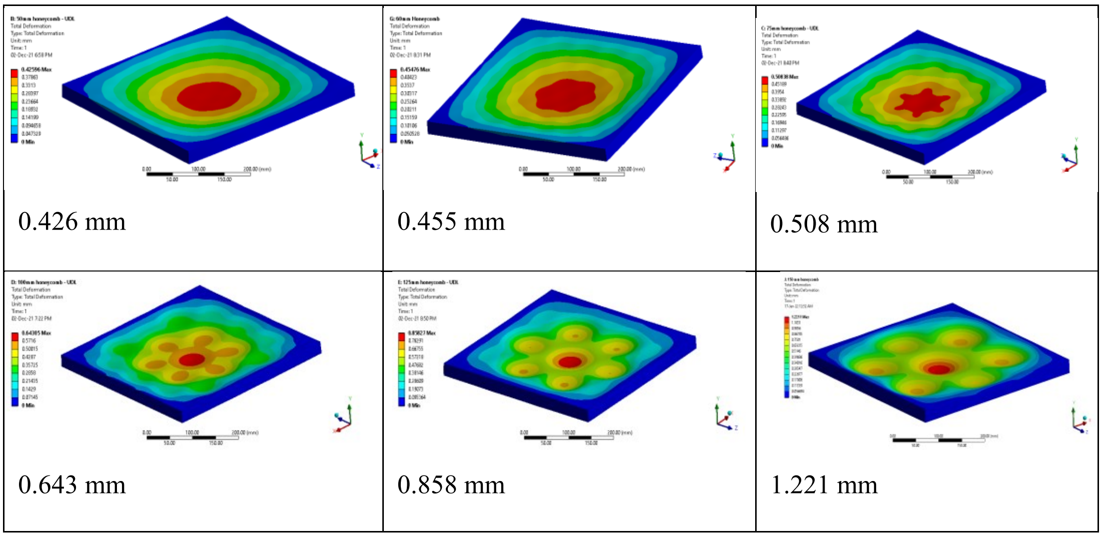

Figure 4-12: Max deformation of honeycomb panels

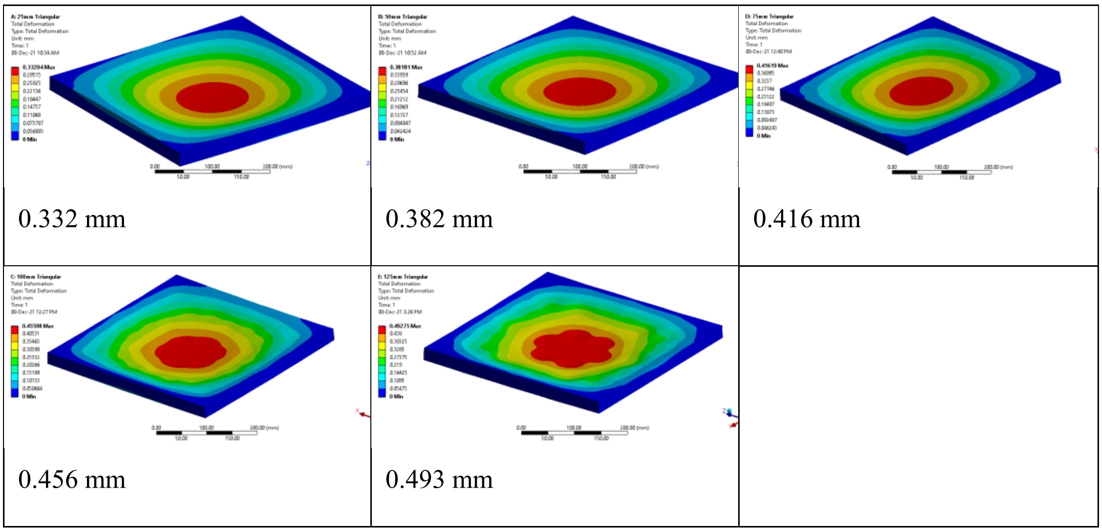

Figure 4-13: Max deformation of square panels

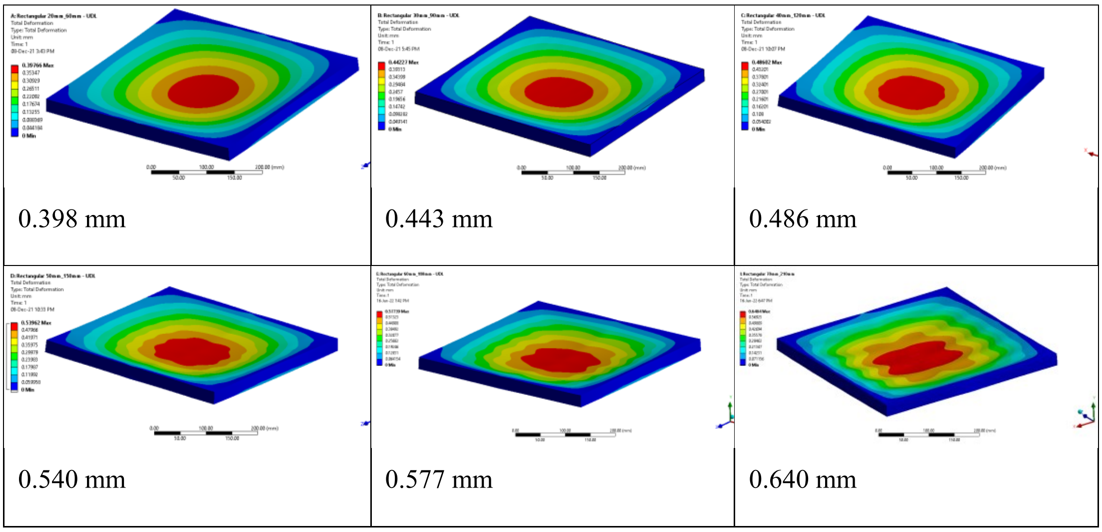

Figure 4-14: Max deformation of triangular panels

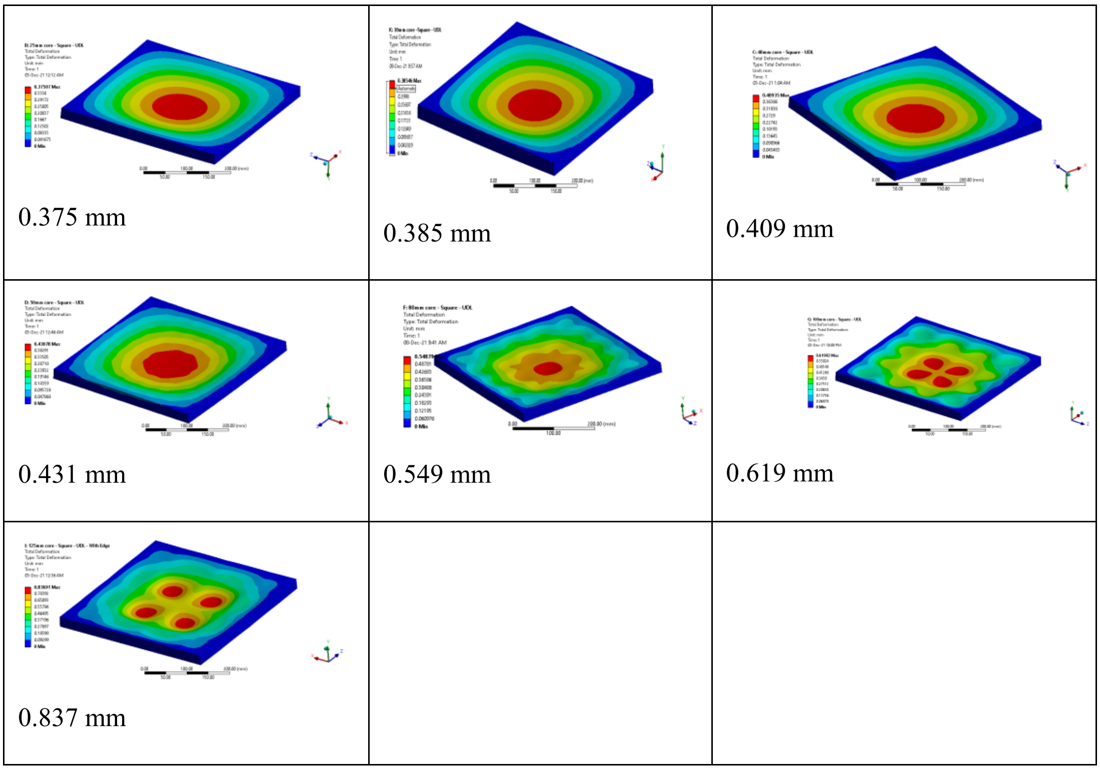

Figure 4-15: Max deformation of rectangular panels

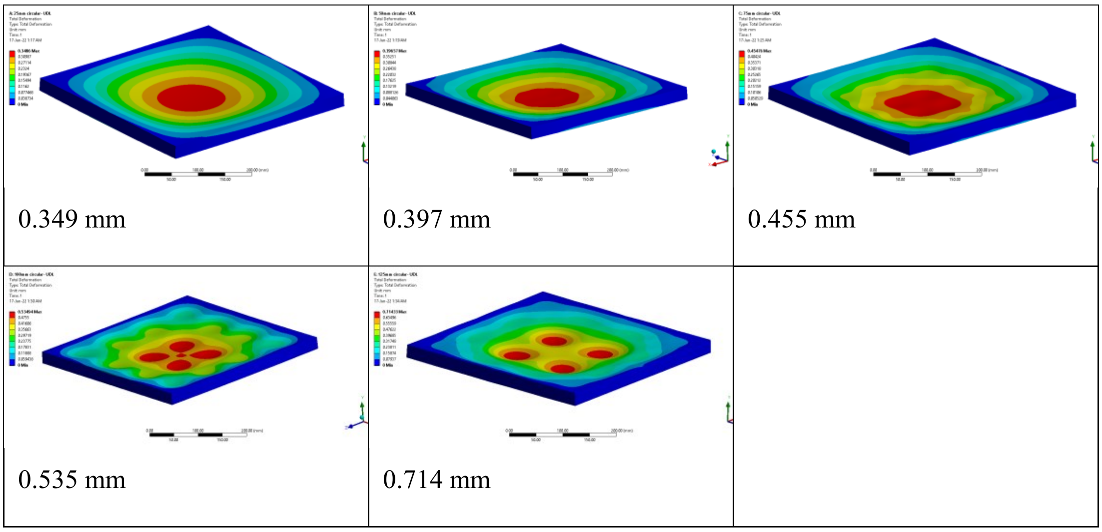

Figure 4-16: Maximum deformation of circular panels

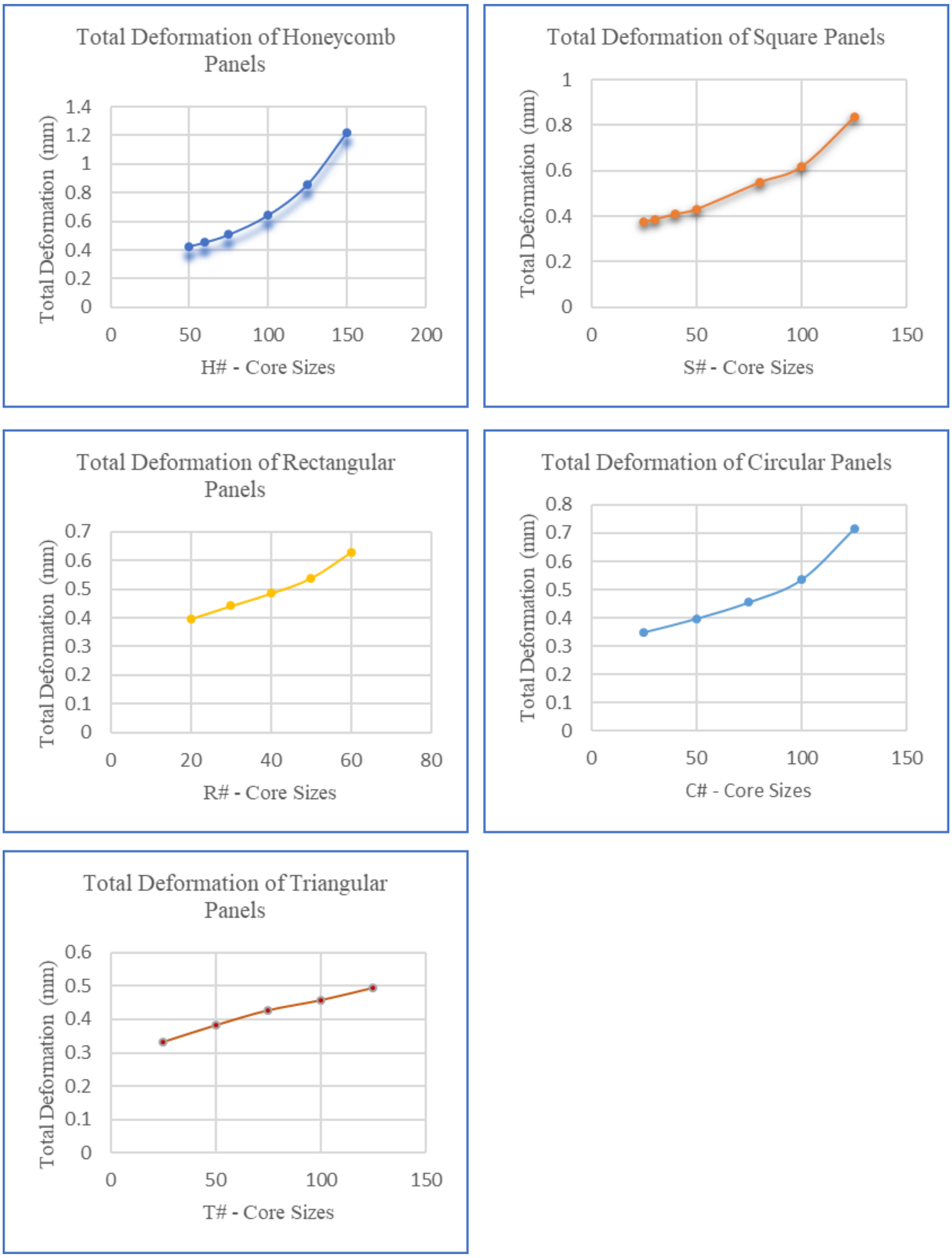

Figure 4-17: Deformation variation with different cell sizes

Table 4-6: Summary of deformation in different cell arrangements

Honeycomb		Square		Triangular		Rectangular		Circular	
Type	**Deformation (mm)**	**Type**	**Deformation (mm)**	**Type**	**Deformation (mm)**	**Type**	**Deformation (mm)**	**Type**	**Deformation (mm)**
H50	0.426	S25	0.375	C25	0.349	R20	0.398	C25	0.349
H60	0.455	S30	0.385	C50	0.397	R30	0.442	C50	0.397
H75	0.508	S40	0.409	C75	0.455	R40	0.486	C75	0.455
H100	0.643	S50	0.431	C100	0.535	R50	0.540	C100	0.535
H125	0.859	S80	0.549	C125	0.714	R60	0.640	C125	0.714
H150	1.221	S100	0.619						
		S125	0.837						

4.3.6.3 Variation of panel volume with maximum stress

The volume variations of the panel with von mises stress are graphically represented in Figure 4-18. It reveals that when volume reduction in the sample panel reduces, von mises stress increases gradually and then comes to a constant value. Since the main objective of this study is to develop the most economical, practically possible, lightweight panel wall with optimum flexural properties, consideration of the minimum volume of the panel is very important. Therefore, a minimum volume with acceptable stress will be the most suitable arrangement. If the volume of the panel wall is minimum, then the weight of the panel wall and material usage will be less. In this situation, the material cost and overall energy also will be less.

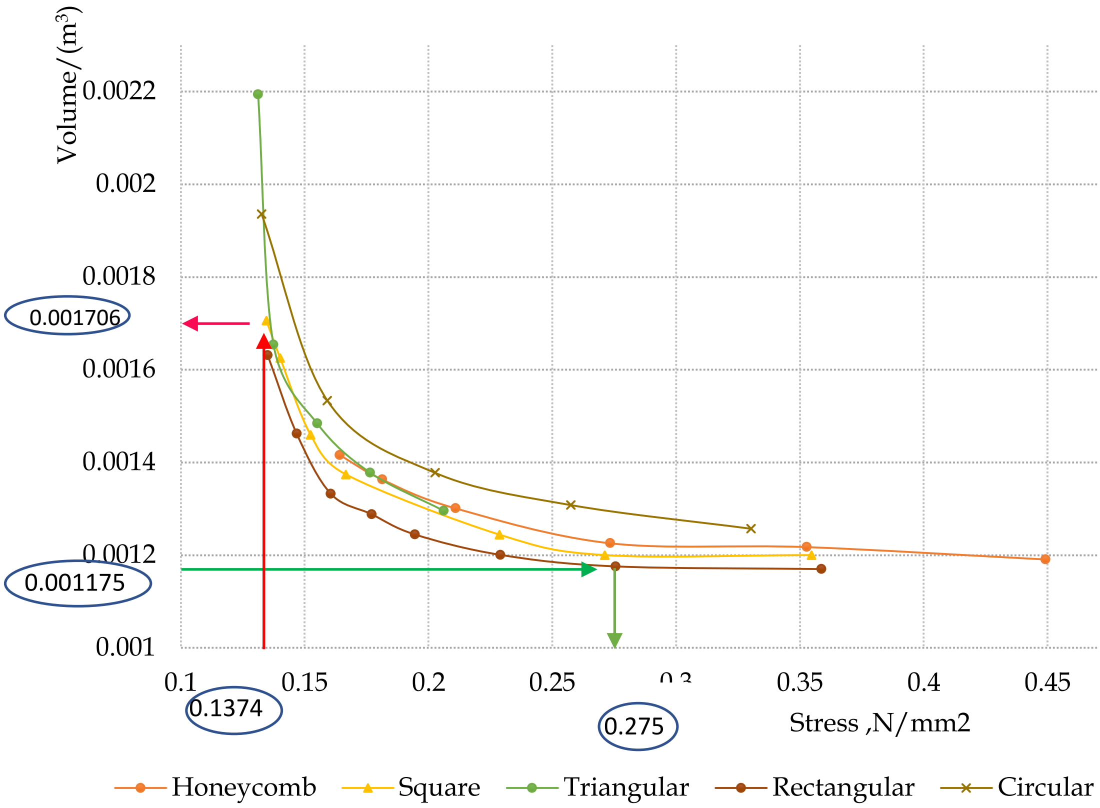

Figure 4-18: Volume of panel wall Vs. Maximum bending stress

When comparing square, rectangular, and honeycomb core arrangements, a significant volume variation cannot observe. The volume of the panels is almost similar to the stress increment. When the stress value is beyond 0.275 MPa, the constant volume of each cell arrangement is observed. Then, any of these core arrangements can be selected considering the volume. However, it should be a practically possible core arrangement.

If we consider the minimum stress in the square core arrangement, which is 0.1374 MPa then the volume is 0.001706 m^3, which is relevant to the 30 mm by 30 mm core size. If this 30mm core arrangement promotes, then production cost and material utilization will be high and also difficulties in manufacturing. Once we select the minimum volume of square core arrangement, then the relevant stress is to be 0.275 N/mm^2. And this value corresponds to the 100 mm core arrangement. So, this shows the least volume of panel walls. Then the cost of the production will be less, and the manufacturing process will be straightforward compared to the 30 mm square core arrangement. Hence, the most suitable core arrangement is square one when choosing the practically possible core arrangement because manufacturing and fabrication is very easy. So, the square core arrangement was selected to develop the panel wall. Figure 4-19 shows the total deformation Vs. Cell sizes in square panel sample.

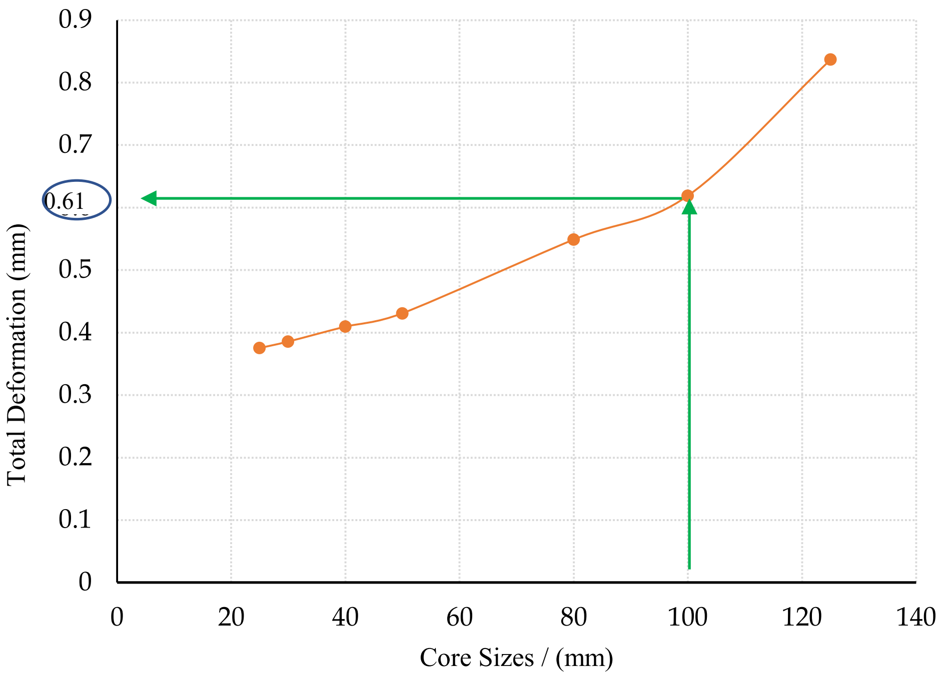

Figure 4-19: Total deformation Vs. core sizes in square panel

4.3.6.4 Check for serviceability requirement

Under the serviceability check, the selected cell arrangement should be satisfied the serviceability requirement according to the building code 2006. For that, deformation behavior was studied. Then, it was observed that the deformation of the 100 mm cell arrangement is 0.61 mm. However, the limiting deformation value in the panel based on building code 2006 is given as (span / 240), which is 1.667 mm. Hence the panel is within the limit.

4.4 Chapter Summary

The different types of sandwich panels are available in the world for a variety of requirements. The usage of the sandwich panel in the construction industry is very rear. Hence, this study aims to develop a partitioning panel wall with better flexural performance using the sandwich panel concept and fill the construction industry's gap. The sandwich panel consists of two face sheets and an internal core arrangement. Hence, panel walls were also developed using a similar concept. Selection of the most suitable inner core causes provides better bending stiffness. Numerical modeling was used to choose the most appropriate internal core arrangement to optimize the flexural properties. Considering the weight and flexural properties, the 100 mm x 100 mm square core configuration was selected as the optimum solution. During this process, young’s modulus was calculated for the particular composite samples. In the end, check the flexural strength and deformations. The deformation should be within the limited serviceability requirements.

5 PREPARATION OF SAMPLE PANELS AND ANALYSIS OF FLEXURAL PERFORMANCE

5.1 General

After developing composite material and selecting a suitable core arrangement, the next step was to develop the panel wall. The panel wall consists of 2 face sheets, including an internal core arrangement. The 3 mm thick composite sheets were utilized for the development of the panels. Initially, the sample panel wall was prepared manually, and then the sample panel wall was prepared using a developed mold. The mold was prepared in the die and mold section in the University of Moratuwa mechanical department, and the 3-point bending test was carried out to investigate flexural performance. This was carried out in the structural laboratory of the Dept. of civil engineering. In the end, the flexural properties of the existing selected panel wall (Durra panel wall) with the FRPC panel wall were compared. The bending stiffness is the main mechanical property of the non-load bearing wall, and research focuses on optimizing the flexural properties.

5.2 Sandwich panel preparation and testing

Fabrication of sandwich panels using 3 mm face sheets, and 19 mm x 19 mm squire core was carried out manually. The composite sheets were developed in 400 mm by 400 mm size according to the procedure described in section 3.3. These composite sheets were used as outer face sheets of the sandwich panel. The same composite sheets were cut into 19 mm strips to fabricate the square core arrangement. Figure 5-1 shows the mild steel molds used to manufacture the composite and prepared composite sheets.

.

Figure 5-1: Mild steel mold with cover plates and prepared composite sheets

5.2.1 Preparation of panel manually

The composite material and panels are prepared manually. The composite material was cut into 19 mm strips to prepare the internal core in the panel. Epoxy glue was used to attach the core to the face sheets. Figure 5-2 shows the manual sandwich panel preparation process.

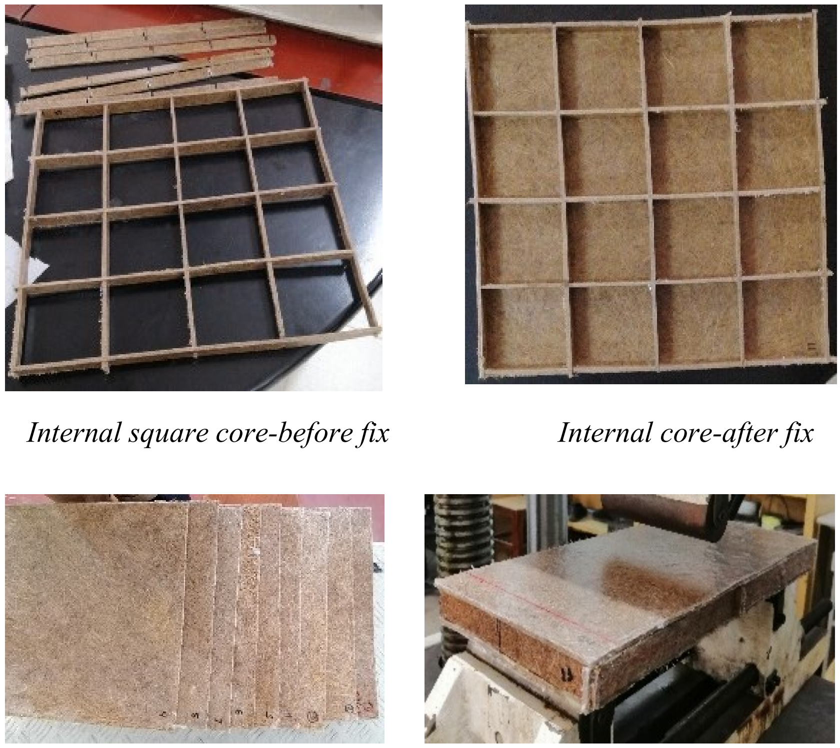

Internal square core-before fix *Internal core-after fix*

400 mm x 400 mm composite sheets *Prepared half sandwich panel*

Figure 5-2: Manual sandwich panel preparation process.

Different adhesive materials shown in Figure 5-3 like epoxy resin and hardeners (Figure 5-3(a-c)), special arylene glue (Figure 5-3 (d)), and blistering glue (Figure 5-3 (e)) were progressively used to check the bond performance between face sheets and core arrangement. Then, it was realized that the different kinds of slow-curing epoxy glues are the most suitable to glue the FRPCs. The “EPI-FIX” adhesive with low hardener proportion was used as an adhesive material. Adhesive material was prepared by mixing 50 % epoxy with 50 % hardener and arranging the curing time for 72 hours for proper bonding.

Epoxy resin and hardener *Special arylene* *Blistering glue*

Figure 5-3: Different types of glue.

5.2.2 Testing of manually prepared samples

After the preparation of the panels, the 3-point bend test was carried out to investigate the flexural performance. The bending test equipment “INSTRON tester, Model 4465” was used for this testing process, and the five numbers of samples of 400 mm x 200 mm x 25 mm were tested. Figure 5-4 shows the sample arrangement for the testing work.This test series observed debonding failure between core and face sheets. Figure 5-5 illustrates the debonding failure of the core and bottom face sheets. This occurs due to the weakness of the adhesive material and poor bond between composite material. After this bonding failure, the continuous deformation could be observed without further increment of applied force. So, the correct flexural capacity of the panel couldn’t be present due to this phenomenon. Hence, the next step was to develop the sandwich panel by minimizing the bond failure. So, an alternative method was adopted to fulfill this requirement. For that, developing the sandwich panel in a monolithically cast was significant.

Instron Tensile equipment *Sample before testing*

Figure 5-4: Sample arrangement for the testing work

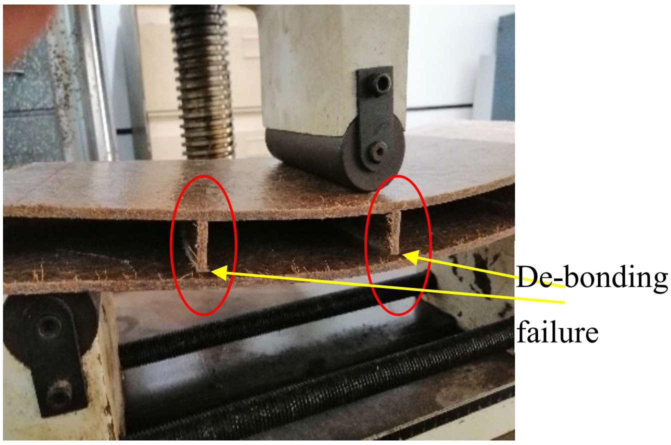

Figure 5-5: De-bonding failure between core and face sheet

5.2.3 Panel wall preparation using the mold

This alternative method was selected to minimize the debonding failure between face sheets and the internal core. The concept was to develop the male and female molds. The final output was to develop the sandwich FRPC panels by combining both male and female panels.

5.2.3.1 Preparation of aluminium mold

Another technique was used to develop the panel walls to minimize the debonding failure. The 30 mm thick two aluminium plates were used for this process. Aluminium is a material that has less tendency to stick the polymer composite material [178]. The handling of these aluminum molds is very easy due to less weight.

5.2.3.2 Preparation of program by "SolidWorks 2018"

A computer program was required to machine the aluminium plates according to the required mold shape. The "*SolidWorks 2018*" is a solid modeling computer-aided design (CAD) and computer-aided engineering (CAE) software. This software was used for this machining work. This software helped to check the pre-arrangement of the mold's digital model and the preferability of using the actual model. Figure 5-6**Error! Reference source not found.** shows the digital pictures of the model in the *" SolidWorks 2018"* interface. After writing the program, the ARIX CNC milling machine was used to cast the mold. Since the tools are costly and machines consume high electric power, try to minimize the repetitive work.

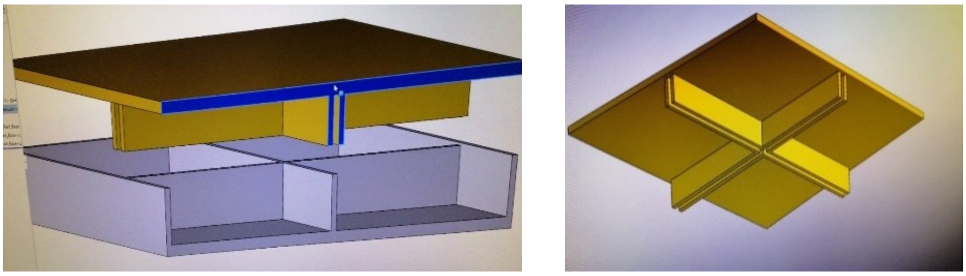

Figure 5-6: Graphical interpretation of mold

5.2.3.3 Surfacing of Aluminium sample to prepare the mold

The two aluminium plates were purchased from "Swistech Aluminium" Pvt Ltd in Sri Lanka. Figure 5-7 shows the photograph of a 450 mm x 250 mm x 30mm aluminium plate. Mold preparation work was carried out "Die and mold section" in the University of Moratuwa mechanical department. The two aluminium plates were fixed to the CNC milling machine and smoothened all surfaces to remove the surface irregularities. Figure 5-8 shows the smoothing process of the aluminium sheet using CNC milling machine to cast the mould.

Figure 5-7: Aluminium plates 450mm x 250 mm x 30mm

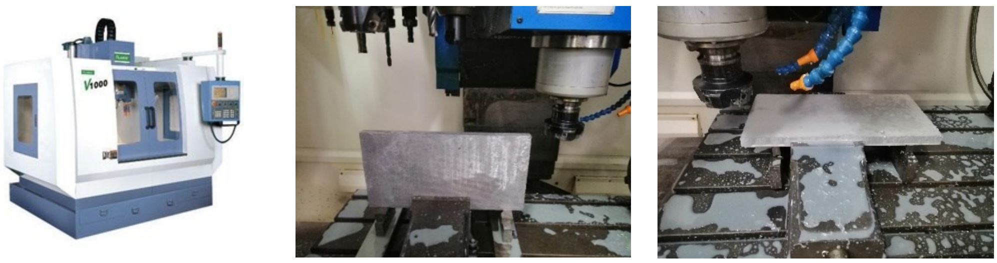

CNC milling machine *Smoothing side faces* *Smoothing surfaces*

Figure 5-8: Aluminum sheet smoothing process

5.2.3.4 Casting the mold

This casting process was carried out using fully automated computerized milling machines (ARIX CNC machine Co. Ltd). This has been installed in the Die and molding section in the University of Moratuwa mechanical department. The 200 mm x 200 mm size male and female molds were prepared. These molds were used to prepare the panel samples monolithically. Figure 5-9 shows the casting process of the mold using a milling machine and prepared male/ Female molds.

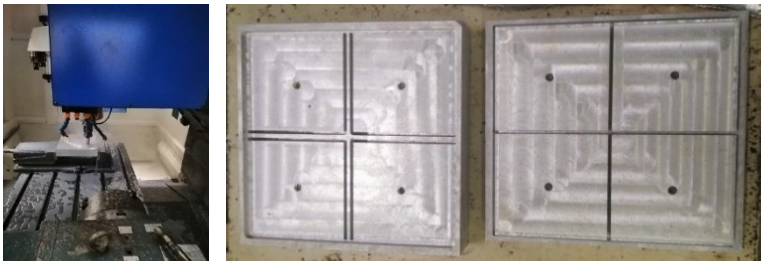

Figure 5-9: Casting work process of the mold and male and female molds

5.2.3.5 Preparation of panel wall sample

The male and female panel samples were developed using these molds. This method was adopted to rectify and minimize the bond failure of the panels. The top and bottom faces were firmly bonded to the internal core due to this method. Figure 5-10 shows the process to prepare the panels using aluminum molds.

Mold placed in hot press equipment | *Male panel .* | *Female panel*

Figure 5-10: Process to prepare the panels

5.2.4 Testing of molded sample

The three-point bend test was carried out for the 200 mm x 200 mm samples illustrated in Figure 5-11. Five samples were tested, and failure loads were noted down. The average failure load of all five samples was 1.1 KN. Then flexural strength was calculated using simple bending formulae, and the flexural strength at the failure was 3.4228 N/mm^2. During this testing process, debonding failure was not observed. The displacement was also noted. When the load is gradually increasing, the displacement value is also increasing.

Figure 5-11: Three-point bend test setup

5.2.5 Comparison of flexural strength with available panel walls

Since the durra panel is the most used panel wall in Sri Lanka, it was decided to find out the flexural strength of the Durra panel by using a 3-point bending test, which was carried out in the structural laboratory of the University of Moratuwa. The Durra panel is the most famous non-load-bearing wall in Sri Lanka. The other selected few types of panel walls such as Acotec panels, Micro panels, and EPC panels' flexural strengths were extracted based on literature.

Five numbers of Durra panels were tested, and failure loads were recorded. Figure 5-12 shows the 3-point bend testing procedure. The average flexural strength was calculated using simple bending formula. The maximum average failure load was 900 N, and the estimated maximum flexural stress was 1.215 N/mm^2. The flexural strength at the failure stage was compared with the average values of FRPC panel samples. The FRPC panel showed the 3.423 N/mm^2 flexural strength. When we compare both values, the FRPC panel showed 2.8 times higher values than the durra panel. Table 5-1 shows the flexural strength of the existing panel wall, and compared values were taken up to study the percentage increment of the FRPC panel. The FRPC panel shows better performance concerning flexural strength. According to the flexural strength shown in Table 5-1, it can be concluded that the innovative FRPC panel shows better flexural performance than all the other selected panels.

Durra board samples *Sample on the testing machine* *Failed sample*

Figure 5-12: The 3-point bend test for durra panel

Table 5-1: Flexural strength of available panels

Panel type	**Flexural strength / (N/mm^2)**	**Variation % comparative to the Durra**
Durra	1.215	100 %
Acotec panel	1.080	-
Micro panel	1.700	40 %
EPCI panel	1.800	48 %
FRPC panel	3.423	280 %

5.3 Chapter Summary

This chapter explains two methods to prepare the panels and study the flexural performance. The first method was to prepare the panel manually. After preparing the panel sample, the axial load was applied using 3-point bending test equipment. Then is observed that it failed due to a weak bond between the core and the face sheets. Because of this situation, there was no possibility of investigating the flexural performance of the panel. So, another alternative method was adopted. That method was to prepare the panel in the molding method. This method helped to minimize the debonding failure and evaluate the flexural strength. The five samples were tested, and average values were taken. This average value needed to be compared to existing panel walls in Sri Lanka.

The most famous and mostly used panel wall in Sri Lanka is Durra boards. Similarly, the five samples were arranged from Durra boards and underwent the 3-point bend test. Then studied the flexural performance and compared them with FRPC panels. The flexural strength of the Durra panel was 1. 215 $N/mm^{2,}$ and the FRPC novel panel was 3.432 N/mm^2. These results revealed that the novel FRPC panel has 2.8 times higher flexural capacity than the Durra panel.

6 FINANCIAL FEASIBILITY AND EMBODIED ENERGY

6.1 General

The production cost for the FRPC panel wall was calculated. Then the cost-benefit analysis was carried out by comparing the cost of the Durra panel wall. The calculated production cost was used to evaluate the Life Cycle Cost for the developed panel wall.

The previous chapter discussed the way to develop the sample panel, which was the outcome of this research study. The calculation of the life cycle cost of this novel product is a vital factor after concluding the right mix proportion of the material and optimizing the construction technologies. As a result, this section aims to determine the actual value of the overall life-cycle cost of panel walls and compare it with the Durra panel wall used in today's construction. After that, the embodied energy of FRPC was analyzed.

The initial production cost of the panel wall was estimated using the 2022-year market values of materials. The most suitable mix design for the composite material is 7:3 polyethylene to coir and 3 cm length of coir, prepared under 4 MPa pressure maintaining 140^0 C temperature. The recommended processing time is 6 min. These parameters were considered for these analyses. This chapter illustrated the cost-benefit analysis, LCC analysis, and EE analysis.

6.2 Evaluate the cost of the product

The production cost for the FRPC panel was calculated and compared with the Durra panel wall. The cost calculation was carried out for the 1.2 m x 2.4 m x 3 mm panel wall. The required area of the 3.0 mm composite sheet is 6.92 m^2 to develop the panel in the above size.

So, the required weight of coir and polyethylene amount was calculated following selected mix design parameters. The LDPE of 16.131 kg and coir of 6.92 kg are required to develop the panel wall. The following calculation shows the total cost incurred for the panel development. In the end, it was revealed that Rs. 4,8785.21 needed to be spent to prepare the 1.2 m x 2.4 m x 3 mm panel wall.

Cost Calculation for 1.2 m x 2.4 m x 3 mm panel wall

i. Required composite panel area:

Face sheets and thickness of the core	=	3	mm
Total area of both face sheets	=	1.2 x 2.4 x 2	
	=	5.76	m^2
Total area of core	=	(2.4 x13 + 1.2 x 25) x 0.019	
	=	1.16	m^2
Total area of panel (1.2m x 2.4)	=	(5.76+1.16) = 6.92	m^2

ii. Cost of the panel wall

Mix proportion	=	7:3 (LDPE : Coir)	
Material requirement	=	533 g	
(400 mmx 400 mmx 3 mm sheets)			
Required material for 1 m x 1 m	=	3.331	Kg
LDPE requirement for 1 m x 1 m	=	2.331	Kg
Coir requirement 1 m x 1m	=	1.000	Kg
LDPE requirement for panel	=	16.131	Kg
Coir requirement for panel	=	6.920	Kg
Cost for LDPE	=	Rs. 65.00	Per Kg
Cost for Coir	=	Rs. 375.00	Per Kg
Total cost for 1.2 m x 2.4 m panel	=	Rs. 3,645.51	
Electricity + Labour	=	Rs. 1,235.00	
Total cost for one panel[only process]	=	Rs. 4,878.51	

The Durra panel wall was manufactured in Minneriya [8.0387° N, 80.9064° E], Polonnaruwa. Therefore, the current market price of the Durra panel was obtained and shown in Table 6-1.

Table 6-1: The current market price of the durra pannel

EFFECTIVE FROM 25th APRIL 2022

#	Product	Thickness	Size	Price at Colombo		
		mm	mm	Without Taxes	VAT @ 8%	With Taxes
1	DURRA - Standard Panel (8' x 4')	50	2438 x 1187	5,830.00	466.40	**6,296.40**
2	DURRA - Standard Panel (8' x 4')	58	2438 x 1187	5,940.00	475.20	**6,415.20**
3	DURRA - Standard Panel (9' x 4')	58	2743 x 1187	6,680.00	534.40	**7,214.40**
4	DURRA - Standard Panel (10' x 4')	58	3048 x 1187	7,425.00	594.00	**8,019.00**
5	# DURRA - Standard Panel (11' x 4')	58	3353 x 1187	8,165.00	653.20	**8,818.20**

According to the given price list, the price of the 1.2 m x 2.4 m x 50 mm thick panel wall, excluding taxes is Rs.5,830.00 at the factory. However, the total cost for a novel FRPC panel wall is Rs. 4,878.51. So, there is a saving of Rs. 951.49 per panel. We can achieve cost savings on partitioning walls by replacing Durra panel walls with FRPC for the high-rise buildings.

6.3 Life cycle cost (LCC) calculation

The design life of the building is given as a fifty-year life cycle according to British standards. Since none of the chosen panel walls have a life cycle of fifty years or more, the replacement cost of panel wall materials must be factored into the LCC measurement process. Further, necessary maintenance costs also were included while calculating the total life-cycle cost of the building.

The total cost of a panel wall over its lifetime, including preparation, construction, procurement, operations, repair, disposal, and any residual value can be specified as the LCC [179]. The amount of the construction expense and the combined sum of operating expenses, electricity costs, and other recurring costs, minus any disposal value at the end, is the net cost of acquiring and repairing a building throughout its life [179], [180], which is given in

Equation 6-1.

$$LCC = Ic + (Mc + Ec + Cc + Oc) + Uc - Rv$$

Equation 6-1

where,

Ic - The initial cost, Mc - maintenance costs,

Ec - The energy costs, Cc - The cleaning costs,

Oc - The overhead and management costs, Uc - The utilization costs,

Rv - The resale value

However, the [LCC = Initial Cost + Present value of (maintenance + demolition) Cost – Present values of Resale cost] equation was used to calculate LLC easily. Among several methods of calculating the LCC exists, the Net Present Value (NPV) method was used to calculate the present value's maintenance and demolition costs [181]. Assuming the resale value after 50 years is negligible.

An investment's net present value [NPV] is the sum of capital that must be spent to satisfy all potential financial demands over the investment's lifetime. This is shown in Equation 6-2.

$$\mathrm{NPV} = \sum_{t=0}^{T} \frac{C_t}{(1+r)^t}, \qquad \textit{Equation 6-2}$$

Where;

C_t - The estimated cost in year t

r - The discount rate

T - The period of analysis in years

The above calculation considers the amount of interest that would be paid on the money spent. In reality, the hateful effect of inflation will erode the value of our investment. As a result, the above formula must be modified by a factor that accounts for inflation. Inflation would raise prices in year "n", resulting in a higher current investment level. The modified factor is known as the "net of inflation discount rate" [NDR], which is shown in Figure 6-3.

$$\text{NDR} = \left(\frac{1 + \text{int}\%}{1 + \text{inf}\%} - 1\right) \qquad \textit{Equation 6-3}$$

where,

int % - The interest rate and inf % - the inflation rate.

This calculation determines LCCs by subtracting the resale value from the original cost-plus repair and recovery costs. A survey was carried out to collect cost information from supplies. Labour costs are determined by a leading construction firm in Colombo that is familiar with current prices. Previous scholarly data were used to collect information about the life span of wall panel components, and facility managers provided forecasts of repair costs [182], [183], [184].

In this study, LCC was calculated on the sample panel wall. In Sri Lanka, reusing building materials is primarily an informal sector practice. As a result, there are no readily accessible and credible sources of price and recyclability statistics in practice. As a result, the reusability was only assessed in terms of potential use. Owing to their ambiguity in alternate reuses, the other alternative reuses or recycles are omitted [182], [185], [184]. The lifetimes and reusability factors were assumed as 50 years and 0.0%, respectively for both the materials. The NPV is worked out based on a discount rate of 4.7 %. Here, consider the 50 years lifetime for a novel panel wall, and the life cycle cost was calculated using the above equation. Summary calculations with details is given in Table 6-2. LCC for novel panel = Rs. [4,878.51 + 8,146.08 + 50.31] – Rs. 0.00 = Rs. 13,075.00. The calculated LCC for the FRPC panel wall is around Rs. 13,075.00.

Here, consider the 50 years lifetime for durra panels based on their manufactures guarantee period. Similarly, the LCC was calculated using this [LCC = Initial Cost + Present value of (maintenance + demolition) Cost – Present values of Resale cost] equation, and maintenance cost was calculated using the NPV method. Factory BOQ value was taken as the initial cost of the product, and assuming the resale value of durra panel after 50 years is zero. Therefore, the calculated LCC value for the Durra panel is Rs. 14,415.92.

According to the previous calculation, LCC for the novel panel is Rs 13,075. When considering the 50 years lifetime, we can have around Rs.1,340.92 cost savings by adopting the navel panel. Details for the cost calculation for the durra panel are given in Table 6-3.

LCC for the Durra panel = Rs. [5,830.00+ 8,535.61 + 50.31] – Rs. 0.00

= Rs. 14,415.92

LCC for the novel panel = **Rs. 13,075.00**

Cost different = **Rs. 1,340.92**

Table 6-2 Details for the LCC calculation in novel panel

FRP composite panel	Initial cost	Rs. 4,878.51	Including Material cost & Transportation cost & Production cost (Lab scale production)
	Maintenance cost –Waterproofing material application	10 yr frequencies Rs.5,280.00/m^2 –both side, each 10 years	The waterproofing manufacturer gives 10 yr warranty
	Maintain aesthetic appearance		Colour washing is not required
	Demolition cost	Rs. 500.00 –only 50th year	Utilize one labor for Max. 1 hrs.
	Resale Value	Rs. 0.00	Difficult to use for usable work

Table 6-3: Details for the LCC calculation in the Durra panel

Durra panel wall	Initial cost	Rs. 5,830.00	At factory BOQ cost according to manufacturer's details (Mass scale production)
	Maintenance cost	5 yr frequencies Rs.2,450/m^2 –both side, each 5 years	Colour washing is required
	Demolition cost	Rs. 500.00-only 50th year	Utilize one labor for Max. 1 hr time
	Resale Value	Rs. 0.00	Difficult to use for usable work due to this was made out of waste paddy straw and Kraft sheets

6.4 Embodied Energy of panel wall

Process analysis, input-output analysis, and hybrid analysis are the three most common approaches for analyzing EE [186]. The EE of a polymer reinforced composite wall panel was estimated using process analysis and compared with durra panels on the market. In-process analysis, the EE of a product was calculated by evaluating every activity that contributes to its production [187]. The input-output analysis employs an economic input-output table, which necessitates calculating the amount of energy consumed by the country's various sectors [188]. However, the data presented in Sri Lanka is insufficient to compile this table. [189] Furthermore, employing case studies to examine the EE of different products is not viable with this method [190]. On the other hand, the hybrid analysis combines process analysis and input-output analysis [191].

Quantitative, qualitative, and mixed methods are the primary methodologies in EE calculation. A mixed approach is a blend of quantitative and qualitative methods that links the gap between them [192]. Qualitative research is the way to go when a researcher needs to obtain information from a variety of people based on their experiences and perspectives [193]. Since EE is novel to the construction industry in Sri Lanka, it is required to gather the viewpoints of industry subject matter experts to achieve the research's goals. Hence, the mixed method is the best approach for this study.

6.4.1 **Embodied energy of FRPC panel wall**

Embodied Energy was calculated for panel wall incorporation of all manufacturing stages. The total energy of material at a given level becomes the embodied energy of the raw material. The data required to estimate the embodied energies were collected from coir fiber manufacturing factories and merchants using and developing polyethylene. Only three forms of energy are considered [194].

- The energy embodied in raw materials
- Transport energy for raw materials
- Energy for development of panel wall

Here, the EE of the FRPC panel wall, a size of 1 m^2 was used to calculate and compare with the Durra board of the same size. This EE calculation was carried out at different levels as above. The prepared coir was purchased from Gampaha [7.0840° N, 80.0098° E] area and transported to university of Moratuwa. The waste polyethylene was collected from Rapid creation, Homagama [6.8433° N, 80.0032° E]. The embodied energy of waste polyethylene is considered zero. The embodied energy calculations of individual materials used to prepare the 1.0 m x 1.0 m x 25 mm FRPC sandwich panel composite are below.

Embodied energy calculation

i. The total area of the panel required

Panel and core thickness	=	3	mm
Total area of both face sheets	=	1.0 m x 1.0 m x 2	
	=	2	m^2
Area of core	=	(1.0 x11 + 1.0 x 11) x 0.019	

	=	0.418	m^2
Total Area of Panel (1.0m x 1.0 m)	=	2.418	m^2

At the initial stage, LDPE's energy intensity and coir's energy intensity (at the shop) are assumed as zero (0 MJ/kg). So, the total embodied energy of material when purchasing is zero. It is required to calculate the EE for transporting material from the available location to UOM. Because the manufacturing process was carried out in UOM. The 750 kg mini truck was used for this purpose and consumed diesel as fuel. The energy intensity of a 750 kg mini truck is 3.2 MJ/ton/km [187]. The actual traveling distance for the material transportation was recorded based on the mileage readings of the used vehicles.

Mix Proportion (LDPE to Coir)	=	7 : 3	
Required amount of (Coir + LDPE) for 1 m x 1 m x 3.0 mm	=	3.331	Kg
LDPE requirement for 1 m x 1 m x 3.0 mm	=	2.331	Kg
Coir requirement for 1 m x 1m x 3.0 mm	=	1.000	Kg
Total Area of panel	=	**2.418**	**m^2**
LDPE requirement for panel	=	**5.636**	**Kg**
Coir requirement for panel	=	**2.418**	**Kg**

Based on the above LDPE and coir requirements, EE was calculated for the transportation of raw materials to the laboratory. Details calculation is given in Table 6-4. The shredder machine and hot press equipment were used to develop the composite material. The energy used for the shredder machine is 0.14 MJ/kg, and the energy used for the hot press machine is 1.75 KWh. The time spent cutting the 5.636 kg amount of polyethylene is 5 minutes, and the time spent preparing the composite from hot press equipment is around 40 minutes. Hence, the energy consumed to develop the required composite amount (2.418 m^2) is given in Table 6-5.

Table 6-4: EE for material transportation to the laboratory

Material	Quantity(kg) for 1 m^2 panel	Transport Distance(km)	Vehicle Used	Embodied Energy (MJ)
Coir	2.418	47 (Gampaha to UOM)	750 kg mini truck	2.418x47x3.2/1000 = 0.3636
Polyethylene	5.636	16 (Homagama to UOM)	750 kg mini truck	5.626x16x3.2/1000 = 0.28805
Total Energy for Transportation				**0.6516 MJ**

Table 6-5: EE to develop the composite

Machine	Required Wt/ kg/ m^2 panel	Time consumed/Minutes	Energy	Embodied Energy (MJ)
Hot-press	5.636 (Polyethylene)	40	0.14 MJ/kg	5.636 x .14 = 0.789
Shredder	2.418 (Coir)	5	1.75 KWh	$1.75 \times 60 \times 5 / 10^3 =$ 0.525
Total Energy for composite preparation / MJ				**1.314 MJ**

The sandwich panel was prepared manually. The skilled labours were utilized. After incorporating all the energy incurred to develop the sandwich panel, the final energy utilized for the panel comes as a summation of the above-described sub-items.

Therefore, the final embodied energy to develop the 1 m x 1 m x 25 mm thick panel wall is 1.9656 MJ (0.6516 + 1.314).

6.4.2 **Embodied energy of selected durra panel**

A documentary review was necessary to determine the EE of Durra panel walls. The work norms and rates for the durra panel board were collected from the ICC Pvt Ltd, Kohuwala, Nugagoda [6.8625° N, 79.8855° E]. The Selected panel size was 1m x1 m. According to their guidelines, the following data (per annum) was used to calculate Embodied Energy.

- Actual billing data for Electricity and Water
- Actual materials used (Straw, Glue, Paper)
- A total of $1m^2$ of board produced
- Greenhouse gas coefficients for Victoria (AGO 2004)
- Embodied energy values for raw materials (Straw, Glue, Paper)

The Durra panels have low embodied energy compared to alternative building materials, a commonly used non-load-bearing walling material in Sri Lanka. Embodied Energy is the energy consumed by all of the processes associated with manufacturing and delivering the product to the site. The EE was calculated as shown below.

EE of durra panel at Minneriya factory	= 5 MJ/m^2
Weight of a 1.2 m x 2.4 m board	= 20 Kg
Mini truck can be transported	= 20 Nos boards
EE of transportation to UOM	= 3.2x 221 kmx20.0 kg/1.2 x 2.4 x1000
	= 4.9 MJ/m^2
Therefore, total EE of Durra panel at UOM	= 9.9 MJ/m^2

In a conclusion, the novel composite panel has less EE compared to the durra panels in 402% ($[EE_{durra\ panel} - EE_{FRPC\ panel}] / EE_{FRPC\ panel} x100$)

6.5 Chapter Summary

The global lack of natural resources and the effects on the environment are both significantly impacted by the construction industry. Because calculating EE and LCC is a common way to gauge the sustainability of building materials, it is crucial to do so when evaluating cost-effectiveness and long-term performance.

Embodied energy is, by definition, the total amount of different types of energy used in the creation of a certain good or service. The whole embodied energy content was considered using process analysis and the hierarchical structure of energy use.

A 1.0 m x 1.0 m panel wall was used to compare the embodied energy. Considering all the scales given to measure the suitability of FRPC, incorporating initial cost, embedded energy, operation cost, and life cycle cost, the FRPC panel wall is the best walling material to build affordable houses compared to Durra panel walls. The EE of the Durra panel wall is 9.9 $MJ/m^{2,}$ and the EE of the FRPC panel wall is 1.9656 MJ/m^2.

7 CONCLUSION AND RECOMMENDATIONS

The use of various matrix and reinforcing materials to create composite materials has sparked a lot of research. These composites are used in a variety of applications. The most popular reinforcing materials for composites are natural or synthetic fibers. Polypropylene, polystyrene, and thermoset materials are the most popular matrix materials used to make composites. Most composite materials are designed for various purposes, such as automobiles, airplanes, marine equipment, and asphalting road material.

Even though waste polyethylene has become a significant problem worldwide, there is a knowledge gap among researchers who employ waste polyethylene to make polymer composites. However, there has been a lot of research using coconut fiber in conjunction with polypropylene, polystyrene, and thermoset to make composites. Therefore, combining coir and waste polyethylene has been highlighted as a different area to research.

While most researchers are interested in using composites in various applications, just a few have set out to produce construction materials. Using composites to make lighter partitioning panel walls is an innovative research topic since partition walls are such an important aspect of building construction.

Once identifying these gaps in knowledge and the necessity of filling them, this study primarily focuses on developing a composite material based on coir and waste polyethylene to determine the possibility of using this composite as a thinner partition wall. The partition wall is developed based on the sandwich panel concept with the required properties.

Finally, the study aims to develop an internal panel wall with better flexural performance and an attractive architectural appearance. In addition, expected to have better characteristics such as lightweight, lesser installation and demolition time, and lower manufacturing costs than the existing panel wall in Sri Lanka. This novel panel wall should also be long-lasting with low embodied energy and life-cycle costs and with good sustainable features.

The various types of natural fibers are available in Sri Lanka and worldwide. The coir fiber, in particular, exhibits unique qualities among these fibers. These fibers have been used in a variety of applications. As a result, researchers have been interested in utilizing coir fiber to develop composites. In the composite development process, several polymers are used as matrix materials.

The waste low-density polyethylene was chosen as the matrix material, and coir was chosen as the reinforcing material in this study. The panel wall was made out of fiber-reinforced polymer (FRP) composite made out of coir fibers mixed with waste polyethylene.

Before commencing the material development process, it is required to examine material characterizations. Therefore, characterizations of coir and polyethylene were carried out.

Under the physical properties of the coir, the diameter, density, surface morphology, and degradability temperature were investigated. Coir's tensile strength was investigated under the mechanical characteristic. SEM investigation was used to characterize the surface morphology, pore size, interfacial bonding between the fiber and matrix, and available pollutants. The FTIR was used to distinguish the chemical characterization of the coir fibers, allowing researchers to identify the molecules and functional groups contained in Sri Lankan coir fibers. X-ray diffraction investigation was used to calculate coir fiber's crystallinity index and crystallite size.

According to the results, the average diameter of the coir fiber was 0.31 mm, and the density was 1.018 g/cm^3. The crystallinity index and crystallite size were found to be 37.28 percent and 0.4331 nm, respectively, lower than other natural fibers reported. The ultimate tensile strength, young's modulus, and elongation of the coir fiber ranged from 94 to 159 MPa, 1.2 to 1.8 GPa, and 21 to 67 percent, respectively, obtained from the tensile test results. According to the thermogravimetric study, Sri Lankan coir fibers are thermally stable below 220^0 C.

In low-density polyethylene, which is made up of repeating methylene groups, the carbon and hydrogen atoms should be seen (CH_2). The FTIR spectrum should have wave numbers in between 1377 cm^{-1} and 1366 cm^{-1}. According to FTIR, results conducted for selected waste polyene are equal to the wave number of low-density polyethylene. Therefore, it can be concluded that the waste polyene chosen is low-density polyethylene.

After that, workable coir to polyethylene ratio was discovered, in which the mechanical properties of the composite were optimized. Tensile and flexural tests were conducted for this purpose. It was determined that when the coir to polyethylene weight ratio was between 10% and 40%, the optimum mechanical properties were obtained.

A variety of production factors have an impact on the mechanical properties of composites. Among them, the two most critical manufacturing conditions are temperature and pressure. As a result, it was necessary to figure out what temperature and pressure would give the composite’s best mechanical properties. Following a series of testing, it was discovered that 140^0C and 4 MPa are the most suitable temperature and pressure for producing composites. The most suitable processing time was observed as 6 minutes.

The composite samples were then prepared to determine the effect of fiber length on the composite's characteristics. The composites were manufactured by varying the fiber length while keeping all other parameters constant, and the specimens were mechanically tested. The optimum tensile strength investigated was a 4 cm fiber length with 40 % coir weight content. The maximum tensile strength was 12.56 N/mm^2. The optimum flexural capacity was obtained for 3 cm fiber length and a 30 % coir to LDPE ratio. The bending stiffness of the panel wall is a significant characteristic. So, it was determined to prepare the composite sheets for the panel wall preparation with a 3 cm fiber length and 30 % fiber content.

The maximum flexural strength of composite material was 33.77 N/mm^2. The impact strength is optimal when the fiber content is 40% and the fiber length is 2 cm. The 1.22 kJ/m^2 was the highest impact strength of the composite.

Next, the water absorption test was carried out for composites. Compared to the other composite samples with varying fiber percentages, the composites with 40% weight reinforcing fiber exhibited a maximum water absorption capacity of 19.78%.

However, after 18 days, water absorption was negligible for all fiber percentages. Then. The water absorption of the composite was again tested by applying the waterproofing chemicals. According to the findings, water absorption of composites can be controlled in considerable amounts after applying a waterproofing chemical. At the same time, the chemical-treated composite demonstrated a slight water absorption for up to 7 days. After that, a considerable amount of water absorption could not be observed. Furthermore, despite the composite sample's cutting edges being waterproofed against water contact, all samples absorbed water to some extent, according to this observation. Hence, it was discovered that the composite material's surface should also be treated to protect against water absorption.

The horizontal burning rates of the coir fiber waste polyethylene composites were more significant, ranging from 25.33 to 31.91 mm/min. Hence, the analyzed samples fall under the HB category according to the UL-94HB standard. Furthermore, the test findings demonstrated that the burning rate increased with the fiber fraction of the composites. It can also be stated that the average horizontal burning rate of the sample is proportional to the coir weight percentage. Coir fiber-reinforced polymer composites are highly flammable and burn rapidly. Hence, it is a significant disadvantage. Therefore, the use of flame-retardant chemicals to control and delay the burning process was proposed for this development.

The mix design and production parameters for a composite material made from coconut fiber and waste polyethylene were finalized. The next phase in this research was to develop a lightweight panel wall with optimal flexural properties using newly produced composite material.

The sandwich panels are available in several shapes and sizes to achieve a variety of needs around the world. The sandwich panel is made up of two face sheets and an interior core. This research aims to use the sandwich panel concept to build a partitioning panel wall with higher flexural performance. The higher flexural performance is achieved by selecting the most appropriate internal core arrangement.

The numerical modeling was performed to determine the best internal core arrangement. Based on the numerical modeling, the 100 mm x 100 mm square core arrangement was the most suitable solution to optimize both the material usage and flexural performance.

Then the panels were prepared in two approaches and assessed flexural performance. The first approach was the manual preparation of the panel. Then, the axial load was applied to the panel samples using 3-point bending test equipment. The failure was then caused by a poor bond between the core and the face sheets. As a result, the second approach was taken up. This strategy was to prepare the panel samples monolithically.

This method assisted in reducing de-bonding failure and determining flexural strength. The five prepared samples were tested, and the average values were calculated. Then, the calculated average failure load was 1.1 KN, and the corresponding maximum bending stress was 3.423 N/mm^2. This average value was compared with the flexural performance of existing panel walls available in Sri Lanka. The Durra panel boards were selected for the comparison since it is the most famous and readily available panel board in Sri Lanka.

The 3-point bending test was carried out for the five Durra panels, and then the maximum average failure load observed was 900 N and the calculated maximum flexural stress was 1.215 N/mm^2. When comparing both values, the FRPC panel showed 2.8 times higher values than the Durra panel. So, the proposed FRPC panel shows better performance concerning flexural strength than the durra panels. When comparing the flexural strength with other panels such as Acotec, Micro, and EPS panels available in Sri Lanka, the innovative panel shows better flexural performance than them. In addition, the deformation of the panels was checked, and it was within the limits of serviceability.

The total manufacturing cost for the novel FRPC panel wall was Rs. 4,878.51. However, according to the given price list, the price of the 1.2 m x 2.4 m x 50 mm thick Durra panel wall, excluding taxes is Rs. 5,830.00. So, there is a saving of Rs. 951.49 per panel. Therefore, a 19.5 % cost saving on partitioning walls by replacing Durra panel walls with FRPC for the high-rise buildings could be achieved.

The construction industry contributes significantly to the global shortage of natural resources and environmental concerns. Therefore, it's a universal approach to measuring the sustainability element of building materials. The concept of calculating EE and LCC is a crucial for assessing cost-effectiveness and long-term performance. The total embodied energy was calculated using a process analysis and hierarchical structure of energy use. The EE of the FRPC panel wall was1.9656 MJ/m^2 and the EE of Durra panel wall was 9.9 MJ/m^2.

Compared to Durra panel walls, the FRPC panel could be identified as the best replacement in view of all the factors considered to measure the suitability of FRPC, including flexural performance, lower production cost, lightweight, and less embedded energy. Therefore, FRPC panel walls are recommended as the novel concept of walling material for the internal partitioning walls for multi-storied buildings.

7.1 Recommendations for future research

Following recommendations can be made for the future works identified through this research study.

- Evaluate the mechanical properties such as axial capacity and impact resistance and physical properties like fire and thermal resistance, sound insulation, biodegradability, fungi, and mold growth for the FRPC panel.
- Evaluate the possibility of using the same composite as a construction material for different applications.
- Investigate similar studies for the treated coir fiber with waste polyethylene to study the performance of the composite and panel walls.
- Investigate similar studies for the different natural and synthetic fibers with other polymers.
- Carry out similar studies by varying the thickness of composite material and thickness of the panel wall.
- Carry out a similar study for thermal resistance, thermal conductivity, fire resistance, and sound insulation as physical properties.

References

[1] R. Mateus, S. Neiva, L. Bragança, P. Mendonça, and M. Macieira, “Sustainability assessment of an innovative lightweight building technology for partition walls – Comparison with conventional technologies,” *Build. Environ.*, vol. 67, pp. 147–159, Sep. 2013, doi: 10.1016/j.buildenv.2013.05.012.

[2] W. A. Al-Awsh, N. A. A. Qasem, O. S. B. Al-Amoudi, and M. A. Al-Osta, “Experimental and numerical investigation on innovative masonry walls for industrial and residential buildings,” *Appl. Energy*, vol. 276, p. 115496, Oct. 2020, doi: 10.1016/j.apenergy.2020.115496.

[3] Q. Wang and C. Zhang, “Fire Safety Analysis of Building Partition Wall Engineering,” *Procedia Eng.*, vol. 211, pp. 747–754, 2018, doi: 10.1016/j.proeng.2017.12.071.

[4] S. Yoon, D. Song, J. Kim, and H. Lim, “Stack-driven infiltration and heating load differences by floor in high-rise residential buildings,” *Build. Environ.*, vol. 157, pp. 366–379, Jun. 2019, doi: 10.1016/j.buildenv.2019.05.006.

[5] M. K. Hassan, K. Singh, and R. Kumar, “Experimental Study on Prefabricated Lightweight Composite Wall Panels under Flexural Loading,” *J. Civ. Eng. Constr.*, vol. 9, no. 4, Art. no. 4, Nov. 2020, doi: 10.32732/jcec.2020.9.4.215.

[6] R. Broun and G. F. Menzies, “Life Cycle Energy and Environmental Analysis of Partition Wall Systems in the UK,” *Procedia Eng.*, vol. 21, pp. 864–873, Jan. 2011, doi: 10.1016/j.proeng.2011.11.2088.

[7] G. A. O. Davies, D. Hitchings, T. Besant, A. Clarke, and C. Morgan, “Compression after impact strength of composite sandwich panels,” *Compos. Struct.*, vol. 63, no. 1, pp. 1–9, Jan. 2004, doi: 10.1016/S0263-8223(03)00119-3.

[8] N. Soares, J. J. Costa, A. R. Gaspar, and P. Santos, “Review of passive PCM latent heat thermal energy storage systems towards buildings’ energy efficiency,” *Energy Build.*, vol. 59, pp. 82–103, Apr. 2013, doi: 10.1016/j.enbuild.2012.12.042.

[9] R. Mateus, S. Neiva, L. Bragança, P. Mendonça, and M. Macieira, “Sustainability assessment of an innovative lightweight building technology for partition walls – Comparison with conventional technologies,” *Build. Environ.*, vol. 67, pp. 147–159, Sep. 2013, doi: 10.1016/j.buildenv.2013.05.012.

[10] F. C. Hahn, M. L. Macht, and D. A. Fletcher, “Polythene Physical and Chemical Properties.,” May 01, 2002. https://pubs.acs.org/doi/pdf/10.1021/ie50426a010 (accessed Oct. 15, 2020).

[11] G. Das and S. Biswas, “Effect of fiber parameters on physical, mechanical and water absorption behaviour of coir fiber–epoxy composites,” *J. Reinf. Plast. Compos.*, vol. 35, no. 8, pp. 644–653, Apr. 2016, doi: 10.1177/0731684415626594.

[12] M. J. Shenton and G. C. Stevens, “Surface modification of polymer surfaces: atmospheric plasma versus vacuum plasma treatments,” *J. Phys. Appl. Phys.*, vol. 34, no. 18, pp. 2761–2768, Sep. 2001, doi: 10.1088/0022-3727/34/18/308.

[13] S. Biswas, S. Kindo, and A. Patnaik, “Effect of fiber length on mechanical behavior of coir fiber reinforced epoxy composites,” *Fibers Polym.*, vol. 12, no. 1, pp. 73–78, Feb. 2011, doi: 10.1007/s12221-011-0073-9.

[14] A. G. Adeniyi, D. V. Onifade, J. O. Ighalo, and A. S. Adeoye, “A review of coir fiber reinforced polymer composites,” *Compos. Part B Eng.*, vol. 176, p. 107305, Nov. 2019, doi: 10.1016/j.compositesb.2019.107305.

[15] J. Guo, X. Luo, S. Tan, O. A. Ogunseitan, and Z. Xu, “Thermal degradation and pollutant emission from waste printed circuit boards mounted with electronic components,” *J. Hazard. Mater.*, vol. 382, p. 121038, Jan. 2020, doi: 10.1016/j.jhazmat.2019.121038.

[16] O. Guven, K. Gökdağ, B. Jovanović, and A. Kideys, “Microplastic litter composition of the Turkish territorial waters of the Mediterranean Sea, and its occurrence in the gastrointestinal tract of fish,” *Environ. Pollut.*, vol. 223, Jan. 2017, doi: 10.1016/j.envpol.2017.01.025.

[17] M. I. Jakhro, A. R. Raisani, G. M. Panezai, S. Parveen, M. Naseem, and G. A. Bhuro, "INFLUENCE OF SALINE WATER ON THE SURVIVAL, GROWTH AND DEVELOPMENT OF CHIKU (ACHRAS ZAPOTA L.) SAPLINGS," p. 7.

[18] H. Galabada, H. Galkanda, P. D. Dharmaratne, and R. U. Halwatura, "Investigation of Mechanical Properties of Mud Concrete with Coconut Fiber Reinforcement," in *2020 Moratuwa Engineering Research Conference (MERCon)*, Jul. 2020, pp. 102–106. doi: 10.1109/MERCon50084.2020.9185220.

[19] H. S. Ramaswamy, B. M. Ahuja, and S. Krishnamoorthy, "Behaviour of concrete reinforced with jute, coir and bamboo fibres," *Int. J. Cem. Compos. Lightweight Concr.*, vol. 5, no. 1, pp. 3–13, 1983.

[20] K. Rohit and S. Dixit, "A Review - Future Aspect of Natural Fiber Reinforced Composite," *Polym. Renew. Resour.*, vol. 7, no. 2, pp. 43–59, May 2016, doi: 10.1177/204124791600700202.

[21] S. M.S, S. K. Marikkannan, E. V, M. Vanmathi, R. Sasikumar, and N. L, "Investigation of Mechanical and Electrical Properties of Kevlar/E-Glass and Basalt/E-Glass Reinforced Hybrid Composites," *Int. J. Mech. Prod. Eng. Res. Dev.*, vol. 8, May 2018, doi: 10.24247/ijmperdjun201863.

[22] V. Chauhan, T. Kärki, and J. Varis, "Review of natural fiber-reinforced engineering plastic composites, their applications in the transportation sector and processing techniques," *J. Thermoplast. Compos. Mater.*, p. 089270571988909, Nov. 2019, doi: 10.1177/0892705719889095.

[23] D. Verma, P. C. Gope, A. Shandilya, A. Gupta, and M. K. Maheshwari, "Coir Fibre Reinforcement and Application in Polymer Composites: A Review," p. 15, 2013.

[24] C. R. Rejeesh and K. K. Saju, "Methods and materials for reducing flammability behaviour of coir fibre based Composite Boards: A Review," *Mater. Today Proc.*, vol. 4, no. 9, pp. 9399–9407, Jan. 2017, doi: 10.1016/j.matpr.2017.06.193.

[25] H. Syed, R. Nerella, and S. R. C. Madduru, "Role of coconut coir fiber in concrete," *Mater. Today Proc.*, vol. 27, pp. 1104–1110, Jan. 2020, doi: 10.1016/j.matpr.2020.01.477.

[26] S. A. Hussain, "Mechanical properties of green coconut fiber reinforced hdpe polymer composite," *Int. J. Eng. Sci. Technol.*, vol. 3, no. 11, p. 12, 2011.

[27] D. S. Mintorogo, W. K. Widigdo, and A. Juniwati, "Application of Coconut Fibres as Outer Eco-insulation to Control Solar Heat Radiation on Horizontal Concrete Slab Rooftop," *Procedia Eng.*, vol. 125, pp. 765–772, Jan. 2015, doi: 10.1016/j.proeng.2015.11.129.

[28] P. Lertwattanaruk and A. Suntijitto, "Properties of natural fiber cement materials containing coconut coir and oil palm fibers for residential building applications," *Constr. Build. Mater.*, vol. 94, pp. 664–669, 2015.

[29] S. Mahzan, A. A. Zaidi, M. I. Ghazali, N. Arsat, and M. N. M. Hatta, "Mechanical properties of medium density fibreboard composites material using recycled rubber and coconut coir," *Int. J. Integr. Eng.*, vol. 2, no. 1, 2010.

[30] D. O. Obada *et al.*, "Effect of variation in frequencies on the viscoelastic properties of coir and coconut husk powder reinforced polymer composites," *J. King Saud Univ. - Eng. Sci.*, vol. 32, no. 2, pp. 148–157, Feb. 2020, doi: 10.1016/j.jksues.2018.10.001.

[31] C. Yu and Y. Lee, "Housing requirements for a ageing society," *Indoor Built Environ.*, vol. 26, no. 4, pp. 441–446, Apr. 2017, doi: 10.1177/1420326X17704285.

[32] D. Myers, J. Pitkin, and J. Park, "Estimation of housing needs amid population growth and change," *Hous. Policy Debate*, vol. 13, pp. 567–596, Jan. 2002, doi: 10.1080/10511482.2002.9521455.

[33] R. Yadav, B.-C. Chen, H. Yuan, and R. Adhikari, *Comparative Analysis of Reinforced Concrete Buildings and Concrete Filled Steel Tube Buildings in Nepal*. 2016.

[34] M. R. B. Naidu and D. S. D. Bhole, “Seismic Analysis of Multi-Storied Building and Critical Study of its Foundations,” vol. 2, no. 10, p. 8.

[35] A. M. Odeh and H. T. Battaineh, “Causes of construction delay: traditional contracts,” *Int. J. Proj. Manag.*, vol. 20, no. 1, pp. 67–73, Jan. 2002, doi: 10.1016/S0263-7863(00)00037-5.

[36] A. Sattainathan Sharma, R. Anjughap Priya, R. Thirugnanam, and P. Rathna Priya, “Comparative Study on Multi-storey Structure of R.C.C and Composite Material,” *Indian J. Sci. Technol.*, vol. 9, no. 2, Jan. 2016, doi: 10.17485/ijst/2016/v9i2/86363.

[37] E. Valero, A. Forster, F. Bosché, E. Hyslop, L. Wilson, and A. Turmel, “Automated defect detection and classification in ashlar masonry walls using machine learning,” *Autom. Constr.*, vol. 106, p. 102846, Oct. 2019, doi: 10.1016/j.autcon.2019.102846.

[38] F. R. Arooz and R. U. Halwatura, “Mud-concrete block (MCB): mix design & durability characteristics,” *Case Stud. Constr. Mater.*, vol. 8, pp. 39–50, Jun. 2018, doi: 10.1016/j.cscm.2017.12.004.

[39] F. R. Arooz, T. D. Babilegedara, and R. U. Halwatura, “Effect of aggregate percentage on compressive strength of self-compacting in-situ cast Mud - Concrete load bearing walls,” in *2017 Moratuwa Engineering Research Conference (MERCon)*, May 2017, pp. 271–276. doi: 10.1109/MERCon.2017.7980494.

[40] T. Adekunle and T. Odeyale, “Innovative and sustainable local material in traditional African architecture ? Socio cultural dimension,” in *Structural Analysis of Historic Construction: Preserving Safety and Significance*, E. Fodde, Ed. CRC Press, 2008, pp. 991–998. doi: 10.1201/9781439828229.ch113.

[41] C. W. Isaac, M. Pawelczyk, and S. Wrona, “Comparative Study of Sound Transmission Losses of Sandwich Composite Double Panel Walls,” *Appl. Sci.*, vol. 10, no. 4, p. 1543, Feb. 2020, doi: 10.3390/app10041543.

[42] S. Selçuk, K. Saim, and K. Zerrin, “Evaluation of Precast Exterior Panel Walls (Used in Tunnel Formwork Applications) in Terms of Environmental Quality,”

Int. Conf. Civ. Archit. Eng., vol. 8, no. 8, pp. 1–11, May 2010, doi: 10.21608/iccae.2010.45072.

[43] M. E. Arslan, B. Aykanat, M. A. Ayyıldız, S. Subaşı, and M. Maraşlı, "Effects of basalt and glass fiber composites usage for strengthening on the cyclic behavior of brick infill walls," *J. Build. Eng.*, vol. 52, p. 104405, Jul. 2022, doi: 10.1016/j.jobe.2022.104405.

[44] P. L. N. Fernando, M. T. R. Jayasinghe, and C. Jayasinghe, "Structural feasibility of Expanded Polystyrene (EPS) based lightweight concrete sandwich wall panels," *Constr. Build. Mater.*, vol. 139, pp. 45–51, May 2017, doi: 10.1016/j.conbuildmat.2017.02.027.

[45] G. Boscato, T. D. Mora, F. Peron, S. Russo, and P. Romagnoni, "A new concrete-glulam prefabricated composite wall system: Thermal behavior, life cycle assessment and structural response," *J. Build. Eng.*, vol. 19, pp. 384–401, Sep. 2018, doi: 10.1016/j.jobe.2018.05.027.

[46] V. Birman and G. A. Kardomateas, "Review of current trends in research and applications of sandwich structures," *Compos. Part B Eng.*, vol. 142, pp. 221–240, Jun. 2018, doi: 10.1016/j.compositesb.2018.01.027.

[47] A. Eyvazian *et al.*, "Mechanical behavior of resin pin-reinforced composite sandwich panels under quasi-static indentation and three-point bending loading conditions," *J. Sandw. Struct. Mater.*, vol. 23, no. 6, pp. 2127–2145, Sep. 2021, doi: 10.1177/1099636220909752.

[48] J. Marx and A. Rabiei, "Tensile properties of composite metal foam and composite metal foam core sandwich panels," *J. Sandw. Struct. Mater.*, vol. 23, no. 8, pp. 3773–3793, Nov. 2021, doi: 10.1177/1099636220942880.

[49] J.-B. Bai, D. Chen, J.-J. Xiong, and C.-H. Dong, "A semi-analytical model for predicting nonlinear tensile behaviour of corrugated flexible composite skin," *Compos. Part B Eng.*, vol. 168, pp. 312–319, Jul. 2019, doi: 10.1016/j.compositesb.2019.01.053.

[50] R. A. W. Mines, C. M. Worrall, and A. G. Gibson, "Low velocity perforation behaviour of polymer composite sandwich panels," *Int. J. Impact Eng.*, vol. 21, no. 10, pp. 855–879, Nov. 1998, doi: 10.1016/S0734-743X(98)00037-2.

[51] A. Kicińska-Jakubowska, E. Bogacz, and M. Zimniewska, "Review of Natural Fibers. Part I—Vegetable Fibers," *J. Nat. Fibers*, vol. 9, no. 3, pp. 150–167, Jul. 2012, doi: 10.1080/15440478.2012.703370.

[52] K. Rohit and S. Dixit, "A Review - Future Aspect of Natural Fiber Reinforced Composite," *Polym. Renew. Resour.*, vol. 7, no. 2, pp. 43–59, May 2016, doi: 10.1177/204124791600700202.

[53] N. A. George and R. Vinayakrishnan, "Photoacoustic evaluation of the thermal diffusivity of coconut shell," *J. Phys. Condens. Matter*, vol. 14, no. 17, pp. 4509–4513, May 2002, doi: 10.1088/0953-8984/14/17/321.

[54] A. K. Mohanty, M. Misra, L. T. Drzal, M. Misra, and L. T. Drzal, *Natural Fibers, Biopolymers, and Biocomposites*. CRC Press, 2005. doi: 10.1201/9780203508206.

[55] P. Sathish, R. Kesavan, and N. Mahaviradhan, "Coconut fiber reinforced composites: a review.," *Int. J. Res. Appl. Sci. Eng. Technol.*, vol. 5, no. 3, pp. 171–172, 2017.

[56] A. K. Mohanty, M. Misra, and L. T. Drzal, *Natural Fibers, Biopolymers, and Biocomposites*. CRC Press, 2005.

[57] Y. Li, Y.-W. Mai, and L. Ye, "Sisal fibre and its composites: a review of recent developments," *Compos. Sci. Technol.*, vol. 60, no. 11, pp. 2037–2055, Aug. 2000, doi: 10.1016/S0266-3538(00)00101-9.

[58] N. Ayrilmis, S. Jarusombuti, V. Fueangvivat, P. Bauchongkol, and R. H. White, "Coir fiber reinforced polypropylene composite panel for automotive interior applications," *Fibers Polym.*, vol. 12, no. 7, pp. 919–926, Oct. 2011, doi: 10.1007/s12221-011-0919-1.

[59] Universiti Sains Malaysia and A. A. Owodunni, "Flame-retardant properties of particleboard made from coconut fibre using modified potato starch as a binder,"

J. Phys. Sci., vol. 31, no. 3, pp. 129–143, Nov. 2020, doi: 10.21315/jps2020.31.3.10.

[60] M. Brahmakumar, C. Pavithran, and R. Pillai, "Coconut fibre reinforced polyethylene composites: effect of natural waxy surface layer of the fibre on fibre/matrix interfacial bonding and strength of composites," *Compos. Sci. Technol.*, vol. 65, no. 3–4, pp. 563–569, Mar. 2005, doi: 10.1016/j.compscitech.2004.09.020.

[61] N. J. Rodríguez *et al.*, "Assessment of coconut fibre insulation characteristics and its use to modulate temperatures in concrete slabs with the aid of a finite element methodology," *Energy Build.*, vol. 43, no. 6, pp. 1264–1272, Jun. 2011, doi: 10.1016/j.enbuild.2011.01.005.

[62] Ö. Andiç-Çakir, M. Sarikanat, H. B. Tüfekçi, C. Demirci, and Ü. H. Erdoğan, "Physical and mechanical properties of randomly oriented coir fiber–cementitious composites," *Compos. Part B Eng.*, vol. 61, pp. 49–54, May 2014, doi: 10.1016/j.compositesb.2014.01.029.

[63] P. Paramasivam, G. K. Nathan, and N. C. Das Gupta, "Coconut fibre reinforced corrugated slabs," *Int. J. Cem. Compos. Lightweight Concr.*, vol. 6, no. 1, pp. 19–27, Feb. 1984, doi: 10.1016/0262-5075(84)90056-3.

[64] K. G. Satyanarayana, K. Sukumaran, P. S. Mukherjee, C. Pavithran, and S. G. K. Pillai, "Natural fibre-polymer composites," *Cem. Concr. Compos.*, vol. 12, no. 2, pp. 117–136, Jan. 1990, doi: 10.1016/0958-9465(90)90049-4.

[65] M. Ali, "Coconut Fibre – Versatile Material and Its applications in engineering."

[66] K. Kochova, F. Gauvin, K. Schollbach, and H. J. H. Brouwers, "Using alternative waste coir fibres as a reinforcement in cement-fibre composites," *Constr. Build. Mater.*, vol. 231, p. 117121, Jan. 2020, doi: 10.1016/j.conbuildmat.2019.117121.

[67] K. Joseph, S. Thomas, and C. Pavithran, "Effect of chemical treatment on the tensile properties of short sisal fibre-reinforced polyethylene composites,"

Polymer, vol. 37, no. 23, pp. 5139–5149, Nov. 1996, doi: 10.1016/0032-3861(96)00144-9.

[68] N. M. S, S. S. P, and P. P. R, “Assessment of Marine Debris and Plastic Polymer Types Along the Panvel Creek, Navi Mumbai, West Coast of India,” *Int. J. Zool. Investig.*, vol. 7, no. 1, Jun. 2021, doi: 10.33745/ijzi.2021.v07i01.023.

[69] A. M. Peterson, R. E. Jensen, and G. R. Palmese, “Room-Temperature Healing of a Thermosetting Polymer Using the Diels−Alder Reaction,” *ACS Appl. Mater. Interfaces*, vol. 2, no. 4, pp. 1141–1149, Apr. 2010, doi: 10.1021/am9009378.

[70] V. K. Thakur and M. K. Thakur, “Processing and characterization of natural cellulose fibers/thermoset polymer composites,” *Carbohydr. Polym.*, vol. 109, pp. 102–117, Aug. 2014, doi: 10.1016/j.carbpol.2014.03.039.

[71] W. Post, A. Susa, R. Blaauw, K. Molenveld, and R. J. I. Knoop, “A Review on the Potential and Limitations of Recyclable Thermosets for Structural Applications,” *Polym. Rev.*, vol. 60, no. 2, pp. 359–388, Apr. 2020, doi: 10.1080/15583724.2019.1673406.

[72] S. Kumar, A. Manna, and R. Dang, “A review on applications of natural Fiber-Reinforced composites (NFRCs),” *Mater. Today Proc.*, vol. 50, pp. 1632–1636, Jan. 2022, doi: 10.1016/j.matpr.2021.09.131.

[73] L. Yan, N. Chouw, L. Huang, and B. Kasal, “Effect of alkali treatment on microstructure and mechanical properties of coir fibres, coir fibre reinforced-polymer composites and reinforced-cementitious composites,” *Constr. Build. Mater.*, vol. 112, pp. 168–182, Jun. 2016, doi: 10.1016/j.conbuildmat.2016.02.182.

[74] T. H. Nam, S. Ogihara, N. H. Tung, and S. Kobayashi, “Effect of alkali treatment on interfacial and mechanical properties of coir fiber reinforced poly(butylene succinate) biodegradable composites,” *Compos. Part B Eng.*, vol. 42, no. 6, pp. 1648–1656, Sep. 2011, doi: 10.1016/j.compositesb.2011.04.001.

[75] S. Biswas, S. Kindo, and A. Patnaik, “Effect of fiber length on mechanical behavior of coir fiber reinforced epoxy composites,” *Fibers Polym.*, vol. 12, no. 1, pp. 73–78, Feb. 2011, doi: 10.1007/s12221-011-0073-9.

[76] V. G. Geethamma, R. Joseph, and S. Thomas, “Short coir fiber-reinforced natural rubber composites: Effects of fiber length, orientation, and alkali treatment,” *J. Appl. Polym. Sci.*, vol. 55, no. 4, pp. 583–594, 1995, doi: 10.1002/app.1995.070550405.

[77] “Survey on Partition Walls Commonly Used in Hong Kong and estimation of the heat release rates (100 %.pdf.”

[78] K. Aghaee and M. Foroughi, “Mechanical Properties of Lightweight Concrete Partition with a Core of Textile Waste,” *Adv. Civ. Eng.*, vol. 2013, pp. 1–7, 2013, doi: 10.1155/2013/482310.

[79] M. Kippel, C. Leyder, A. Frangi, and M. Fontana, “Fire Tests on Loaded Cross-laminated Timber Wall and Floor Elements,” *Fire Saf. Sci.*, vol. 11, pp. 626–639, 2014, doi: 10.3801/IAFSS.FSS.11-626.

[80] D. Gawatre, K. M, G. D, S. Karle, and M. Haris, “Review Paper on Thermocol Sandwich Concrete Bricks,” vol. 13, pp. 272–276, Jan. 2020.

[81] O. Faruk, A. K. Bledzki, H.-P. Fink, and M. Sain, “Biocomposites reinforced with natural fibers: 2000–2010,” *Prog. Polym. Sci.*, vol. 37, no. 11, pp. 1552–1596, Nov. 2012, doi: 10.1016/j.progpolymsci.2012.04.003.

[82] “A comprehensive review on material selection for polymer matrix composites subjected to impact load | Elsevier Enhanced Reader.” https://reader.elsevier.com/reader/sd/pii/S2214914720300556?token=FBF05740B714B45A738862563B1311249BEEFB3D4A50382DDE75DFDD96F485492A41C8528C426C8BA276F72D47B5C4D3 (accessed Apr. 21, 2020).

[83] L. Yan, B. Kasal, and L. Huang, “A review of recent research on the use of cellulosic fibres, their fibre fabric reinforced cementitious, geo-polymer and polymer composites in civil engineering,” *Compos. Part B Eng.*, vol. 92, pp. 94–132, May 2016, doi: 10.1016/j.compositesb.2016.02.002.

[84] P. J. Herrera-Franco and A. Valadez-González, "Mechanical properties of continuous natural fibre-reinforced polymer composites," *Compos. Part Appl. Sci. Manuf.*, vol. 35, no. 3, pp. 339–345, Mar. 2004, doi: 10.1016/j.compositesa.2003.09.012.

[85] V. Barbosa, E. C. Ramires, I. A. T. Razera, and E. Frollini, "Biobased composites from tannin–phenolic polymers reinforced with coir fibers," *Ind. Crops Prod.*, vol. 32, no. 3, pp. 305–312, Nov. 2010, doi: 10.1016/j.indcrop.2010.05.007.

[86] H. Syed, R. Nerella, and S. R. C. Madduru, "Role of coconut coir fiber in concrete," *Mater. Today Proc.*, p. S2214785320305824, Feb. 2020, doi: 10.1016/j.matpr.2020.01.477.

[87] A. E. E. Putra, I. Renreng, H. Arsyad, and B. Bakri, "Investigating the effects of liquid-plasma treatment on tensile strength of coir fibers and interfacial fiber-matrix adhesion of composites," *Compos. Part B Eng.*, vol. 183, p. 107722, Feb. 2020, doi: 10.1016/j.compositesb.2019.107722.

[88] C.-L. Hwang, V.-A. Tran, J.-W. Hong, and Y.-C. Hsieh, "Effects of short coconut fiber on the mechanical properties, plastic cracking behavior, and impact resistance of cementitious composites," *Constr. Build. Mater.*, vol. 127, pp. 984–992, Nov. 2016, doi: 10.1016/j.conbuildmat.2016.09.118.

[89] K. P. Marimuthu, S. M. Kumar, V. R. Kumar, and H. K. Govindaraju, "Characterization of Mechanical Properties of Epoxy Reinforced with Glass Fiber and Coconut Fiber," *Mater. Today Proc.*, vol. 16, pp. 661–667, 2019, doi: 10.1016/j.matpr.2019.05.143.

[90] D. Verma and P. C. Gope, "The use of coir/coconut fibers as reinforcements in composites," in *Biofiber Reinforcements in Composite Materials*, Elsevier, 2015, pp. 285–319. doi: 10.1533/9781782421276.3.285.

[91] N. Mathura and D. Cree, "Characterization and mechanical property of Trinidad coir fibers," *J. Appl. Polym. Sci.*, vol. 133, no. 29, Aug. 2016, doi: 10.1002/app.43692.

[92] M. Ho *et al.*, “Critical factors on manufacturing processes of natural fibre composites,” *Compos. Part B Eng.*, vol. 43, no. 8, pp. 3549–3562, Dec. 2012, doi: 10.1016/j.compositesb.2011.10.001.

[93] M. G. Lomelí-Ramírez, R. R. Anda, K. G. Satyanarayana, G. I. B. de Muniz, and S. Iwakiri, “Comparative Study of the Characteristics of Green and Brown Coconut Fibers for the Development of Green Composites,” *BioResources*, vol. 13, no. 1, pp. 1637–1660, Jan. 2018.

[94] A. Widnyana, I. Rian, I. W. Surata, and T. Nindhia, “Tensile Properties of coconut Coir single fiber with alkali treatment and reinforcement effect on unsaturated polyester polymer,” *Mater. Today Proc.*, vol. 22, pp. 300–305, Jan. 2020, doi: 10.1016/j.matpr.2019.08.155.

[95] K. M. M. Rao and K. M. Rao, “Extraction and tensile properties of natural fibers: Vakka, date and bamboo,” *Compos. Struct.*, vol. 77, no. 3, pp. 288–295, Feb. 2007, doi: 10.1016/j.compstruct.2005.07.023.

[96] V. S. Sreenivasan, S. Somasundaram, D. Ravindran, V. Manikandan, and R. Narayanasamy, “Microstructural, physico-chemical and mechanical characterisation of Sansevieria cylindrica fibres – An exploratory investigation,” *Mater. Des.*, vol. 32, no. 1, pp. 453–461, Jan. 2011, doi: 10.1016/j.matdes.2010.06.004.

[97] S. C. Chin, K. F. Tee, F. S. Tong, H. R. Ong, and J. Gimbun, “Thermal and mechanical properties of bamboo fiber reinforced composites,” *Mater. Today Commun.*, vol. 23, p. 100876, Jun. 2020, doi: 10.1016/j.mtcomm.2019.100876.

[98] A. N, M. Ç. EngiN, T. W. Hong, Ka. T, and A. R. G, “Physical, Chemical, Morphological and Thermal Characterization of Natural Fibers,” *TEKSTİL VE KONFEKSİYON*, Sep. 2019, doi: 10.32710/tekstilvekonfeksiyon.375784.

[99] D. Ravindran, V. Manikandan, and R. Narayanasamy, “Microstructural, physico-chemical and mechanical characterisation of Sansevieria cylindrica fibres – An exploratory investigation,” *Mater. Des.*, vol. 32, no. 1, pp. 453–461, Jan. 2011, doi: 10.1016/j.matdes.2010.06.004.

[100] A. Bezazi, A. Belaadi, M. Bourchak, F. Scarpa, and K. Boba, “Novel extraction techniques, chemical and mechanical characterisation of Agave americana L. natural fibres,” *Compos. Part B Eng.*, vol. 66, pp. 194–203, Nov. 2014, doi: 10.1016/j.compositesb.2014.05.014.

[101] N. Sgriccia, M. C. Hawley, and M. Misra, “Characterization of natural fiber surfaces and natural fiber composites,” *Compos. Part Appl. Sci. Manuf.*, vol. 39, no. 10, pp. 1632–1637, Oct. 2008, doi: 10.1016/j.compositesa.2008.07.007.

[102] A. A. M. Moshi, D. Ravindran, S. R. S. Bharathi, S. Indran, S. S. Saravanakumar, and Y. Liu, “Characterization of a new cellulosic natural fiber extracted from the root of Ficus religiosa tree,” *Int. J. Biol. Macromol.*, vol. 142, pp. 212–221, Jan. 2020, doi: 10.1016/j.ijbiomac.2019.09.094.

[103] Y. Liu *et al.*, “Characterization of silane treated and untreated natural cellulosic fibre from corn stalk waste as potential reinforcement in polymer composites,” *Carbohydr. Polym.*, vol. 218, pp. 179–187, Aug. 2019, doi: 10.1016/j.carbpol.2019.04.088.

[104] A. da Silva Moura, R. Demori, R. M. Leão, C. L. Crescente Frankenberg, and R. M. Campomanes Santana, “The influence of the coconut fiber treated as reinforcement in PHB (polyhydroxybutyrate) composites,” *Mater. Today Commun.*, vol. 18, pp. 191–198, Mar. 2019, doi: 10.1016/j.mtcomm.2018.12.006.

[105] S. Indran and R. E. Raj, “Characterization of new natural cellulosic fiber from Cissus quadrangularis stem,” *Carbohydr. Polym.*, vol. 117, pp. 392–399, Mar. 2015, doi: 10.1016/j.carbpol.2014.09.072.

[106] K. M. M. Rao and K. M. Rao, “Extraction and tensile properties of natural fibers: Vakka, date and bamboo,” *Compos. Struct.*, vol. 77, no. 3, pp. 288–295, Feb. 2007, doi: 10.1016/j.compstruct.2005.07.023.

[107] R. Roy, B. K. Sarkar, and N. R. Bose, “Behaviour ofE-glass fibre reinforced vinylester resin composites under impact fatigue,” *Bull. Mater. Sci.*, vol. 24, no. 2, pp. 137–142, Apr. 2001, doi: 10.1007/BF02710090.

[108] J. S. Binoj, R. Edwin Raj, V. S. Sreenivasan, and G. Rexin Thusnavis, “Morphological, physical, mechanical, chemical and thermal characterization of sustainable Indian Areca fruit husk fibers (Areca Catechu L.) as potential alternate for hazardous synthetic fibers,” *J. Bionic Eng.*, vol. 13, no. 1, pp. 156–165, Mar. 2016, doi: 10.1016/S1672-6529(14)60170-0.

[109] S. M.R., S. Siengchin, J. Parameswaranpillai, M. Jawaid, C. I. Pruncu, and A. Khan, “A comprehensive review of techniques for natural fibers as reinforcement in composites: Preparation, processing and characterization,” *Carbohydr. Polym.*, vol. 207, pp. 108–121, Mar. 2019, doi: 10.1016/j.carbpol.2018.11.083.

[110] J. C. dos Santos, L. Á. de Oliveira, L. M. G. Vieira, V. Mano, R. T. Freire, and T. H. Panzera, “Eco-friendly sodium bicarbonate treatment and its effect on epoxy and polyester coir fibre composites,” *Constr. Build. Mater.*, vol. 211, pp. 427–436, 2019.

[111] P. G. Baskaran, M. Kathiresan, P. Senthamaraikannan, and S. S. Saravanakumar, “Characterization of New Natural Cellulosic Fiber from the Bark of *Dichrostachys Cinerea*,” *J. Nat. Fibers*, vol. 15, no. 1, pp. 62–68, Jan. 2018, doi: 10.1080/15440478.2017.1304314.

[112] T. Theivasanthi, F. L. Anne Christma, A. J. Toyin, S. C. B. Gopinath, and R. Ravichandran, “Synthesis and characterization of cotton fiber-based nanocellulose,” *Int. J. Biol. Macromol.*, vol. 109, pp. 832–836, Apr. 2018, doi: 10.1016/j.ijbiomac.2017.11.054.

[113] N. R. J. Hyness, N. J. Vignesh, P. Senthamaraikannan, S. S. Saravanakumar, and M. R. Sanjay, “Characterization of New Natural Cellulosic Fiber from *Heteropogon Contortus* Plant,” *J. Nat. Fibers*, vol. 15, no. 1, pp. 146–153, Jan. 2018, doi: 10.1080/15440478.2017.1321516.

[114] K. Mayandi, N. Rajini, P. Pitchipoo, J. T. W. Jappes, and A. V. Rajulu, “Extraction and characterization of new natural lignocellulosic fiber *Cyperus pangorei*,” *Int. J. Polym. Anal. Charact.*, vol. 21, no. 2, pp. 175–183, Feb. 2016, doi: 10.1080/1023666X.2016.1132064.

[115] A. Al-Khanbashi, K. Al-Kaabi, and A. Hammami, "Date palm fibers as polymeric matrix reinforcement: Fiber characterization," *Polym. Compos.*, vol. 26, no. 4, pp. 486–497, 2005, doi: 10.1002/pc.20118.

[116] R. C. Asensio, M. S. A. Moya, J. M. de la Roja, and M. Gómez, "Analytical characterization of polymers used in conservation and restoration by ATR-FTIR spectroscopy.," *Anal. Bioanal. Chem.*, vol. 395, pp. 2081–2096, 2009.

[117] S. Bolduc *et al.*, "Banana fiber / low-density polyethylene recycled composites for third world eco-friendly construction applications – Waste for life project Sri Lanka," *J. Reinf. Plast. Compos.*, vol. 37, no. 21, pp. 1322–1331, 2018, doi: 10.1177/0731684418791756.

[118] J. Brandon, M. Goldstein, and M. D. Ohman, "Long-term aging and degradation of microplastic particles: Comparing in situ oceanic and experimental weathering patterns.," *Mar. Pollut. Bull.*, vol. 110, no. 1, pp. 299–308, 2016.

[119] C. Elanchezhian, B. V. Ramnath, G. Ramakrishnan, M. Rajendrakumar, V. Naveenkumar, and M. K. Saravanakumar, "Review on mechanical properties of natural fiber composites.," *Mater. Today Proc.*, vol. 5, no. 1, Part 1, pp. 1785–1790, Jan. 2018, doi: 10.1016/j.matpr.2017.11.276.

[120] G. Das and S. Biswas, "Effect of fiber parameters on physical, mechanical and water absorption behaviour of coir fiber–epoxy composites," *J. Reinf. Plast. Compos.*, vol. 35, no. 8, pp. 644–653, 2016.

[121] A. A. Pérez-Fonseca, M. Arellano, D. Rodrigue, R. González-Núñez, and J. R. Robledo-Ortíz, "Effect of coupling agent content and water absorption on the mechanical properties of coir-agave fibers reinforced polyethylene hybrid composites," *Polym. Compos.*, vol. 37, no. 10, pp. 3015–3024, Oct. 2016, doi: 10.1002/pc.23498.

[122] M. M. Rahman and M. A. Khan, "Surface treatment of coir (Cocos nucifera) fibers and its influence on the fibers' physico-mechanical properties," *Compos. Sci. Technol.*, vol. 67, no. 11–12, pp. 2369–2376, Sep. 2007, doi: 10.1016/j.compscitech.2007.01.009.

[123] Amandeep Singh, "CHARACTERIZATION AND MECHANICAL ANALYSIS OF CHEMICALLY TREATED COIR FIBRE-POLYESTER COMPOSITES," 2013, doi: 10.13140/RG.2.2.16740.27522.

[124] L. S. Kuburi *et al.*, "Effects of Coir Fiber Loading on the Physio-mechanical and Morphological Properties of Coconut Shell Powder Filled Low Density Polyethylene Composites," *Procedia Manuf.*, vol. 7, pp. 138–144, 2017, doi: 10.1016/j.promfg.2016.12.036.

[125] W. D. C. Jr and D. G. Rethwisch, *Callister's Materials Science and Engineering*. John Wiley & Sons, 2020.

[126] N. M. Abdullah and I. Ahmad, "Potential of using polyester reinforced coconut fiber composites derived from recycling polyethylene terephthalate (PET) waste," *Fibers Polym.*, vol. 14, no. 4, pp. 584–590, Apr. 2013, doi: 10.1007/s12221-013-0584-7.

[127] J. Chen and N. Chouw, "Effect of the interface condition on the bond between flax FRP tube and coconut fibre reinforced concrete composites," *Constr. Build. Mater.*, vol. 167, pp. 597–604, Apr. 2018, doi: 10.1016/j.conbuildmat.2018.01.152.

[128] R. M. N. Arib, S. M. Sapuan, M. M. H. M. Ahmad, M. T. Paridah, and H. M. D. K. Zaman, "Mechanical properties of pineapple leaf fibre reinforced polypropylene composites," *Mater. Des.*, vol. 27, no. 5, pp. 391–396, Jan. 2006, doi: 10.1016/j.matdes.2004.11.009.

[129] G. L. E. Prasad, B. S. K. Gowda, and R. Velmurugan, "A Study on Impact Strength Characteristics of Coir Polyester Composites," *Procedia Eng.*, vol. 173, pp. 771–777, 2017, doi: 10.1016/j.proeng.2016.12.091.

[130] G. Das and S. Biswas, "Effect of fiber parameters on physical, mechanical and water absorption behaviour of coir fiber–epoxy composites," *J. Reinf. Plast. Compos.*, vol. 35, no. 8, pp. 644–653, Apr. 2016, doi: 10.1177/0731684415626594.

[131] N. Venkateshwaran, A. Elaya Perumal, and D. Arunsundaranayagam, “Fiber surface treatment and its effect on mechanical and visco-elastic behaviour of banana/epoxy composite,” *Mater. Des.*, vol. 47, pp. 151–159, May 2013, doi: 10.1016/j.matdes.2012.12.001.

[132] V. Narayanan, A. Elayaperumal, and M. Jagatheeshwaran, “Effect of fiber length and fiber content on mechanical properties of banana fiber/epoxy composite,” *J. Reinf. Plast. Compos.*, vol. 30, pp. 1621–1627, Oct. 2011, doi: 10.1177/0731684411426810.

[133] T. Alsaeed, B. F. Yousif, and H. Ku, “The potential of using date palm fibres as reinforcement for polymeric composites,” *Mater. Des.*, vol. 43, pp. 177–184, Jan. 2013, doi: 10.1016/j.matdes.2012.06.061.

[134] S. Biswas, S. Kindo, and A. Patnaik, “Effect of fiber length on mechanical behavior of coir fiber reinforced epoxy composites,” *Fibers Polym.*, vol. 12, no. 1, pp. 73–78, Feb. 2011, doi: 10.1007/s12221-011-0073-9.

[135] L. Mwaikambo and M. Ansell, “The effect of chemical treatment on the properties of hemp, sisal, jute and kapok for composite reinforcement,” *Macromol. Mater. Eng.*, vol. 272, pp. 108–116, Dec. 1999, doi: 10.1002/(SICI)1522-9505(19991201)272:1%3C108::AID-APMC108%3E3.0.CO;2-9.

[136] S. Misra, M. Misra, S. S. Tripathy, S. K. Nayak, and A. K. Mohanty, “The influence of chemical surface modification on the performance of sisal-polyester biocomposites,” *Polym. Compos.*, vol. 23, no. 2, pp. 164–170, 2002, doi: 10.1002/pc.10422.

[137] M. M. Kabir, H. Wang, K. T. Lau, and F. Cardona, “Chemical treatments on plant-based natural fibre reinforced polymer composites: An overview,” *Compos. Part B Eng.*, vol. 43, no. 7, pp. 2883–2892, Oct. 2012, doi: 10.1016/j.compositesb.2012.04.053.

[138] E. Canedo, L. Carvalho, S. Farias Neto, and A. Lima, “Moisture Transport Process in Vegetable Fiber Composites: Theory and Analysis for Technological Applications,” 2013, pp. 37–62. doi: 10.1007/978-3-642-37469-2_2.

[139] A. Ab, A. Rashdi, S. Sapuan, K. Abdan, M. Mohamad, and M. M. H. Megat Ahmad, “Water Absorption Behaviour of Kenaf Reinforced Unsaturated Polyester Composites and Its Influence on Their Mechanical Properties,” *Pertanika J. Sci. Technol.*, vol. 18, Jul. 2010.

[140] S. Zakaria and L. Kok Poh, “Polystyrene-Benzoylated Efb Reinforced Composites,” *Polym.-Plast. Technol. Eng.*, vol. 41, no. 5, pp. 951–962, Jan. 2002, doi: 10.1081/PPT-120014397.

[141] A. Ramezani Kakroodi, Y. Kazemi, and D. Rodrigue, “Mechanical, rheological, morphological and water absorption properties of maleated polyethylene/hemp composites: Effect of ground tire rubber addition,” *Compos. Part B Eng.*, vol. 51, pp. 337–344, Aug. 2013, doi: 10.1016/j.compositesb.2013.03.032.

[142] A. Pandian, M. Vairavan, W. J. Jebbas Thangaiah, and M. Uthayakumar, “Effect of Moisture Absorption Behavior on Mechanical Properties of Basalt Fibre Reinforced Polymer Matrix Composites,” *J. Compos.*, vol. 2014, pp. 1–8, Mar. 2014, doi: 10.1155/2014/587980.

[143] M. K. Gupta and R. K. Srivastava, “Mechanical, thermal and water absorption properties of hybrid sisal/jute fiber reinforced polymer composite,” *INDIAN J ENG MATER SCI*, p. 8, 2016.

[144] M. A. H. Alharbi, S. Hirai, H. A. Tuan, S. Akioka, and W. Shoji, “Effects of chemical composition, mild alkaline pretreatment and particle size on mechanical, thermal, and structural properties of binderless lignocellulosic biopolymers prepared by hot-pressing raw microfibrillated Phoenix dactylifera and Cocos nucifera fibers and leaves,” *Polym. Test.*, vol. 84, p. 106384, Apr. 2020, doi: 10.1016/j.polymertesting.2020.106384.

[145] W. Z. W. Zahari, R. N. R. L. Badri, H. Ardyananta, D. Kurniawan, and F. M. Nor, “Mechanical Properties and Water Absorption Behavior of Polypropylene / Ijuk Fiber Composite by Using Silane Treatment,” *Procedia Manuf.*, vol. 2, pp. 573–578, 2015, doi: 10.1016/j.promfg.2015.07.099.

[146] P. Upadhyaya, M. Garg, V. Kumar, and A. K. Nema, “The Effect of Water Absorption on Mechanical Properties of Wood Flour/Wheat Husk Polypropylene Hybrid Composites,” vol. 2012, May 2012, doi: 10.4236/msa.2012.35047.

[147] B. K. Kim, O. H. Kwon, W. H. Park, and D. Cho, “Thermal, mechanical, impact, and water absorption properties of novel silk fibroin fiber reinforced poly(butylene succinate) biocomposites,” *Macromol. Res.*, vol. 24, no. 8, pp. 734–740, Aug. 2016, doi: 10.1007/s13233-016-4102-9.

[148] A. Paul, K. Joseph, and S. Thomas, “Effect of surface treatments on the electrical properties of low-density polyethylene composites reinforced with short sisal fibers,” *Compos. Sci. Technol.*, vol. 57, no. 1, pp. 67–79, Jan. 1997, doi: 10.1016/S0266-3538(96)00109-1.

[149] “Mechanical and Water Absorption Properties of Natural Fibers/Polymer Biocomposites: Polymer-Plastics Technology and Engineering: Vol 49, No 7.” https://www.tandfonline.com/doi/abs/10.1080/03602551003682067 (accessed May 26, 2022).

[150] G. Kalaprasad *et al.*, “Effect of fibre length and chemical modifications on the tensile properties of intimately mixed short sisal/glass hybrid fibre reinforced low density polyethylene composites,” *Polym. Int.*, vol. 53, no. 11, pp. 1624–1638, Nov. 2004, doi: 10.1002/pi.1453.

[151] M. N. Ichazo, C. Albano, J. González, R. Perera, and M. V. Candal, “Polypropylene/wood flour composites: treatments and properties,” *Compos. Struct.*, vol. 54, no. 2, pp. 207–214, Nov. 2001, doi: 10.1016/S0263-8223(01)00089-7.

[152] X. Li and L. Tabil, “A Study on Flax Fiber-Reinforced Polyethylene Biocomposites,” *Appl. Eng. Agric.*, vol. 25, pp. 525–531, Jul. 2009, doi: 10.13031/2013.27454.

[153] B. Mitra, “Environment Friendly Composite Materials: Biocomposites and Green Composites,” *Def. Sci. J.*, vol. 64, no. 3, pp. 244–261, May 2014, doi: 10.14429/dsj.64.7323.

[154] K. Murali Mohan Rao, K. Mohana Rao, and A. V. Ratna Prasad, “Fabrication and testing of natural fibre composites: Vakka, sisal, bamboo and banana,” *Mater. Des.*, vol. 31, no. 1, pp. 508–513, Jan. 2010, doi: 10.1016/j.matdes.2009.06.023.

[155] Akash, K. V. Sreenivasa Rao, N. S. Venkatesha Gupta, and D. S. Arun kumar, “Mechanical Properties of Sisal/Coir Fiber Reinforced Hybrid Composites Fabricated by Cold Pressing Method,” *IOP Conf. Ser. Mater. Sci. Eng.*, vol. 149, p. 012092, Sep. 2016, doi: 10.1088/1757-899X/149/1/012092.

[156] K. Ramanaiah, A. V. Ratna Prasad, and K. Hema Chandra Reddy, “Mechanical, thermophysical and fire properties of sansevieria fiber-reinforced polyester composites,” *Mater. Des.*, vol. 49, pp. 986–991, Aug. 2013, doi: 10.1016/j.matdes.2013.02.056.

[157] M. W. Chai, S. Bickerton, D. Bhattacharyya, and R. Das, “Influence of natural fibre reinforcements on the flammability of bio-derived composite materials,” *Compos. Part B Eng.*, vol. 43, no. 7, pp. 2867–2874, Oct. 2012, doi: 10.1016/j.compositesb.2012.04.051.

[158] ASTM, “Standard Test Method for Water Absorption of Plastics,” West Conshohocken, United States, 2010.

[159] N. Saba, M. Jawaid, and M. T. H. Sultan, “An overview of mechanical and physical testing of composite materials,” in *Mechanical and Physical Testing of Biocomposites, Fibre-Reinforced Composites and Hybrid Composites*, Elsevier Ltd, 2019, pp. 1–12. doi: 10.1016/B978-0-08-102292-4.00001-1.

[160] A. Atiqah, M. Jawaid, M. R. Ishak, and S. M. Sapuan, “Moisture Absorption and Thickness Swelling Behaviour of Sugar Palm Fibre Reinforced Thermoplastic Polyurethane,” *Procedia Eng.*, vol. 184, pp. 581–586, 2017, doi: 10.1016/j.proeng.2017.04.142.

[161] C. A. Echeverria, W. Handoko, F. Pahlevani, and V. Sahajwalla, “Cascading use of textile waste for the advancement of fibre reinforced composites for building applications,” *J. Clean. Prod.*, 2018, doi: 10.1016/j.jclepro.2018.10.227.

[162] Z. Kamble and B. K. Behera, “Mechanical properties and water absorption characteristics of composites reinforced with cotton fibres recovered from textile waste,” *J. Eng. Fibers Fabr.*, vol. 15, pp. 1–8, 2020, doi: 10.1177/1558925020901530.

[163] T. E. Hamouda *et al.*, “Evaluation of Mechanical and Physical Properties of Hybrid Composites from Food Packaging and Textiles Wastes,” *J. Polym. Environ.*, 2019, doi: 10.1007/s10924-019-01369-3.

[164] I. Bektas, C. Guler, H. Kalaycioglu, F. Mengeloglu, and M. Nacar, “Manufacture of Particleboards using Sunflower Stalks (helianthus annuus l.) And Poplar Wood (populus alba L.),” *J. Compos. Mater.*, vol. 39, no. 5, pp. 467–473, 2005, doi: 10.1177/0021998305047098.

[165] Emily, “Polyester Flammability – How Does It Stand Up To Heat?,” *THe creative folk*, 2022. https://www.thecreativefolk.com/polyester-flammability/ (accessed Mar. 21, 2022).

[166] City of Phoenix, “Flammable Fabrics,” *City of Phoenix*, 2021. https://www.phoenix.gov/fire/safety-information/home/fabrics (accessed Mar. 21, 2022).

[167] M. Bar, A. Ramasamy, and A. Das, “Flame Retardant Polymer Composites,” *Fibres Polym.*, vol. 16, pp. 705–717, Nov. 2014, doi: 10.1007/s12221-015-0705-6.

[168] V. Medri *et al.*, “Production and characterization of lightweight vermiculite/geopolymer-based panels,” *Mater. Des.*, vol. 85, pp. 266–274, Nov. 2015, doi: 10.1016/j.matdes.2015.06.145.

[169] J. Assaad, E. Chakar, and G.-P. Zéhil, “Testing and modeling the behavior of sandwich lightweight panels against wind and seismic loads,” *Eng. Struct.*, vol. 175, pp. 457–466, Nov. 2018, doi: 10.1016/j.engstruct.2018.08.041.

[170] S. Darzi, H. Karampour, B. P. Gilbert, and H. Bailleres, “Numerical study on the flexural capacity of ultra-light composite timber sandwich panels,” *Compos.*

Part B Eng., vol. 155, pp. 212–224, Dec. 2018, doi: 10.1016/j.compositesb.2018.08.022.

[171] Y. Du, N. Yan, and M. T. Kortschot, “Light-weight honeycomb core sandwich panels containing biofiber-reinforced thermoset polymer composite skins: Fabrication and evaluation,” *Compos. Part B Eng.*, vol. 43, no. 7, pp. 2875–2882, Oct. 2012, doi: 10.1016/j.compositesb.2012.04.052.

[172] Y. H. Mugahed Amran, R. Alyousef, H. Alabduljabbar, F. Alrshoudi, and R. S. M. Rashid, “Influence of slenderness ratio on the structural performance of lightweight foam concrete composite panel,” *Case Stud. Constr. Mater.*, vol. 10, p. e00226, Jun. 2019, doi: 10.1016/j.cscm.2019.e00226.

[173] D. Zhang, D. Jiang, Q. Fei, and S. Wu, “Experimental and numerical investigation on indentation and energy absorption of a honeycomb sandwich panel under low-velocity impact,” *Finite Elem. Anal. Des.*, vol. 117–118, pp. 21–30, Sep. 2016, doi: 10.1016/j.finel.2016.04.003.

[174] W.-S. Chang, E. Ventsel, T. Krauthammer, and J. John, “Bending behavior of corrugated-core sandwich plates,” *Compos. Struct.*, vol. 70, no. 1, pp. 81–89, Aug. 2005, doi: 10.1016/j.compstruct.2004.08.014.

[175] M. Ma, W. Yao, W. Jiang, W. Jin, Y. Chen, and P. Li, “Fatigue Behavior of Composite Sandwich Panels Under Three Point Bending Load,” *Polym. Test.*, vol. 91, p. 106795, Nov. 2020, doi: 10.1016/j.polymertesting.2020.106795.

[176] M. Giglio, A. Gilioli, and A. Manes, “Numerical investigation of a three point bending test on sandwich panels with aluminum skins and Nomex^{TM} honeycomb core,” *Comput. Mater. Sci.*, vol. 56, pp. 69–78, Apr. 2012, doi: 10.1016/j.commatsci.2012.01.007.

[177] A. Mostafa, “Numerical analysis on the effect of shear keys pitch on the shear performance of foamed sandwich panels,” *Eng. Struct.*, vol. 101, pp. 216–232, Oct. 2015, doi: 10.1016/j.engstruct.2015.07.010.

[178] C. Frazão, J. Barros, R. Toledo Filho, S. Ferreira, and D. Gonçalves, “Development of sandwich panels combining Sisal Fiber-Cement Composites and

Fiber-Reinforced Lightweight Concrete," *Cem. Concr. Compos.*, vol. 86, pp. 206–223, Feb. 2018, doi: 10.1016/j.cemconcomp.2017.11.008.

[179] R. Emmanuel, "Estimating the environmental suitability of wall materials: preliminary results from Sri Lanka," *Build. Environ.*, vol. 39, no. 10, pp. 1253–1261, 2004.

[180] R. Arooz and R. Halwatura, "Life cycle costing and embodied energy analysis of self-compacting in-situ cast mud-concrete load-bearing walling system (MCW) - An innovative earth based walling material application for energy efficient buildings.," presented at the iiSBE Forum of Young Researchers in Sustainable Building, Prague, Czech Republic, Jul. 2019.

[181] V. Biolek and T. Hanák, "LCC estimation model: A construction material perspective," *Buildings*, vol. 9, no. 8, p. 182, 2019.

[182] B. Reza, R. Sadiq, and K. Hewage, "Sustainability assessment of flooring systems in the city of Tehran: An AHP-based life cycle analysis," *Constr. Build. Mater.*, vol. 25, no. 4, pp. 2053–2066, 2011.

[183] B. Han, R. Wang, L. Yao, H. Liu, and Z. Wang, "Life cycle assessment of ceramic façade material and its comparative analysis with three other common façade materials," *J. Clean. Prod.*, vol. 99, pp. 86–93, Jul. 2015, doi: 10.1016/j.jclepro.2015.03.032.

[184] G. M. Nicoletti, B. Notarnicola, and G. Tassielli, "Comparative Life Cycle Assessment of flooring materials: ceramic versus marble tiles," *J. Clean. Prod.*, vol. 10, no. 3, pp. 283–296, Jun. 2002, doi: 10.1016/S0959-6526(01)00028-2.

[185] Ajla Aksamija, "Comparative Analysis of Flooring Materials: Environmental and Economic Performance," *PERKINS WILL Res. J.*, vol. 02, no. 01, pp. 55–66, 2010.

[186] K. I. Praseeda, B. V. V. Reddy, and M. Mani, "Embodied energy assessment of building materials in India using process and input–output analysis," *Energy Build.*, vol. 86, pp. 677–686, Jan. 2015, doi: 10.1016/j.enbuild.2014.10.042.

[187] D. M. K. W. Dissanayake, C. Jayasinghe, and M. T. R. Jayasinghe, “A comparative embodied energy analysis of a house with recycled expanded polystyrene (EPS) based foam concrete wall panels,” *Energy Build.*, vol. 135, pp. 85–94, Jan. 2017, doi: 10.1016/j.enbuild.2016.11.044.

[188] J. Nässén, J. Holmberg, A. Wadeskog, and M. Nyman, “Direct and indirect energy use and carbon emissions in the production phase of buildings: An input–output analysis,” *Energy*, vol. 32, no. 9, pp. 1593–1602, Sep. 2007, doi: 10.1016/j.energy.2007.01.002.

[189] W. P. S. Dias and S. P. Pooliyadda, “Quality based energy contents and carbon coefficients for building materials: A systems approach,” *Energy*, vol. 29, no. 4, pp. 561–580, Mar. 2004, doi: 10.1016/j.energy.2003.10.001.

[190] R. Fay, G. Treloar, and U. Iyer-Raniga, “Life-cycle energy analysis of buildings: a case study,” *Build. Res. Inf.*, vol. 28, no. 1, pp. 31–41, Jan. 2000, doi: 10.1080/096132100369073.

[191] R. H. Crawford, “Validation of a hybrid life-cycle inventory analysis method,” *J. Environ. Manage.*, vol. 88, no. 3, pp. 496–506, Aug. 2008, doi: 10.1016/j.jenvman.2007.03.024.

[192] J. W. Creswell and J. W. Creswell, *Qualitative inquiry & research design: choosing among five approaches*, 2nd ed. Thousand Oaks: Sage Publications, 2007.

[193] Igor Pietkiewicz and Jonathan A. Smith, “A practical guide to using Interpretative Phenomenological Analysis in qualitative research psychology,” *Czas. Psychol. Psychol. J.*, vol. 20, no. 1, Aug. 2014, doi: 10.14691/CPPJ.20.1.7.

[194] R. Emmanuel, “Estimating the environmental suitability of wall materials: preliminary results from Sri Lanka,” *Build. Environ.*, vol. 39, no. 10, pp. 1253–1261, Oct. 2004, doi: 10.1016/j.buildenv.2004.02.012.

Annex 1

The maximum stress of five different core arrangements for different cell sizes

1. Maximum stress - square panels

25 mm × 25 mm 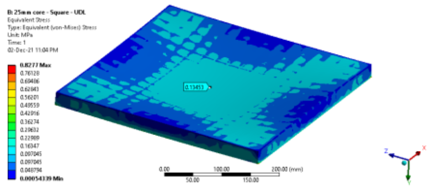 0.135 MPa	30 mm × 30 mm 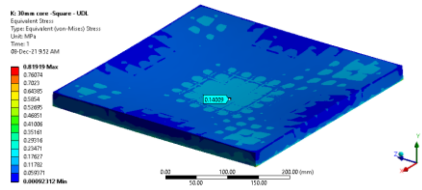 0.140 MPa
40 mm × 40 mm 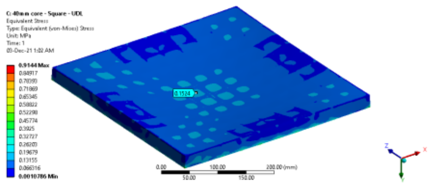 0.152 MPa	50 mm × 50 mm 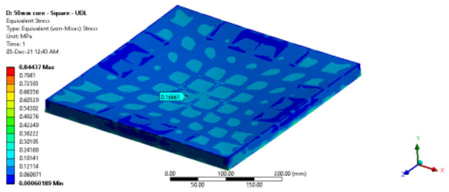 0.167 MPa
80 mm × 80 mm 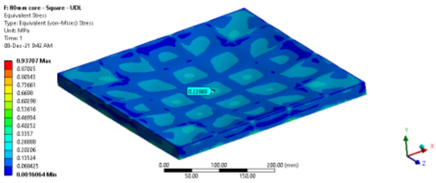 0.229 MPa	100 mm × 100 mm 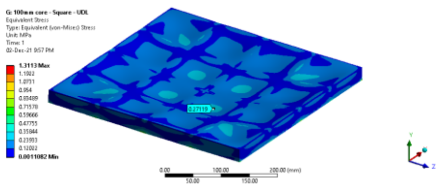 0.271 MPa
125 mm × 125 mm 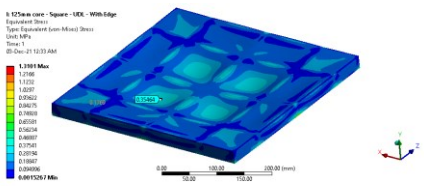 0.355 MPa	

2. Maximum stress -rectangular panels

20 mm × 60 mm 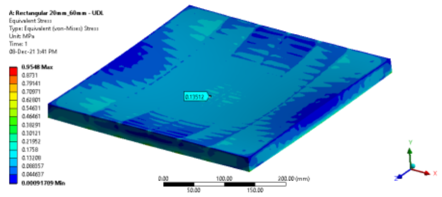 0.135 MPa	30 mm × 90 mm 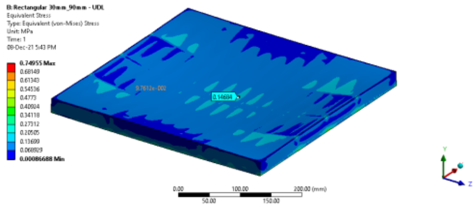 0.147 MPa
40 mm × 120 mm 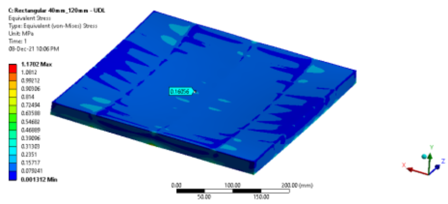 0.161 MPa	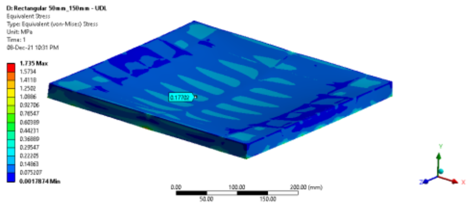 50 mm × 150 mm 0.177 MPa
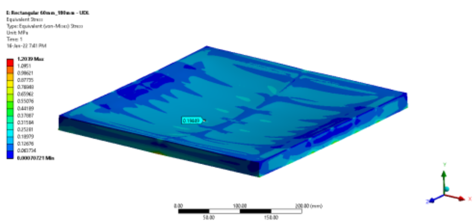 60 mm × 180 mm 0.194 MPa	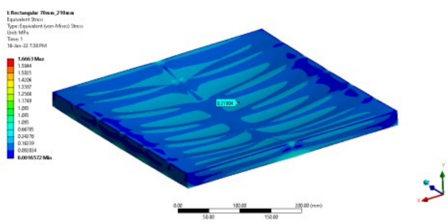 70 mm × 210 mm 0.219 MPa

3. Maximum stress - circular panels

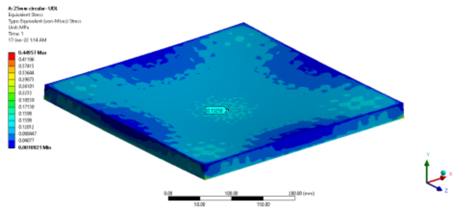 25 mm diameter 0.133 MPa	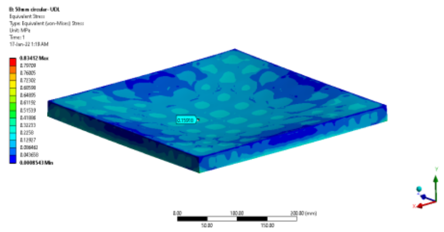 50 mm diameter 0.159 MPa
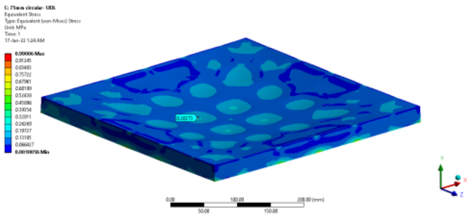 0.159 MPa 0.203 MPa	100 mm diameter 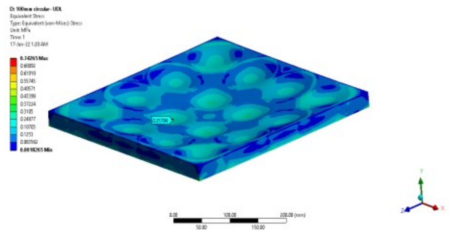 0.258 MPa
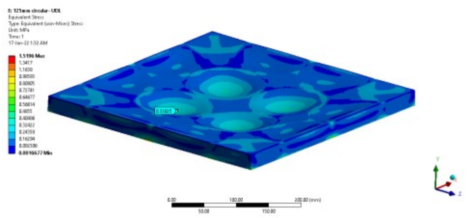 125 mm diameter 0.330 MPa	

4. Maximum stress -Triangular panels

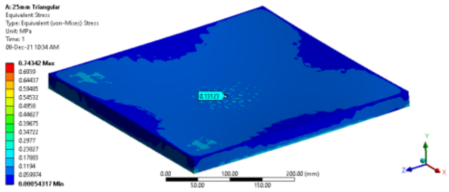 25 mm 0.131 MPa	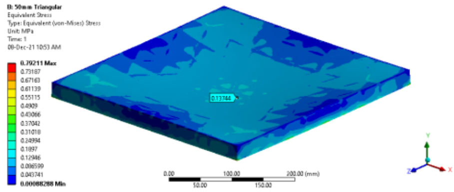 50 mm 0.137 MPa
75 mm 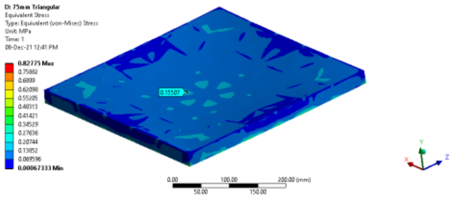 0.155 MPa	100 mm 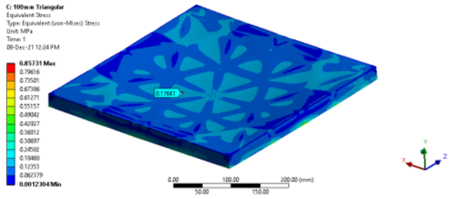 0.176 MPa
125 mm 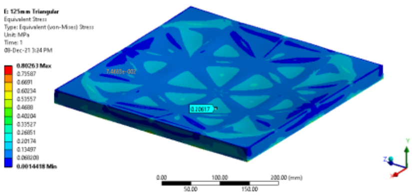 0.206 MPa	

5. Maximum stress - honeycomb panels

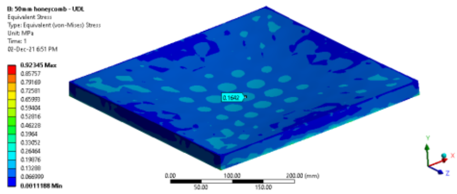 50 mm × 50 mm 0.164 MPa	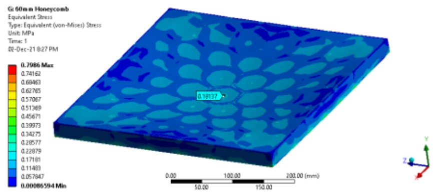 60 mm × 60 mm 0.181 MPa
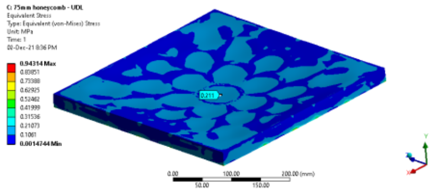 75 mm × 75 mm 0.211 MPa	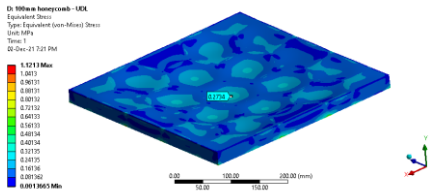 100 mm × 100 mm 0.273 MPa
125 mm × 125 mm 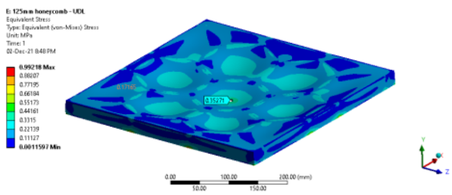 0.353 MPa	150 mm × 150 mm 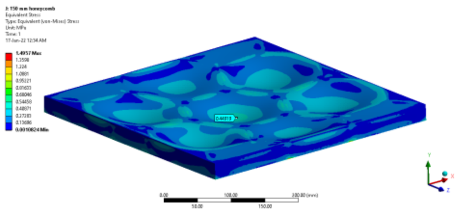 0.449 MPa